CHALMERS

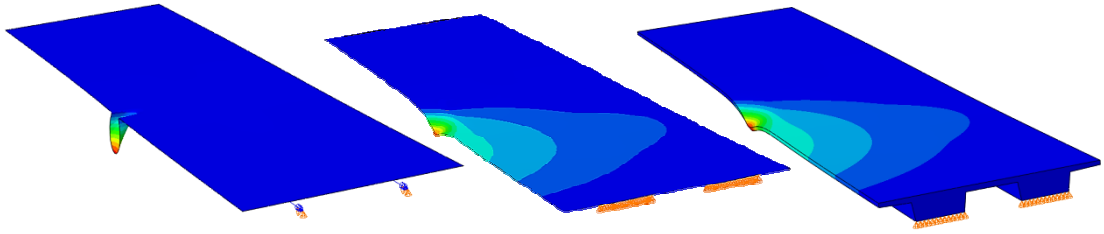

Load distribution in 3D structural analysis of a two girder concrete bridge

An investigation of how different FE-modelling techniques influence sectional forces

Master of Science Thesis in the Master's Programme Structural Engineering and Building Technology

LINUS LAGGAR
SOFIE STRÖM

Department of Civil and Environmental Engineering
Division of Structural engineering
Concrete structures
CHALMERS UNIVERSITY OF TECHNOLOGY
Göteborg, Sweden 2013

Master's Thesis 2013:65

MASTER'S THESIS 2013:65

Load distribution in 3D structural analysis of a two girder concrete bridge

An investigation of how different FE-modelling techniques influence sectional forces

Master of Science Thesis in the Master's Programme Structural Engineering and Building Technology

LINUS LAGGAR

SOFIE STRÖM

Department of Civil and Environmental Engineering
Division of Structural engineering
Concrete structures
CHALMERS UNIVERSITY OF TECHNOLOGY
Göteborg, Sweden 2013

Load distribution in 3D structural analysis of a two girder concrete bridge
An investigation of how different FE-modelling techniques influence sectional forces

Master of Science Thesis in the Master's Programme Structural Engineering and Building Technology

LINUS LAGGAR
SOFIE STRÖM

Examensarbete / Institutionen för bygg- och miljöteknik,
Chalmers tekniska högskola 2013:

Department of Civil and Environmental Engineering
Division of Structural engineering
Concrete structures
Chalmers University of Technology
SE-412 96 Göteborg
Sweden
Telephone: + 46 (0)31-772 1000

Cover:
Deformation figures of FE-models, representing a case study bridge, established in the FE-software Brigade/Plus. From left to right: FE-model established by beam and shell elements, shell elements and continuum elements. The cantilever is loaded with concentrated load.

Chalmers Reproservice
Göteborg, Sweden 2013

Load distribution in 3D structural analysis of a two girder concrete bridge
An investigation of how different FE-modelling techniques influence sectional forces

Master of Science Thesis in the Master's Programme Structural Engineering and Building Technology

LINUS LAGGAR
SOFIE STRÖM
Department of Civil and Environmental Engineering
Division of Structural engineering
Concrete structures
Chalmers University of Technology

ABSTRACT

The purpose of this Master's project was to investigate how different finite element modelling techniques in three-dimensional structural analysis influenced the distribution of shear forces and bending moments for a case study bridge. It was examined how the different modelling techniques described the load effect and which model that was the most suitable to describe the results of interest. The structure that was analysed was a two girder concrete bridge in two spans with an overlaying bridge deck slab. The case study bridge was represented by three different FE-models in the FE-software Brigade/Plus, where the models were established by different finite element types. The first FE-model was created by beam elements representing the girders and orthotropic shell elements representing the bridge deck slab, where the slab was not assigned any stiffness in longitudinal direction of the bridge. The second FE-model was created entirely of isotropic shell elements and the third model was established by continuum elements. To do a comprehensive investigation, specific load cases of concentrated loads as well as moving vehicle loads were studied, and sectional forces in critical sections of the bridge were compared.

The results from the analysis showed that the FE-model created by beam elements and orthotropic shell elements could be used to design the girders longitudinally. However, this model could not describe the structural behaviour of the slab. To design the bridge deck slab and consider the longitudinal load distribution, the models established by isotropic shell elements and continuum elements could be used. If output data was of interest in the girders at sections where loads were applied, it was to be aware of that shear forces were not described in a correct way at those sections, due to how shear forces were calculated and presented by *Free Body Cut*. In sections where no loads were applied, shear forces were described in the girders in a correct way and advantageous of the load distribution in the slab were taken into account. The results also showed that the FE-model established by continuum elements described a greater interaction between the girders when the cantilever was loaded, compared to the models established by structural elements. For moving vehicle loads all three FE-models could be used to design the girders.

Key words: FE-modelling, Finite element method, FEM, beam elements, shell elements, continuum elements, bridge design, load distribution, Free Body Cut, Brigade/Plus

Strukturanalys av lastspridningen i 3D för en tvåbalksbro i betong

En undersökning av hur olika modelleringstekniker med finita element påverkar tvärkrafter och moment

Examensarbete inom *Structural Engineering and Building Technology*

LINUS LAGGAR
SOFIE STRÖM
Institutionen för bygg- och miljöteknik
Avdelningen för Konstruktionsteknik
Betongbyggnad
Chalmers tekniska högskola

SAMMANFATTNING

Syftet med det här examensarbetet är att undersöka hur olika modelleringstekniker med finita element påverkar fördelningen av tvärkrafter och moment. Genom en fallstudie har en tvåbalksbro med överliggande brobaneplatta studerats. Bron var av betong och var i två spann. Tre olika FE-modeller skapades med olika elementtyper i programvaran Brigade/Plus. Den första FE-modellen var uppbyggd av balkelement som representerade balkarna och ortotropa skalelement som representerade brobaneplattan, där plattan inte tilldelades någon styvhet i longitudinell riktning av bron. Den andra FE-modellen skapades helt av isotropa skalelement och den tredje var uppbyggd av kontinuumelement. Både specifika lastfall med koncentrerade laster och lastfall med fordonslaster studerades där snittkrafter i kritiska snitt i bron jämfördes. Resultaten från analysen visade att en FE-modell uppbyggd av balkelement och ortotropa skalelement kunde användas för att dimensionera balkarna longitudinellt. Modellen kunde dock inte beskriva plattans strukturella respons. För att beskriva den longitudinella lastspridningen i plattan kunde modellerna som var uppbyggda av isotropa skalelement och kontinuumelement användas. För utdata i balkarna, i snitt där last var pålagd, var det dock viktigt att vara medveten om att tvärkraft inte beskrevs korrekt. Detta var en följd av att *Free Body Cut* användes för att beräkna och presentera snittkrafter. I de obelastade tvärsnitten beskrevs den gynnsamma longitudinella spridningen av tvärkraft. Resultaten från modellen uppbyggd av kontinuumelement visade också på en bättre samverkan mellan balkarna då konsolen belastades, jämfört med FE-modellerna uppbyggda av strukturella element. För rörliga fordonslaster kunde alla tre FE-modellerna användas för utformning av balkarna.

Nyckelord: FE-modellering, finita elementmetoden, FEM, balkelement, skalelement, kontinuumelement, brodesign, lastfördelning, Free Body Cut, Brigade/Plus

Contents

Preface

This Master's project was conducted in collaboration with Inhouse Tech Infra Göteborg AB in the spring 2013, for the department of Civil and Environmental Engineering at the division of Structural engineering at Chalmers University of Technology.

We want to send a great thanks to the company Inhouse Tech Infra Göteborg AB, Gothenburg, Sweden, and our supervisor Max Fredriksson for good advice and guidance during the work. We also want to thank Mario Plos that was our supervisor from Chalmers University of Technology and Scanscot Technology AB, Lund, Sweden, for helping us with the FE-software Brigade/Plus.

Linus Laggar and Sofie Ström
Gothenburg, 2013.

Notations

A	Cross-sectional area [m^2]
E	Young's Modulus [Pa]
G	Shear modulus [Pa]
I	Moment of inertia [m^4]
M	Bending moment [Nm]
q	Load [N/m]
t	Torque load [Nm/m]
V	Shear force [N]
w	Deflection [m]
ε	Strain [-]
γ	Shear angle [-]
κ	Curvature [1/m]
φ	Angle [º]
ν	Poisson's ratio [-]

1 Introduction

In the process from idea to a physical bridge structure there is an iterative process in design. To achieve an optimal performance, effective modelling techniques are very important. In the last years there have been stricter requirements and recommendations in Swedish bridge design and application of the finite element method (FEM) has been increasingly used. The complexity of mathematics in FE-modelling places great demands on improved knowledge of the engineers.

1.1 Background

Bridge design was traditionally performed by two-dimensional analyses where the longitudinal and transversal structural behaviour were treated separately. Assumptions regarding the interaction between the two directions were then introduced and sectional forces to be used in design were calculated.

Stricter requirements from the Swedish Transport Administration (Trafikverket) regarding design of bridges, where the structural behaviour should be described in its entirety, has led to that the traditional way of analysing bridges is no longer sufficient. Accordingly, a three-dimensional finite element model needs to be established and analysed to account for the complex interaction between longitudinal and transversal direction.

The theory of finite elements has been developed mathematically for a long time, but before the computer capacity was sufficient the advanced mathematics in finite element methods was not applicable in the engineering analysis. As the computer capacity has increased, the finite element method has started to be used more for practical engineering problems.

A finite element model where the structural parts are assigned linear elastic material properties can describe the structural behaviour in the ultimate limit state. FE-models are complex and it can be difficult to establish a model which represents the real structural behaviour in good way. Results obtained from a FE-model can be hard to interpret and the output data needs in some cases to be post-processed before it is useful in design. Introducing assumptions and simplifications of the structural behaviour can lead to less complicated models which still represent a realistic structural response. This places great demands on understanding the structural behaviour since absence of knowledge of structural response easily can result in implemented errors and oversights in the finite element model.

The finite element method consists of advanced theories and mathematical models. Different ways of modelling can be used to describe the same structural problem. Which method that suits best can vary depending on the results of interest.

1.2 Purpose and objectives

The purpose of this Master's project was to investigate if simplified FE-models, established by structural elements, could be used to describe the structural response sufficiently well compared to a fully three-dimensional FE-model based on continuum mechanics. The project aimed to investigate if there were differences of the distribution of shear forces and bending moments in the bridge deck slab depending

on which modelling technique that was used and if the FE-models were able to describe the interaction between the girders.

The intention was to state advantages and disadvantages with the different modelling techniques and come to a conclusion when the FE-models preferably can be used in design.

1.3 Scope

The structure modelled in the case study was a two span concrete bridge which was continuous over the mid support. This is a bridge type that is common for new bridges in Sweden, and therefore relevant for the investigation. The bridge was simplified to only consist of two longitudinal girders with an overlaying bridge deck slab and was symmetric both in longitudinal and transversal direction.

The bridge was modelled by three different modelling techniques. The first model was established by beam and shell elements where beam elements represented the girders and shell elements represented the bridge deck slab. The shell elements were assigned stiffness in transversal direction only of the bridge. In the second model the entire bridge was established by isotropic shell elements and the last model was established by continuum elements.

The analysis was performed for situations where the bridge was subjected to specific load cases of concentrated loads and moving vehicle loads. The material response was assumed to be linear elastic and the sectional forces of interest, used in the comparison of the modelling techniques, were shear forces and bending moments.

1.4 Method

In this Master's project three different FE-models were established using different modelling techniques. The FE-models were representing a case study bridge and an investigation of how different modelling techniques describe variation and distribution of shear forces and bending moments in the bridge deck slab and along the girders was made.

The FE-models were established and analysed in Brigade/Plus 5.1-1, a FE-software for bridge engineering based on the more general FE-software Abaqus. Two of the FE-models that were used in the analysis were established by structural elements where simplifications of the structural behaviour and geometry were made and the third was established by continuum elements based on continuum mechanics. The first FE-model was chosen to be established by beam elements representing the girders and shell elements representing the bridge deck slab, where the slab was not assigned any stiffness in longitudinal direction of the bridge. The second FE-model was established entirely of shell elements where the slab was assigned isotropic material properties to take the longitudinal distribution in the bridge deck slab into account. The third model was established by continuum elements without any simplifications of the mathematical model and the geometry of the case study bridge.

In order to understand the underlying theories and assumptions in FE-software, a literature study of FE-theory and FE-modelling was performed. To ensure that the different theories represented the different structural parts included in the three FE-models satisfactorily, the reliability and reasonableness of the established models

were verified both analytically and visually. Also element based tie constraints, used to constrain the beam elements and shell elements in model 1, were studied.

To state general conclusions about the advantages and disadvantages of using different modelling techniques two specific load cases of concentrated loads, applied on the bridge deck slab between the girders and on the cantilever, were studied. The distribution of loads in the bridge deck slab was compared between the FE-models and the interaction between the girders was investigated. The conclusions made from the specific load cases was thereafter used to interpret the results from an FE-analysis of moving vehicle loads from Load model 1, defined in Eurocode 1-2 Chapter 4.3.2 (CEN, 2003).

2 Finite element method

The Swedish Transport Administration (Trafikverket) has made stricter requirements regarding design of bridges. The new requirements were stated in TK Bro 2009 where the calculation model for system analysis should, with respect to loads, geometry and deformations, describe the structural behaviour in its entirety (Trafikverket1, 2011). Modelling of bridges in two dimensions is therefore no longer sufficient in order to meet the new requirements, unless a clear two-dimensional structural behaviour can be distinguished. The consequence of the new requirements is that a three-dimensional FE-model needs to be established and analysed in order to capture the interaction between the structural behaviour in longitudinal and transversal direction (Trafikverket2, 2011).

In this chapter the background and important theories of the finite element method are presented and element types used in this Master's project are shortly explained.

2.1 Background and history of FEM

The theory of finite elements has been developed mathematically for a long time, but before the computer capacity was sufficient the advanced mathematics in finite element methods was not applicable in engineering analysis. The last decades, the computer capacity that was needed in order to perform FE-analyses of complex structures, were only available at research departments and large companies (Rombach, 2011). As the computers capacities have increased, the finite element method has become a standard tool in structural engineering design.

In finite element modelling the problem domain is divided into elements where each element is given different properties depending of which structural behaviour that should be represented (Liu & Quek, 2003). The finite element modelling is used to establish a system of differential equations. The equation system is solved by a numerical method that gives an approximate solution. With mesh refinement the number of elements will increase and the approximate solution converges to become close to the exact solution (Rugarli, 2010).

Bridge design has traditionally been performed by two-dimensional analyses where the transversal behaviour of the structure was analysed separately and taken into account in the longitudinal direction. The interaction of load distribution in transversal and longitudinal direction was thereby assumed by the structural engineer. In this way, a two-dimensional analysis may disguise important effects from the transversal direction. In recent years, three-dimensional linear elastic FE-modelling has been commonly used in bridge design (Davidson, 2003). A three-dimensional FE-analysis is preferably used with respect to accuracy in modelling and to represent a global structural behaviour, where the interaction between longitudinal and transverse direction is included.

Advanced finite element software is a good engineering tool to describe a structural behaviour. In order to establish a model which represents the real structural behaviour in a good way, the knowledge of the underlying theories and assumptions is essential.

2.2 Mathematical models for structural behaviour

To be able to create reliable FE-models with reasonable structural behaviours, the theories of beams and plates are studied. A plate can carry load in two directions in contrast to a beam that only can carry load in one direction. Despite this, plates are generalisations of beams and contain the beam theory.

Both beam and plate theories solve equilibrium conditions based on a predetermined assumption of the deformations. It is important to be aware of the different simplifications in the different theories before they are applied and used in a FE-model. If the simplifications are considered not to describe the behaviour of a structure sufficiently well continuum mechanics could advantageously be used. In continuum mechanics the equilibrium conditions are solved based on strain-displacement relations, and do not introduce assumptions of the deformations. The theory is thereby considered to reflect the real structural behaviour.

To determine whether the simplifications in beam and plate theory are valid to be introduced in the FE-models, the theories will be explained more in detail in this chapter.

2.2.1 Beam theory

There are two well known beam theories used in FE-modelling, Euler-Bernoulli beam theory and Timoshenko beam theory. Euler-Bernoulli beam theory is based on the fundamental assumption of plane sections normal to the beam axis remains plane and normal to the beam axis in the deformed shape (Ottosen & Petersson, 1992). This theory is applicable for slender beams.

Deriving the differential equation for a three dimensional beam structure, based on the equilibrium conditions, kinematic and constitutive relations will give raise to a complex set of equations to be solved (Ottosen & Petersson, 1992). Therefore it is favourable to introduce assumptions that simplify the problem formulation significantly, provided that the geometry of the structure is such that it is possible.

Beams are good examples of structures where assumptions about the structural behaviour can be made, which simplify the problem formulation of beam bending. The physical structure is three-dimensional but since beams are dominated by extension in the axial plane it becomes possible to make simplifications about the structural deformations (Ottosen & Petersson, 1992).

When a beam with an arbitrary cross-sectional area is loaded with a distributed load in vertical direction the deflections will occur in the same direction only, see Figure 2.1. This holds true if the cross-section of the beam is symmetric to its vertical plane. In Euler-Bernoulli beam theory these assumptions are made in order to simplify the problem formulation from a three-dimensional problem to two dimensions. The complex set of equations is then reduced.

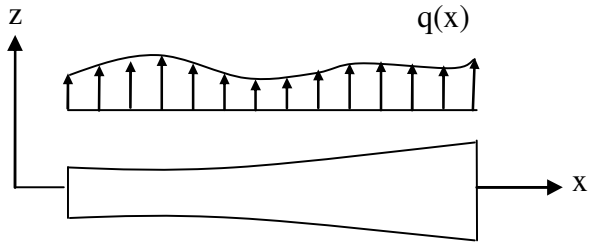

Figure 2.1 A beam with an arbitrary cross-section, loaded with a distributed load, adapted from Ottosen och Petersson (1992).

The equilibrium conditions of a beam problem can be stated by looking at an infinitesimal part of the beam, see Figure 2.2. In the horizontal direction, it is assumed that no normal forces will occur. This hold true for deflections that are small compared to the depth of the beam, when the supports are constrained (Blaauwendraad, 2010). Therefore the horizontal equilibrium only states the assumption of no resulting forces.

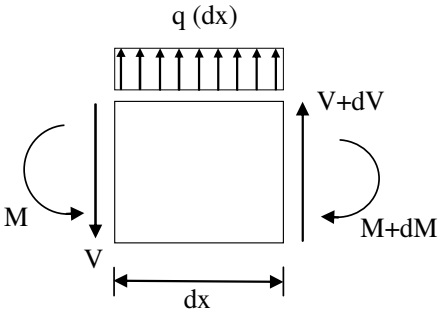

Figure 2.2 Equilibrium conditions for an infinitesimally part of a beam loaded vertically, adapted from Ottosen och Petersson (1992).

This means that, if looking at the equilibrium conditions for the element, the equilibrium in vertical direction and moment equilibrium will be of interest. The vertical equilibrium gives the expression in equation 2-1 and 2-2.

$$qdx - V + (V + dV) = 0 \tag{2-1}$$

$$\frac{dV}{dx} = -q \tag{2-2}$$

Moment equilibrium from the same infinitesimal element is presented in equation 2-3. If qdx and dV are infinitesimally the relation that the derivative of the moment force is equal to the shear force can be stated, see equation 2-4.

$$M + qdx\frac{dx}{2} + (V + dV)dx - (M + dM) = 0 \tag{2-3}$$

$$\frac{dM}{dx} = V \tag{2-4}$$

The kinematic relation in beam theory is, as mentions earlier, based on Euler-Bernoulli beam theory of plane sections remain plane and normal to the beam axis even after deformation. To clarify this, two points at the cross-sectional plane of a beam in the unloaded state is defined, and the longitudinal axis of the beam is the normal to the plane between these points, see Figure 2.3 (a). The theory implies that the position of the two points will change when the beam is loaded, but both the distance between the points and the normal to the plane will remain, see Figure 2.3 (b).

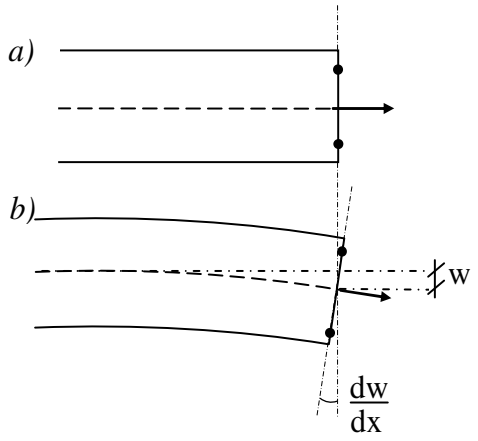

Figure 2.3 Deformation of a beam when the section rotates, using Euler-Bernoulli beam theory; (a) undeformed beam and (b) deformed beam. Adapted from Ottosen och Petersson (1992).

The kinematic relations together with the equilibrium conditions give the equations of strain and shear strain, see equation 2-5 and 2-6.

$$\varepsilon_{xx} = -z\frac{d^2w}{dx^2} \tag{2-5}$$

$$\varepsilon_{yy} = \varepsilon_{zz} = \gamma_{xy} = \gamma_{yz} = \gamma_{xz} = 0 \tag{2-6}$$

The last assumption that is needed to formulate the differential equation for a beam, based on Euler-Bernoulli beam theory, is a constitutive relation where a small slope of the curvature is assumed. The curvature can then be expressed as the second derivative of the deflection, see equation 2-7, and the moment is then given by the expression in equation 2-8.

$$\kappa = \frac{d^2w}{dx^2} \tag{2-7}$$

$$M = -EI\kappa \tag{2-8}$$

When all needed relations are known, the differential equation for Euler-Bernoulli beams can be derived. Combining equation 2-1to 2-8, the differential equation can be stated, see equation 2-9.

$$EI\frac{d^4w}{dx^4} - q = 0 \tag{2-9}$$

From the differential equation, based on Euler-Bernoulli beam theory, all forces of interest can be derived when the deflection has been determined. By linear elasticity and consideration of Hook's law, also stresses can be calculated.

Even though the beam theory involves a number of assumptions it still reflects the real structural behaviour of beams satisfactorily (Ottosen & Petersson, 1992). It should be remembered that the approximation of no shear strain vertically along the beam means that the theory only consider flexural deformations. As long as the beam holds a high ratio between length and height of the beam cross-section, the real shear strain is generally small and Euler-Bernoulli beam theory is generally a good approximation.

Timoshenko's beam theory is a more general way of explaining the beam theory, where the angular change between the normal of the deformed plane and the beam axis is taken into account. The theory keeps the assumption that the sections remain plane, but not necessarily normal to the beams axis in the deformed position (Rugarli, 2010). In Timoshenko beam theory, both flexural and shear deformations are taken into account, when the beam deforms due to loading. Therefore Timoshenko's beam theory is advantageously applied on non-slender beams to account for a more correct structural behaviour (Blaauwendraad, 2010).

2.2.2 Plate theory

A plate is a collective term for systems in which forces are transferred in two directions. Plates are distinguished in two main categories depending on if they are loaded in their plane or loaded out of plane (Blaauwendraad, 2010). A slab is loaded out of plane and does not show any membrane like behaviour (Rugarli, 2010).

Two commonly used plate theories that imply out of plane loading are Kirchhoff plate theory and Mindlin-Reissner plate theory. Similar in both theories is that the three-dimensional plate is reduced to a two-dimensional problem.

Since the plate structure generally is a structure with a small thickness, it is dominated by its in plane dimensions. The set of equations can therefore be reduced by its coordinate in the direction of the plate thickness (Ottosen & Petersson, 1992). To be able to do this, it must be assumed that all dependent variables are independent of the thickness and that all external loads only are applied in the normal direction to the plane of the plate (Liu & Quek, 2003). By these assumptions the plate become a two dimensional structure and since the dominating dimensions are in the plane there is also an assumption of a plane stress situation. Plane stress implies that the stresses over the height of the plate is very small and can be neglected (Ottosen & Petersson, 1992).

As in Euler-Bernoulli beam theory, Kirchhoff plate theory assumes that shear deformations are small and can be neglected. The assumption of plane sections remain

plane after deformation, and the beam axis is kept normal to the deformed plane is also made in Kirchhoff plate theory. These are assumptions that simplify the problem and give good results for sufficiently thin plates (Rugarli, 2010).

As in beam theory it is assumed that no normal forces will occur due to constrained supports. This hold true for small deflections compared to the depth of the plate (Blaauwendraad, 2010). According to this assumption, the structure will have no strains in the longitudinal direction. This means that application of load, instead will lead to a rotation of the cross-section.

Introducing these assumptions of the structural behaviour of plates, the problem formulations can be simplified significantly. By looking at a small element of a plate, see Figure 2.4, the kinematic, constitutive and equilibrium relations can be derived.

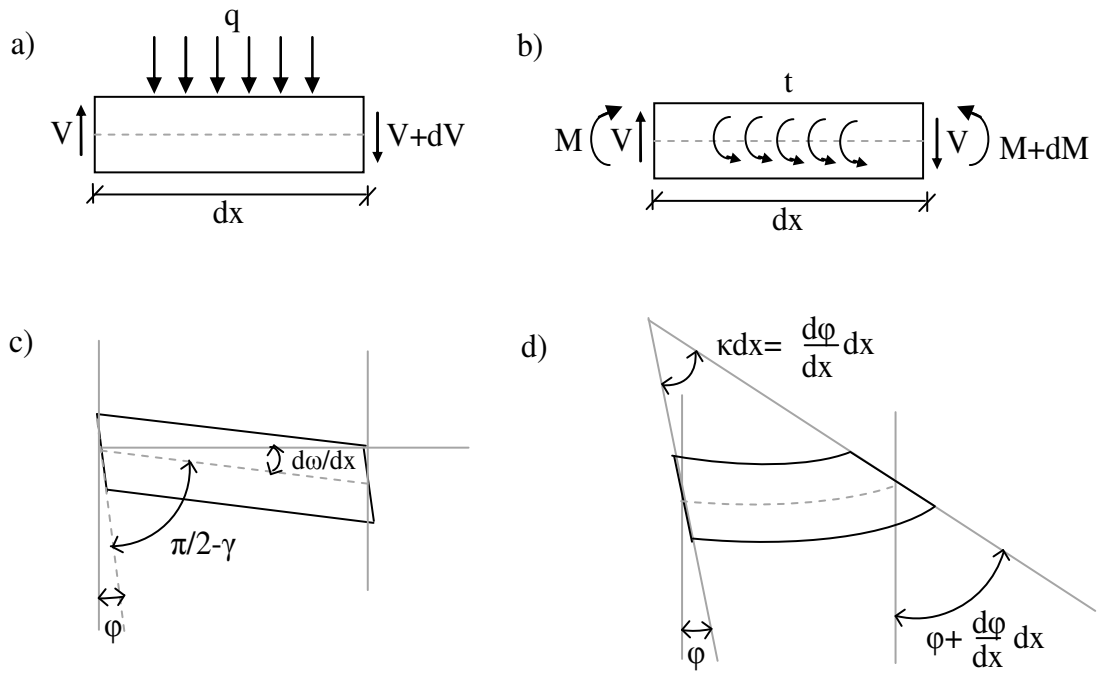

Figure 2.4 Equilibrium conditions for a infinitesimally plate. (a) Vertical equilibrium, (b) moment equilibrium, (c) shear deformation and (d) bending deformation. Adapted from Blaauwendraad (2010).

The kinematic relation is given from Figure 2.4 (c) and (d) where the shear angle and curvature can be derived respectively, see equation 2-10 and 2-11.

$$\gamma = \varphi + \frac{d\omega}{dx} \tag{2-10}$$

$$\kappa = \frac{d\varphi}{dx} \tag{2-11}$$

The constitutive relation of bending and shear is then given by equation 2-12 and 2-13, respectively. The equilibrium conditions is derived from Figure 2.4 (a) that

gives the vertical equilibrium and (b) that gives the moment equilibrium, see equation 2-14 and 2-15, respectively.

$$M = EI\kappa \tag{2-12}$$

$$V = GA\gamma \tag{2-13}$$

$$\frac{dV}{dx} + q = 0 \tag{2-14}$$

$$\frac{dM}{dx} - V + t = 0 \tag{2-15}$$

The relations from equation 2-10 to 2-15, together with the assumption that shear deformations are negligible results in the governing differential equation for Kirchhoff plates, see equation 2-16.

$$\frac{d^4\omega}{dx^4} + 2\frac{d^4\omega}{dx^2dy^2} + \frac{d^4\omega}{dy^4} = \frac{12(1-\upsilon^2)}{Et^3}t \tag{2-16}$$

The analogy between beam and plate theory can be seen in the first term in the differential equation. The term relates to the load bearing capacity in longitudinal direction which can be seen to correspond to the beam action. The main difference between plate and beam theory is that the differential equation for plates must include the fact that plates carry load in two directions. This can be seen in the third term in the expression of the differential equation. The second term treats the torsion capacity. As in the case for beams, sectional forces and moments can be derived when the deflection has been determined since the differential equation is based on the field relations. By linear elasticity and by Hook's law also stresses can be calculated.

Mindlin-Reissner plate theory is an extension of Kirchhoff plate theory which takes shear deformations into account. Mindlin-Reissner plate theory is more generalized where the assumption of plane sections remain plane after deformation is kept but not necessarily the normal of the plane (Rugarli, 2010). In thick plates, shear deformations occur to a greater extent than in thin plates, hence Mindlin-Reissner plate theory is preferably used.

2.3 Finite element types

In finite element modelling there are different finite element types with various structural properties. Often more than one element type can be used to describe the same structural problem. All finite element types can be assigned different shapes and different number of nodes and the formulation of the mathematical model can be chosen to, in the best way, represent the real structural behaviour (Simulia, 2009). In each integration point in the finite elements, the material response is evaluated. Elements with one node in each corner of the elements are called first order elements

and use linear interpolation. Elements with one intermediate node between the corner nodes are called second order elements and use quadratic interpolation.

If the structural model is analysed by inappropriate element types it does not matter how detailed the model is made or how dense the mesh is; the analysis is wrongly stated and the FE-model does not reflect the real problem in a good way.

The most common element types are from the categories truss, beam, shell and continuum finite elements where the last three element types are used in this Master's project and described below.

2.3.1 Beam elements

The most common beam theory is Euler-Bernoulli beam theory, described in Section 2.2.1. The solid beam elements available in Brigade/Plus are based on Euler-Bernoulli beam theory. It is important to evaluate if the simplifications in the theory is correct to use for a certain problem or if other finite elements that take the deformation in the plane into account may be used (Simulia, 2009).

Beam elements can be two-dimensional or three-dimensional and are represented by lines in FE-modelling (Liu & Quek, 2003). The deformation of a beam is only in the direction perpendicular to its longitudinal axis. Every node in a three-dimensional beam element consists of six degrees of freedoms, i.e. three translations and three rotations.

Beam elements are generally easy to use in FE-modelling and are therefore relatively inexpensive in terms of computational cost, compared to other finite element types. The beam elements are good at describing bending and bending failure but cannot describe shear cracking or shear failure.

The differential equation for beam theory is derived from the field equations and therefore all sectional forces of interest can be found when the deflection is known, see 2.2.1. This leads to the advantage that sectional forces easily can be calculated at any arbitrary node, without post-processing, when the FE-analysis has been performed.

2.3.2 Shell elements

Plate structures, e.g. slabs, carry load in its plane and distribute the load in both longitudinal and transversal direction to the supports. In FE-modelling, plate structures are often treated as special cases of shell structures analysed by shell elements (Liu & Quek, 2003).

Shell elements are often formulated by a combination of two-dimensional plane stress solid elements and plate elements, where the plate theory is implemented, but can also be formulated by defining shape functions (Liu & Quek, 2003). A difference between plate elements and shell elements is that shell elements can describe membrane forces in the plane of the shell, but plate elements cannot.

In Brigade/Plus different plate theories are implemented, (Simulia, 2009). If a four node, quadrilateral stress-displacement shell element is used, these elements allow for transverse shear deformations. For this element type, plate theory for thick plates is used when the shell thickness increases, see Kirchhoff plate theory in Section 2.2.2,

and thin plate theory is used when the shell thickness decreases, see Mindlin-Reissner plate theory in Section 2.2.2.

A common shape of the shell elements, often used in modelling, is rectangular shape but other shapes are also available in many FE-software. A mesh of rectangular elements should have regular element sides and it should be sought to have elements with perpendicular corners.

Shell elements are represented by surfaces in FE-modelling and they have six degrees of freedom in every node, three rotations and three translations (Simulia, 2009). They are good at describe bending and bending failure and can to some extent describe in-plane shear.

Analogous to beam elements and beam theory the differential equation for plate theory is derived from the field equations, see Section 2.2.2. All sectional forces of interest can therefore be calculated from the system of differential equations when the deflection is known.

2.3.3 Continuum elements

Typical continuum problems are structures with thick members loaded generically in space, but all kind of structures can be modelled by continuum elements (Rugarli, 2010). Beam and shell structures are often modelled by structural elements where introduced assumptions about the behaviour are made. This leads to an approximated mathematical problem where the structural behaviour is described in a line or surface respectively (Liu & Quek, 2003). In reality beams and plates are volumes.

The continuum elements are based on a strain-displacement relation in continua, and no assumptions of the structural behaviour are introduced. For that reason a structure, modelled by continuum elements, is in general more accurate with regard to the structural behaviour, compared to a structure modelled by structural elements (Simulia, 2009).

Continuum elements are represented by volumes and have three degrees of freedom in every node, translation in three directions (Rugarli, 2010). When establish a model, using continuum elements, the interpretation of results becomes more difficult compared to e.g. a model established by beam or shell elements. Only deflection and stresses are easily obtained from the FE-analysis. This creates a need of post-processing of results before any sectional forces can be found and used in design.

Continuum elements can have combinations of solid and structural properties and also have many different shapes. Some continuum elements are more or less sensitive to distortions, for example triangular and tetrahedral elements (Simulia, 2009). In order to get a reliable model, the element shape should be structured with regular element sides. Hexahedral elements, for example, should have perpendicular corners (Rugarli, 2010).

A disadvantage with continuum elements is that it is in general difficult to create a mesh without distortions. A relatively dense mesh is needed to describe the structural behaviour satisfactorily. Generally, high order elements are good to use if the problem induces high bending. If first order elements are used, many elements must be used over the height of the cross-section to describe bending in a good way. For these

reasons it is more expensive in terms of computational cost to use continuum elements compared to structural elements (Liu & Quek, 2003).

Another disadvantage with a model established by continuum elements is that it is difficult to predict critical sections. This is because it is not possible to visualise contour plots of sectional forces of the FE-model.

2.4 Interaction by tie constraints

When different element types are used within a FE-model, the different structural parts must be connected to each other to create an interactive structure. In Brigade/Plus this can be made in different ways and in this Master's project surface based tie constraints have been used.

A surface based tie constraint, is a stiff links between nodes, where all active degrees of freedom within the constrained nodes will be equal (Simulia, 2009). Tie constraints are good to use to interact different element types or to avoid mesh disturbance if the mesh density is rapidly changed within the model.

To interact two structural parts in a FE-model, a master surface and a slave surface have to be defined. The surfaces can be chosen as element-based or node-based, see Figure 2.5 and Figure 2.6, respectively. For an element-based master surface stiff links, orthogonal to the master surface, are coupled to the nodes in the slave surface within a position tolerance. The position tolerance is either chosen as the default value, where the tolerance is selected by the software and is based on the distance between the surfaces, or specified by the user. The tied region can also be chosen to a set of nodes. For a node-based master surface the slave nodes are directly constrained to the closest master node, if the slave nodes are within the tolerance distance from the master node.

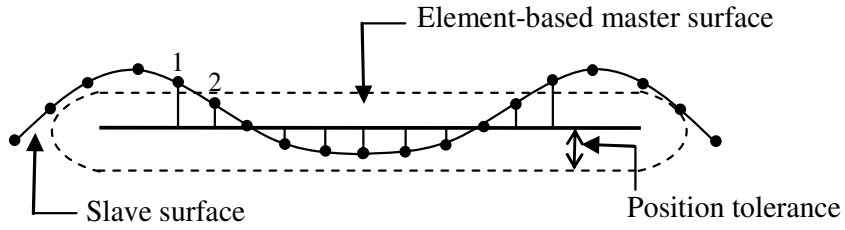

Figure 2.5 Surface-based master surface constrained to the slave surface within the position tolerance, adapted from (Simulia, 2009).

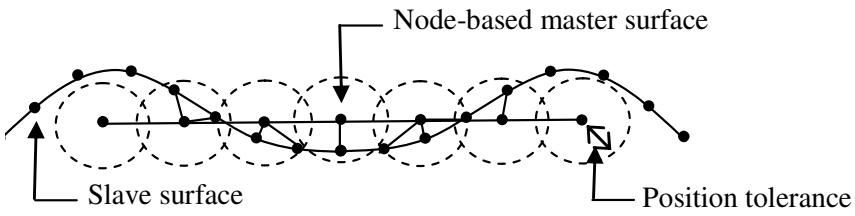

Figure 2.6 Node-based master surface constrained to the slave surface within the position tolerance, adapted from (Simulia, 2009).

For both element-based and node-based master surfaces, slave nodes are not constrained unless they are within the tolerance region or included in the set to be constrained. Unconstrained nodes will remain unconstrained during the FE-simulation and will not interact with the master surface as a part of the constraint.

In Brigade/Plus, there are two formulations of how the slave nodes projects on the master surface, surface-to-surface formulation and node-to-surface formulation. The position tolerance criterion is dependent on which constraint formulation that is used, why surface restrictions need to be taken into account. For a surface-to-surface formulation all nodes to an element edge that is within the position tolerance will be constrained, i.e. both node number 1 and 2 in Figure 2.5 will be constrained. For a node-to-surface formulation only the nodes within the position tolerance will be constrained, i.e. node number 1 in Figure 2.5 will not be constrained.

Due to how the node-to-surface approach formulates the projection from the slave surface to the master surface, the node-to-surface formulation is somewhat more efficient for complex surfaces than the surface-to-surface formulation. In addition to that there are generally more master nodes per tie constraint in a surface-to-surface formulation compared to a node-to-surface formulation. For that reason the surface-to-surface formulation may be more costly to use in terms of computational cost. The same occurs if the mesh of the master surface is very fine compared to the slave surface and could also affect the accuracy of the solution. The master surface should be chosen as the surface with the coarser mesh for the best accuracy of the solution.

2.5 Free Body Cut

Free Body Cut is a feature in Brigade/Plus which calculates sectional forces for FE-models established by continuum elements or shell elements (Scanscot Technology AB, 2013). Because continuum elements only are able to describe deformations and stresses, Free Body Cuts can be created to get e.g. shear forces and bending moments in specific sections. *Free Body Cut* can also be used to distribute loads over a specific width. For that reason, sectional forces are advantageously calculated by the feature *Free Body Cut* to get sectional forces to be used in design when load effects is to be distributed over certain widths.

The great advantage with *Free Body Cut* is that it can be used in analyses where the combined load effects from different load cases are of interest. In design of bridge structures there are often many load combinations and load positions to take into account and each load position is analysed separately. Without the use of *Free Body Cut* in FE-models established by continuum elements, the sectional forces for the maximum stress component are calculated for each point individually. The contribution from all load cases and load positions obtained by linear analysis are then combined and superimposed, see Figure 2.7. A disadvantage with this is that the sectional forces may be calculated from stress distributions that are not possible to arise from any of the examined load cases. For this reason continuum elements faced many constraints and the process of finding sectional forces was not useful in design.

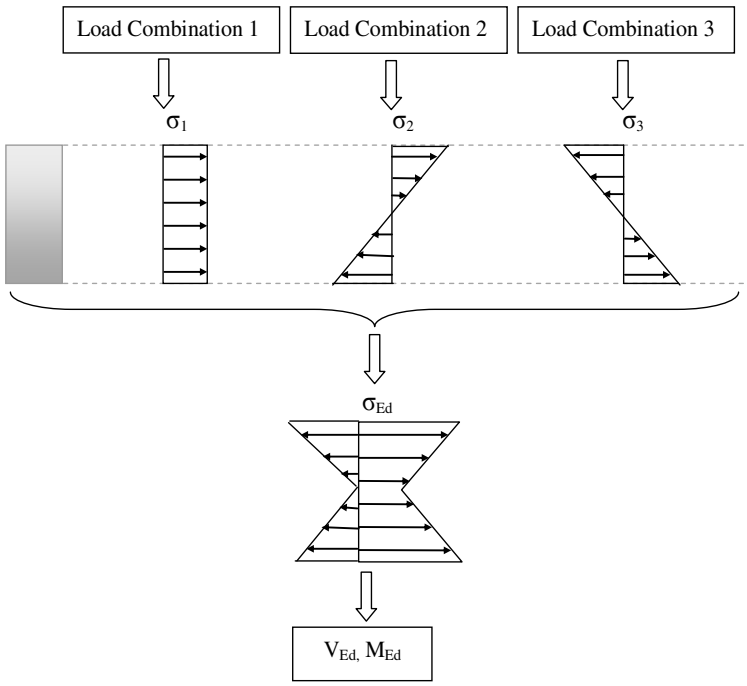

Figure 2.7 Calculation of sectional forces by post-processing. The stresses were here summarised independently for each point and the design profile for sectional forces became often unrealistic.

With the *Free Body Cut* feature in Brigade/Plus it is possible to perform analyses for FE-models established by continuum elements when the effect from load combinations is to be examined. Instead of combining the maximum possible stress components for all load combinations into sectional forces, *Free Body Cut* calculates the sectional forces for each load case separately, see Figure 2.8. Thereafter the sectional forces are summarised to get the design sectional forces for the chosen section.

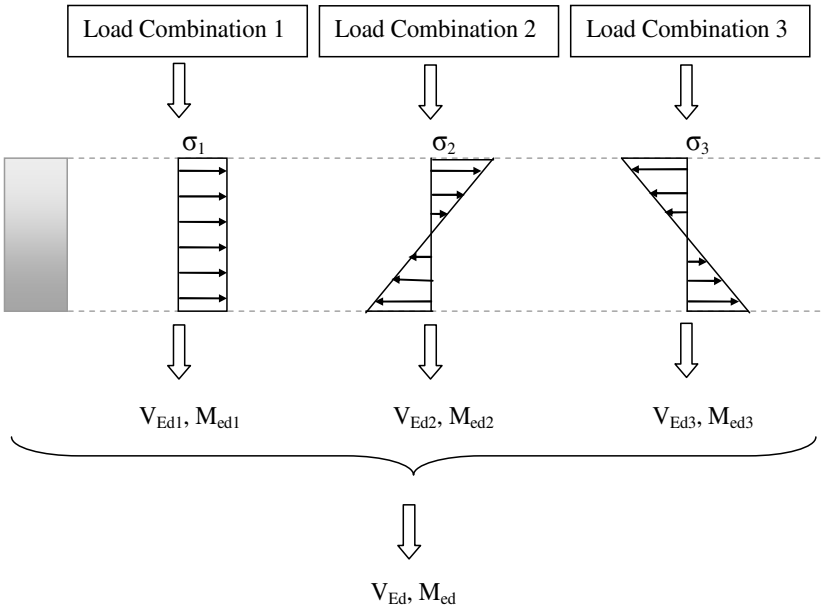

Figure 2.8 Calculation of sectional forces by Free Body Cut.

The first step to generate a Free Body Cut is to select a surface containing the element sides where sectional forces are to be calculated, see Figure 2.9. For the selected surface, a normal vector must be defined to expose one of the sides of the surface. Sectional forces are then calculated at that surface.

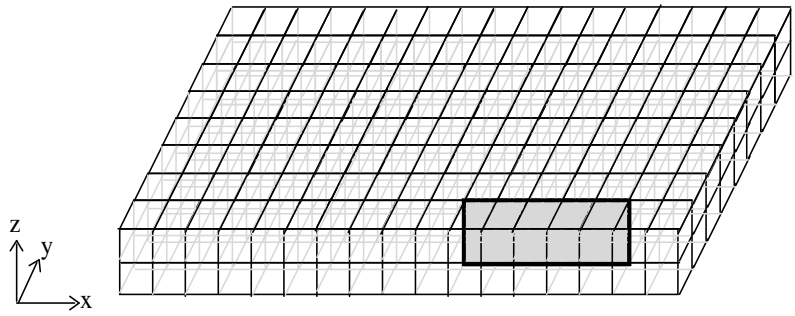

Figure 2.9 A Free Body Cut surface in a continuum.

For the chosen surface, *Free Body Cut* calculates the gravity centre of the surface by the weighted centre of gravity for all element sides in the cut. Thereafter the average normal vectors for all element sides within the surface are summarised to calculate the resultant normal direction. If the normal direction for any individual element within the Free Body Cut surface deviate more than 60 degrees from the chosen normal vector for the surface, these element surfaces will be excluded in the calculations. The choice of element shape is for that reason of importance and a structured mesh is important to not generate an unreliable result. Therefore, irregular and polygonal elements should be avoided.

Sectional forces are calculated in the global coordinate system by integrating the internal nodal forces around the calculated gravity centre. Finally, the sectional forces can be transformed to the local coordinate system of the cut.

If the sectional forces are of interest along a section, a number of Free Body Cut surfaces can be defined along that section, see Figure 2.10. Sectional forces are then calculated for each Free Body Cut surface.

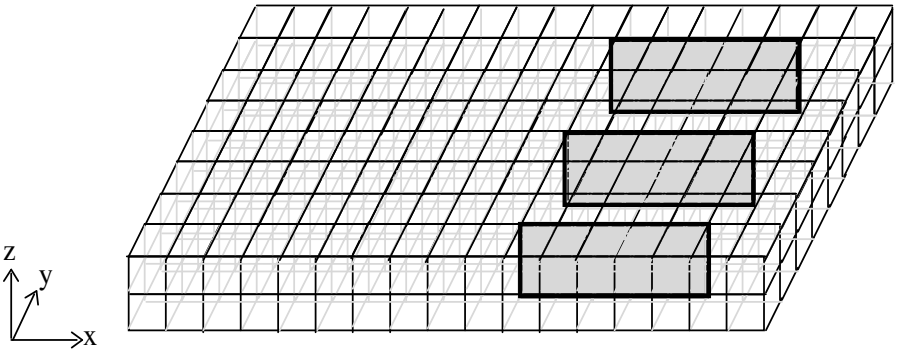

Figure 2.10 Free Body Cut surface defined along a section where sectional forces are of interest.

2.6 Output data in Brigade/Plus

To create output data in Brigade/Plus, to present in the graphs, two different methods can be used. The most common method is to use the feature *path* and the other method is to use *Free Body Cut*.

One difference between the methods is about the workability of the creation of the output data. Paths are created in the mesh after the FE-simulation. Critical sections can then first be obtained by looking at the deformed shape of the FE-model and by looking at contour plots of the results of interest. Free Body Cuts, on other hand, must be created before the FE-simulation, and it is therefore not possible to study the deformed shape or the contour plots to find critical sections.

The two methods also differ in how results are presented. With the feature *path*, the output data is collected at the element nodes. The nodal values are average values, interpolated from the integration points of the elements sharing the same node. An exception of this is when a path is created at sections where the discontinuities of the results exceed the chosen tolerance. At these nodes, two values are given, namely the average value from the element pair from each side of the discontinuity. Figure 2.11 show a mesh where a path is created between node 1 and 8. For a shear force variation, node 3 is given an interpolated nodal value from the integration points in the four elements sharing node 3. Node 6, on other hand, is given two values of the shear force due to a higher discontinuity; one value from the integration points in the elements on the left side of the node and one value from the integration points in the elements on the right side, see the striped contour and the shaded grey contour, respectively, in Figure 2.11.

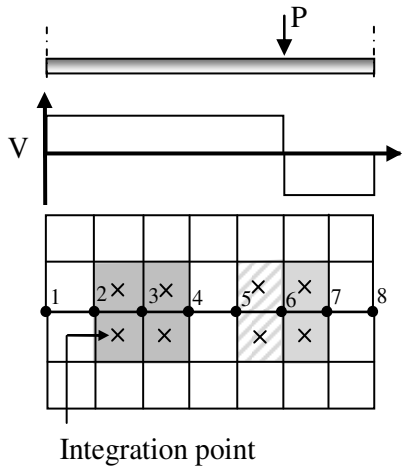

Figure 2.11 Schematic sketch of a path in a mesh, where the sectional forces in the nodes are interpolated from the integration points.

Free Body Cut does not define the shear forces and bending moments as nodal values. As explained in Section 2.5, a normal vector to the Free Body Cut surface has to be defined to expose one of the sides of the surface. Sectional forces are then calculated from the internal nodal forces from the elements of the exposed surface and are then collected in the gravity centre of the surface, see Figure 2.12.

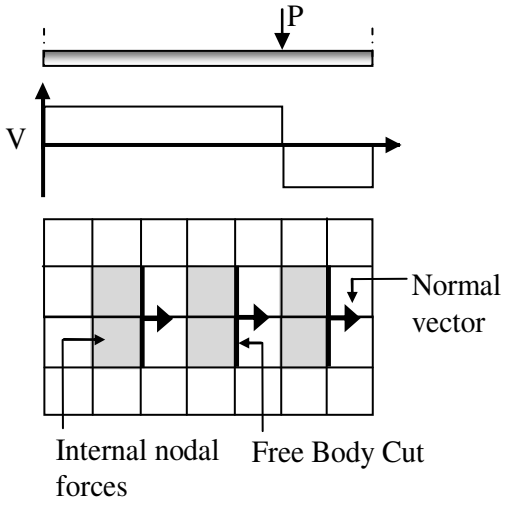

Figure 2.12 Schematic sketch of Free Body Cuts in a mesh, where the sectional forces in the Free Body Cut surfaces are calculated from the internal element forces.

3 Modelling process

Establishing a FE-model that sufficiently well represents the real structural behaviour requires several steps in the process of FE-modelling. Some steps require that the structural engineer does choices of the model and other steps are performed by the software. It is important that the engineer is aware of and understand how the different steps affect the outcome.

In this chapter an introduction of the finite element modelling process will be presented and common errors and pitfalls when establishing a FE-model will be disclosed. The chapter will also present different modelling techniques of the case study bridge and discuss the advantages and disadvantages of these.

3.1 Modelling process

FE-modelling is an iterative process where a FE-model is assigned geometry, structural properties and material properties to describe a physical problem satisfactorily, see Figure 3.1. It is important to decide what degree of accuracy that is needed and adjust the simplifications according to this. How comprehensive a model has to be depends on the parameters sought and the mathematical model can in some cases be simplified where details and complex geometries preferably are omitted. In other cases, a comprehensive mathematical model with a fully three-dimensional formulation with complex effects is needed (Bathe, 1996). By increasing the complexity gradually and verify the results, the risk of implementing errors in the model is minimized. A more complex FE-model describes the real structural behaviour more accurate than a less complex FE-model, but the cost of generating the FE-model will increase.

The modelling process starts by formulating the physical structure that is going to be analysed into a mathematical problem (Liu & Quek, 2003). The structural engineer simplifies the problem and introduces assumptions of the structural complexity so that the structural behaviour is idealised. The force pattern can then be easily understood and calculated (Rombach, 2011). The engineer needs to be aware of that all choices made in FE-modelling affect the governing differential equation and consequently also the structural behaviour of the model.

Liu and Quek (2003) advocate that the general rule of thumb is, that when a structure can be assumed within acceptable tolerances to be simplified into a one-dimensional or two-dimensional structure, this should always be done. The creation of a one-dimensional or two-dimensional FE-model is much easier and efficient.

One step in the selection of structural behaviour of the mathematical model is to assign proper element types to the model. Different parts could be assigned different structural properties depending on which behaviour they should represent. From this, a finite element solution of the mathematical model is made and a governing differential equation is formulated by the software. The solution will be approximate but with an increasing number of equations, i.e. an increasing number of elements, the solution will converge to the correct solution (Liu & Quek, 2003).

In the interpretation of the results, it could be detected if the model needs to be improved or supplemented. If the element types or chosen mesh density do not give reasonable structural behaviour, parameters need to be changed or refinements of the

mesh need to be made until the model represents the physical problem sufficiently well.

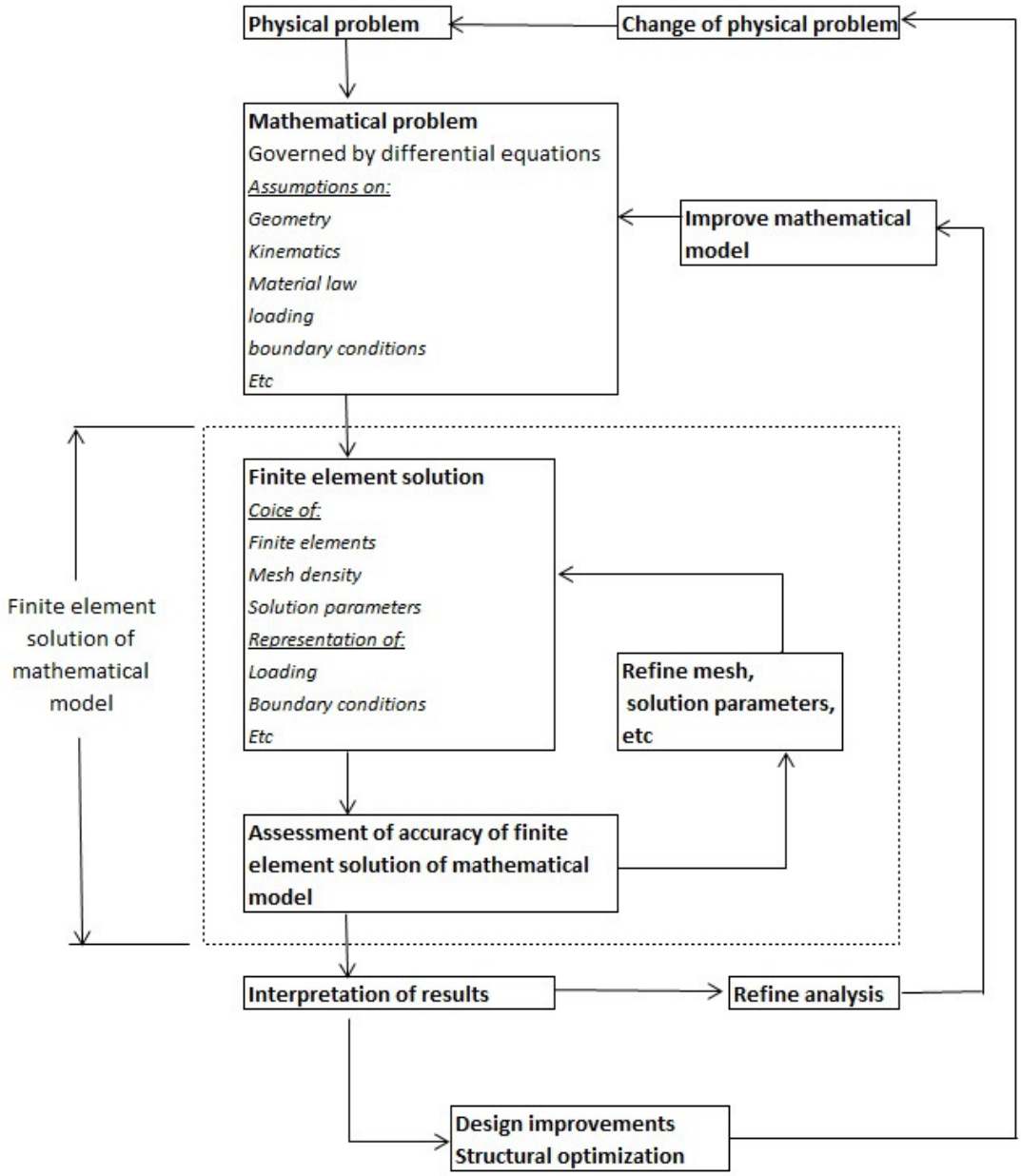

Figure 3.1 The finite element modelling process, adapted from Bathe (1996).

3.2 Misstatements in establishment of a FE-model

Improved computer capacity and lowered hardware cost has led to a development where FE-software have been increasingly used in practical engineering problems. The improved FE-software and more user friendly interfaces have led to that the calculations in the FE-software are often trusted without a critical approach. This has led to a misuse where wrongly established FE-models and associated errors in results have been used in design (Rombach, 2011).

To make use of the software correctly it is important that the user understands the theories that are implemented in the FE-software and have good knowledge about structural behaviour. If there are gaps in the knowledge, it is difficult to establish a reliable FE-model (Blaauwendraad, 2010).

Blaauwendraad (2010) describes a study made in Netherlands where eighteen structural engineers were asked to solve the same structural problem using six different FE-codes. The obtained results showed a substantial difference depending on modelling technique, even if the same FE-software was used. The presented results were so widely spread that it could not be coupled as the results from the same given structural problem. Studies like these illustrate the difficulties of FE-modelling and demonstrate the importance of having good knowledge of the FE-theory.

As mentioned before, everywhere the structural engineer chooses input data, structural theories and mathematical formulations, simplifications and assumptions are introduced to the FE-model. In all choices, possible errors could arise and be implemented into the model (Liu & Quek, 2003). Typical sources of errors in result are from the simplifications made in the mathematical models and choice of element types (Rugarli, 2010). Rugarli (2010) points out that in reality, there are neither any Kirchhoff or Mindlin-Reissner plates, only generic solids.

3.3 Modelling techniques for the case study bridge

The case study bridge to be modelled and analysed in this Master's project is a two girder concrete bridge with an overlaying bridge deck slab. Establishing a FE-model of the structure can be made in several ways using different modelling techniques. Models established differently have their respective advantages and disadvantages and which model that is best suited for the problem depends on the parameters sought in the analysis. For that reason, it is good to consider the results of interest in advance.

The bridge structure can be modelled using only one element type for the whole structure or it can be modelled by subdividing the structure and use different element types for the different structural parts. Figure 3.2 shows some possible alternatives of how to establish the FE-model for the case study bridge.

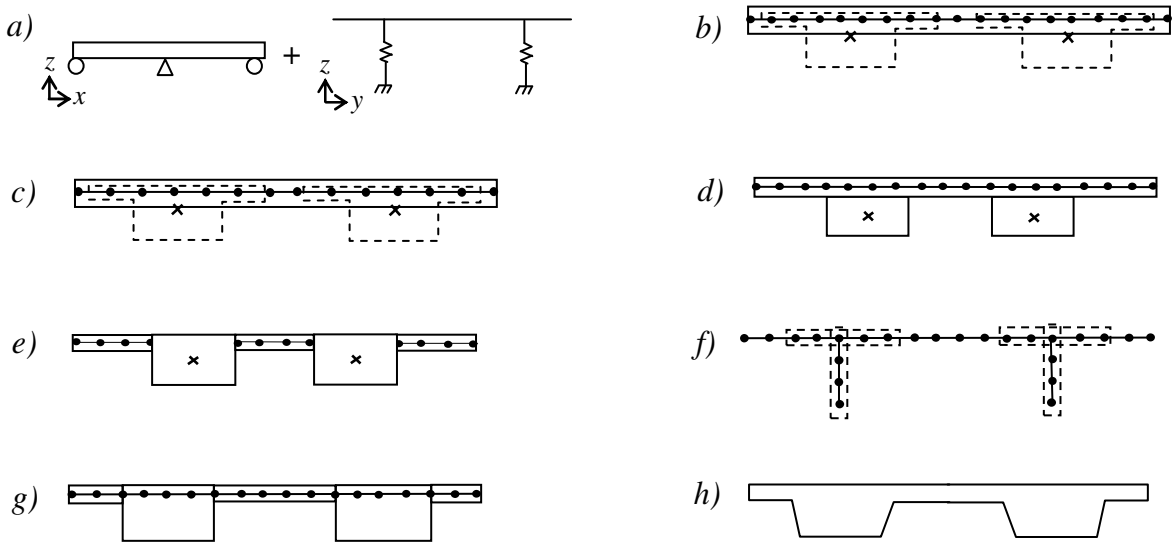

Figure 3.2 *Different possible modelling techniques for structural analysis of the case study bridge; (a) two-dimensional models where the transversal and longitudinal behaviour are studied separately, (b) a beam grillage FE-model, (c) three-dimensional FE-model with orthotropic shell elements overlapping the flange of the beam elements, (d) three-dimensional FE-model with isotropic shell elements above the beam elements, (e) three-dimensional FE-model with isotropic shell elements and beam elements, (f) three-dimensional FE-model with isotropic shell elements for both the bridge deck slab and girders, (g) three-dimensional FE-model with isotropic shell elements for both the bridge deck slab and girders and (h) three-dimensional FE-model with continuum elements for the entire bridge structure.*

The model in Figure 3.2 (a) is the traditional way of analysing a bridge structure in two dimensions, where the transversal and longitudinal effects are studied separately. Initially a transversal model is used where the effects from different traffic load positions in transversal direction of the bridge are studied and lane factors are calculated. The lane factors describe the magnitude of the load acting on the girders and are later used in the load definition of the model that describes the longitudinal structural behaviour.

If a structure shows a clear two-dimensional behaviour with simple load positions and load combinations this model is relatively simple to use. If a clear three-dimensional behaviour may be expected much work is needed to formulate the lane factors for all conceivable load positions.

A disadvantage with this model is that it does not account for the true longitudinal load distribution in the slab. The lane factor includes for a load distribution longitudinally in the slab, but it is assumed by the engineer.

In (b), both the girders and the slab are represented by beam elements. This model is a beam grillage model where the transversal beam elements, that represent the bridge deck slab, are spanning over the longitudinal girders.

The beam grillage model is easy to establish and is good to use if sectional forces longitudinally along the girders and transversally in the slab are of interest. However, the model is conservative and simplifies the load distribution in the bridge deck slab to only transfer load transversally. For that reason it is not possible to use the model when designing the bridge deck slab longitudinally.

In the model in (c), the bridge deck slab is represented by shell elements assigned orthotropic properties without any stiffness in longitudinal direction of the bridge. The orthotropic properties make the model comparable with model (b).

The girders are represented by beam elements with equivalent cross-sectional properties equal to the girders of the analysed bridge structure. The slab is placed within the flange of the girders.

This model separates the load distribution so that the slab transfers the load transversally and the girders longitudinally. In this way of modelling, sectional forces to be used in design longitudinally are obtained for the girders, see Figure 3.3.

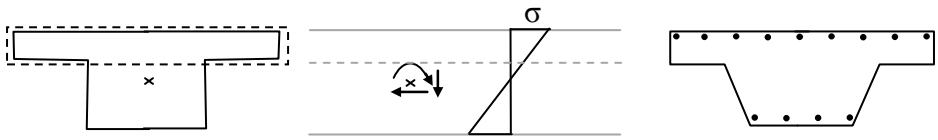

Figure 3.3 *A bridge deck slab modelled with orthotropic shell elements that only have stiffness in transversal direction of the bridge deck slab, and a girder modelled with beam elements with a T-cross-section.*

The model in (d) as well as the model in (e) is established by beam and shell elements. The shell elements are given isotropic properties and therefore the bridge deck slab can be designed, where the longitudinal distribution of load is taken into account. However, there will be difficulties in the interpretation of results since the model consist of two structural parts which transfer loads in longitudinal direction, modelled by two different element types. Both parts will obtain separate resultant sectional forces longitudinally, and if they are used directly in design it will lead to a situation where both the slab and the girders will be given top and bottom reinforcement, see Figure 3.4. In order to get a reasonable reinforcement layout in the bridge cross-section the output data need to be post-processed before it can be used in design. If load combinations are used in design, the post-processing might be very comprehensive and may increase the workload so that it will not be practically possible.

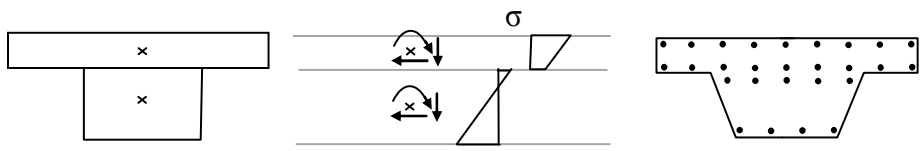

Figure 3.4 *A bridge deck slab modelled with isotropic shell elements and a girder modelled with beam elements with rectangular cross-section. The reinforcement layout shows the disadvantage of modelling with isotropic shell elements.*

In the model in (f) as well as the model in (g) the entire structure is established by shell elements. The difference between the two models is how the girders are represented. In (f) the girders are represented by vertical shell elements with thickness assigned to represent the width of the girders. The horizontal elements over the section of the girders could be stiffened so that no deformations over the girders occur, but it is to be aware of how this affects the structural behaviour. In the model in (g), the depth of the girders is represented by using an offset. The centre of gravity is then placed in the gravity centre of the offset of the shell.

When using these models, where shell elements are used to represent the whole structure, it is important to ensure that the FE-software uses appropriate plate theory. By increasing the plate thickness to represent the girders it may be necessary to evaluate which plate theory that holds true for the structural behaviour. For structures with high and narrow girders, the way of modelling in (f) is more suitable. If the girders are low and wide, model (g) is preferable to use to represent the girders.

In both models, the shell elements are assigned isotropic properties. By this, these models can be used to design the bridge deck slab where the longitudinal load distribution is taken into account. The models can also be used to design the girders longitudinally.

The last model (h) is established entirely of continuum elements where the structural geometry can be created without simplifications. The elements are assigned isotropic material properties and the model can therefore be used to design the bridge deck slab and take the longitudinal load distribution into account. The model can also be used to design the girders longitudinally.

4 The case study bridge

The bridge structure, which was modelled with different modelling techniques, was a two girder concrete bridge with an overlaying bridge deck slab. The structural response of a physical bridge cannot be predicted exactly since all the properties of the real bridge cannot be described in the FE-model. Nevertheless, it is important to define the FE-models to reflect the sought structural behaviour in the best way.

Initially, this chapter describes the structure that was chosen to be analysed with its geometry and material properties. The different loading conditions that were accounted for in the analysis are presented. Thereafter the different FE-models that were established are explained.

4.1 Geometry and material properties

The geometry of the structure was selected with the intention to represent a typical modern Swedish road bridge. The bridge was chosen to be 50 meters long with two equally long spans, see Figure 4.1. The bridge was continuous over the mid support.

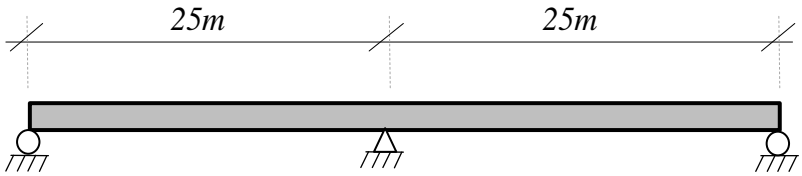

Figure 4.1 Schematic sketch of the bridge structure longitudinally.

To obtain a comprehensive structural system and to limit the risk of implementation of errors in the FE-models, the geometry of the structure was simplified. The bridge was chosen to be straight without curvature or inclination and to be symmetric both in longitudinal and transversal direction of the bridge.

The bridge consisted of two longitudinal girders with an overlaying bridge deck slab and the cross-section was chosen to be constant along the bridge. The slab was given the width of 12 meters and a height of 300 mm with decreasing height over the cantilevering part, see Figure 4.2. The girders were 2.6 meters wide at the bottom, with increasing width over the height of the girders.

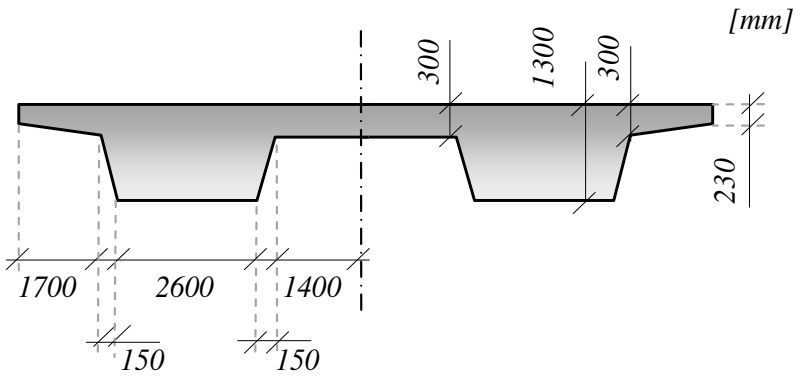

Figure 4.2 Schematic sketch of the cross-section of the bridge structure.

The cross-section was homogeneous and consisted of concrete with linear elastic material response. However, it is good to keep in mind that reinforced concrete is a highly non-linear material in reality, due to cracking of the concrete and yielding of reinforcement.

The Young's modulus of the concrete was chosen to 34 GPa and the shear modulus to 17 GPa. Poisson's ratio was chosen to 0.2.

To simplify the model, the supports, i.e. columns and bearings, were not included in the model. Instead, boundary conditions were applied to prevent translations and rotations significant for columns with bearings and transversal beams between the longitudinal girders.

To be able to examine the load effect globally, when different loads were acting on the bridge deck slab, the whole bridge structure was modelled without the use of symmetry.

4.2 Load conditions

The structural behaviour of the bridge was examined by subjecting the bridge deck slab to two specific load cases of concentrated loads. To study the load distribution longitudinally in the bridge deck slab and to investigate the interaction of the girders, a concentrated load was subjected to one node on the slab between the girders, see Figure 4.3. The loading point was deliberately chosen to be closer to one of the girders.

In the second study, the load was applied on an area of 0.5x0.25 m^2 on the edge of the cantilever, see Figure 4.4. This loading point was chosen to examine if there would be an interaction between the girders. Both loads had a magnitude of 360 kN, which was intended to represent an typical vehicle load for road bridges.

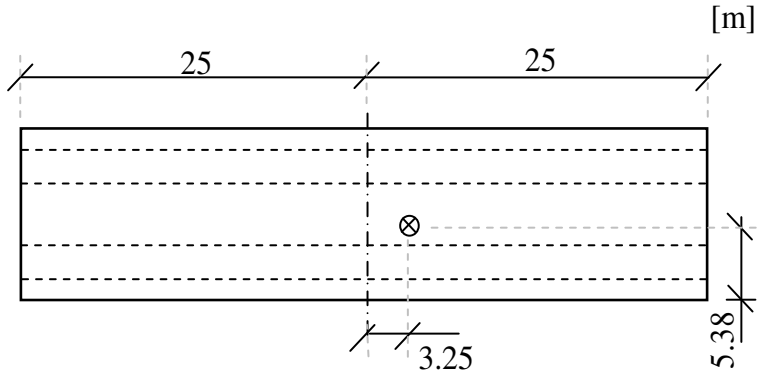

Figure 4.3 Position of the concentrated load applied on the bridge deck slab between the girders.

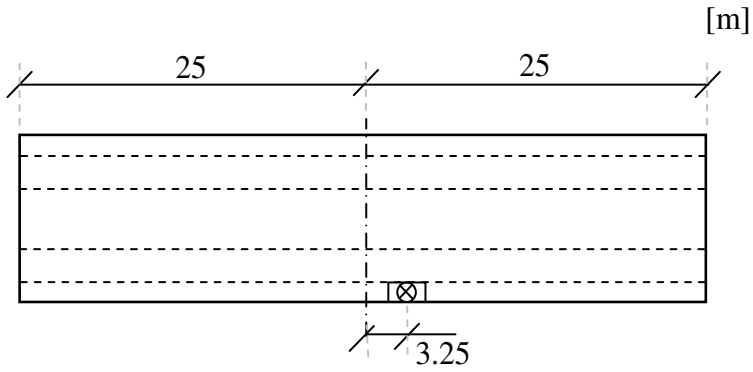

Figure 4.4 Position of the load applied on the edge of the cantilever.

To compare sectional forces to be used in design, traffic loads adopted from Eurocode were also studied. In Brigade/Plus different design codes from Eurocode 1-2 chapter 4.3.2 (CEN, 2003) that takes vehicle loads into account, are implemented and can be used together with the Swedish national parameters defined in TRVFS 2011:12, (Scanscot Technology AB, 2013). With the function of live loads, in Brigade/Plus, it is possible to subject the structure with traffic loads to examine the structural response. From this, sectional forces determined with the different modelling techniques, can be compared.

For the live load function in Brigade/Plus a traffic area needs to be defined where the traffic load can be imposed. The whole bridge deck was chosen as the live load area and longitudinal traffic loading lines were created, see Figure 4.5. The traffic lines represent the centre of the vehicles.

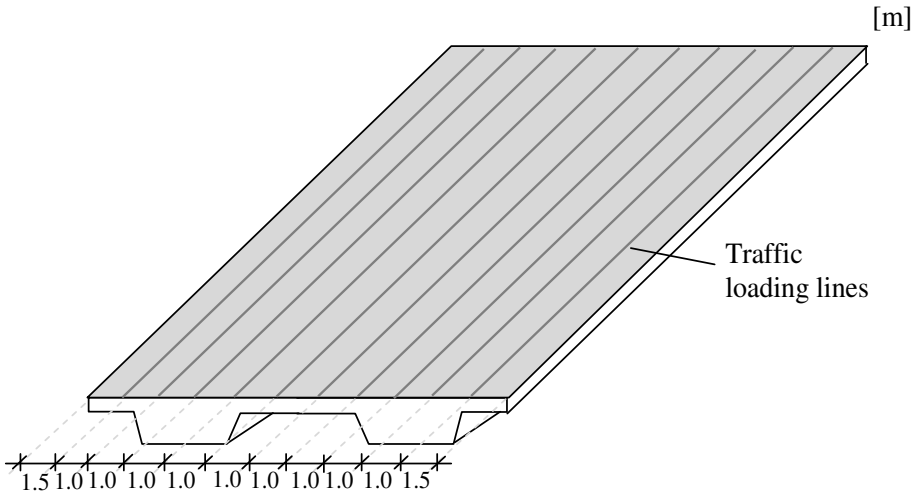

Figure 4.5 The bridge with chosen traffic area (shaded grey area) and traffic loading lines. The spacing between the lines was 1 meter.

The design code defines a traffic lane width to be 3 meters and, consequently, the first traffic loading line shall be created 1.5 meters from the edge of the cantilever (Scanscot Technology AB, 2013). The spacing between the traffic lines was chosen to 1 meter, see Figure 4.5. Brigade/Plus automatically controls the load positions in order to avoid overlapping of vehicles.

Choosing a step length for the traffic loading lines defines the distance for the vehicles to move between each calculation. A smaller step gives more possible load

positions longitudinally for the traffic but does also influence the computational time. In this Master's project it was chosen to have a step length of 1.2 meters, which also is defined as the distance between two wheel axles.

Eurocode defines four different load models, LM1-4, which contains different types of vehicles. In addition to these, the Swedish transport Administration defines national load models and all of these are possible to import in Brigade/Plus. In this Master's project only LM1 was imported in the FE-analyses. LM1 often governs the design values and gives comprehensive and adequate results where design values for traffic loads can be compared. This load model consists of lane surface loads with, general moving surface load and vehicle loads according to Figure 4.6.

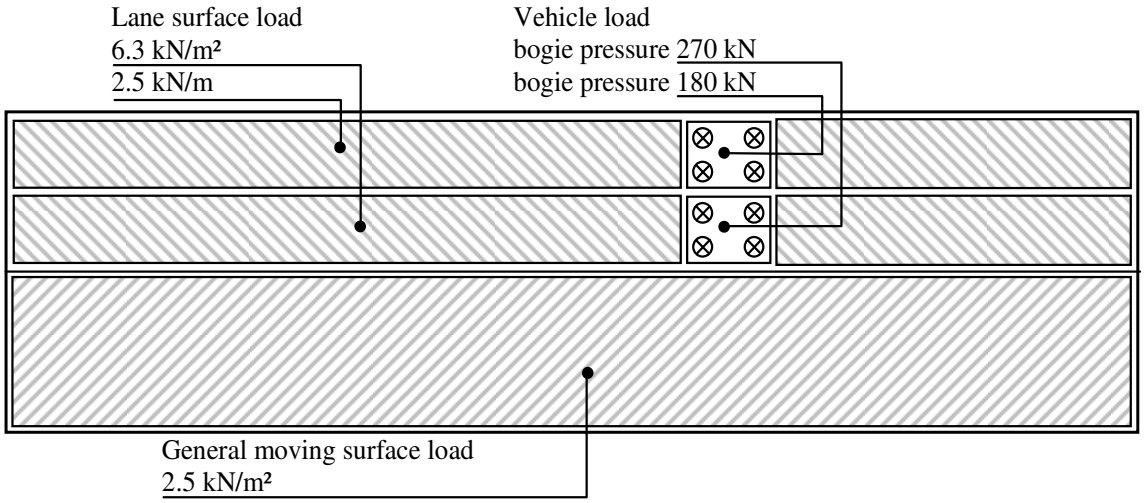

Figure 4.6 Example of one load combination of load model 1 acting on the bridge.

4.3 Bridge model 1 – Beam/Shell model

Bridge model 1 was established by structural elements, where beam elements were used to represent the girders and orthotropic shell elements without any stiffness in longitudinal direction of the bridge were used to represent the bridge deck slab, see Figure 4.7. The advantages and disadvantages with this model were explained in Section 3.3 with corresponding Figure 3.2 (c). This model was chosen in this Master's project in order to represent a FE-model established by structural elements with simplified load distribution. The model is similar to the beam grillage model, see Figure 3.2 (b), but the bridge deck slab is easier to model with a shell compared to transversal beams.

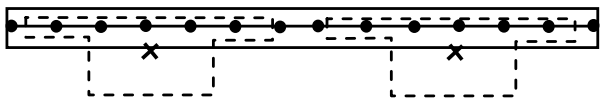

Figure 4.7 Three-dimensional model with orthotropic shell elements overlapping the flange of the beam elements.

As mentioned in Section 2.3.1, Euler-Bernoulli beam theory is implemented in the beam elements available in Brigade/Plus. Since the girders were slender in the chosen bridge structure, beam elements could advantageously be used in the FE-model.

The bridge deck slab was dominated by its in-plane dimensions and was subjected with load normal to its plane. Therefore, shell elements were a good approximation in the FE-model and represented the transversal distribution of load sufficiently well. Depending on the thickness of the slab, in relation to its length and width, Brigade/Plus uses the favourable plate theory, see Section 2.3.2.

In Brigade/Plus it is possible to choose among different standard cross-sectional shapes for the beam elements and the cross-sectional properties will be represented as properties of the element in the gravity centre of the cross-section. The girder cross-section of the case study bridge had varying width over the girders which meant that none of the predefined cross-sections in Brigade/Plus matched perfectly. In order to assign the cross-sectional properties of the girders to the beam elements in a correct way, an equivalent T-cross-section was used, see Figure 4.9 (a). The properties of the equivalent cross-section that were chosen to fit the cross-sectional properties of the case study bridge, were the gravity centre in vertical direction and the moment of inertia for bending longitudinally. In addition, the cross-sectional height was kept. The beam elements were placed in the gravity centre of the girders.

The overlaying slab was modelled with a shell having the same geometry as the bridge deck slab of the case study bridge, see Figure 4.9 (b). In Brigade/Plus the orthotropic elasticity properties were defined in a stiffness matrix, see Figure 4.8. The intention with the FE-model was to separate the longitudinal and transversal distribution of load for the different structural parts. Therefore, the stiffness parameters which account for the stiffness in transversal direction of the bridge were assigned to the stiffness matrix only. Due to no contraction or elongation of the slab, perpendicular to the load, Poisson's ratio was set to zero.

$$\begin{vmatrix} E_{1(1-\nu_{23}\nu_{32})}\Upsilon & E_{1(\nu_{21}+\nu_{31}\nu_{23})}\Upsilon = E_{2(\nu_{12}+\nu_{32}\nu_{13})}\Upsilon & E_{1(\nu_{31}+\nu_{21}\nu_{32})}\Upsilon = E_{3(\nu_{13}+\nu_{12}\nu_{23})}\Upsilon & 0 & 0 & 0 \\ 0 & E_{2(1-\nu_{13}\nu_{31})}\Upsilon & E_{2(\nu_{32}+\nu_{12}\nu_{31})}\Upsilon = E_{3(\nu_{23}+\nu_{21}\nu_{13})}\Upsilon & 0 & 0 & 0 \\ 0 & 0 & E_{3(1-\nu_{12}\nu_{21})}\Upsilon & 0 & 0 & 0 \\ 0 & 0 & 0 & G_{12} & 0 & 0 \\ 0 & 0 & 0 & 0 & G_{13} & 0 \\ 0 & 0 & 0 & 0 & 0 & G_{23} \end{vmatrix}$$

where, $\Upsilon = \frac{1}{1-\nu_{12}\nu_{21}-\nu_{23}\nu_{32}-\nu_{31}\nu_{13}-2\nu_{21}\nu_{32}\nu_{13}}$

Figure 4.8 Stiffness matrix defining the orthotropic material properties in Brigade/Plus, adapted from (Simulia, 2009).

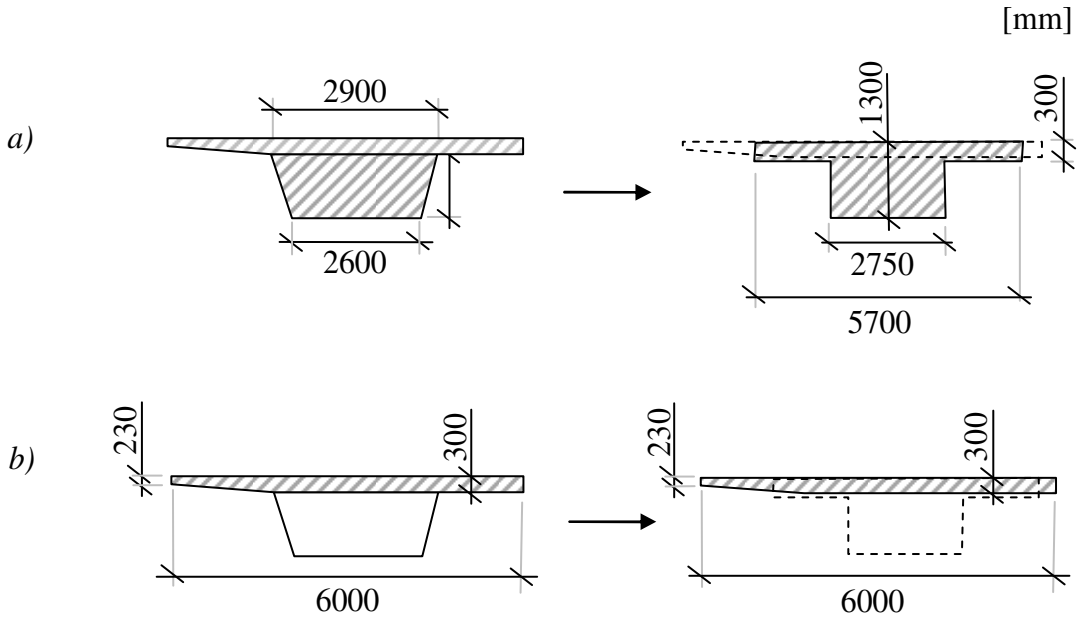

Figure 4.9 *Beam elements with equivalent T-cross-section and a slab of shell elements overlapping the flange of the girders; (a) the moment of inertia for bending longitudinally of the case study bridge was represented by beam elements and (b) the stiffness in the transversal direction of the bridge deck slab for the case study bridge was represented by the shell elements assigned transversal stiffness only.*

To represent the real structural behaviour, the beam elements were coupled with stiff tie constraints to the nodes in the shell that were located above the girders, see Figure 4.10. The beam elements were chosen as the master surface and the surface was chosen as node-based. Consequently the node-to-node formulation was used, see Section 2.4. The position tolerance of the tied region was chosen so that the width of the shell that was constrained was 2.6 meters. The width of the girders was relatively big compared to the length of the span and therefore the constrained width does have significant influence of the load effect. In order to understand the effect of the tie constraints an additional investigation was made, see Appendix A.

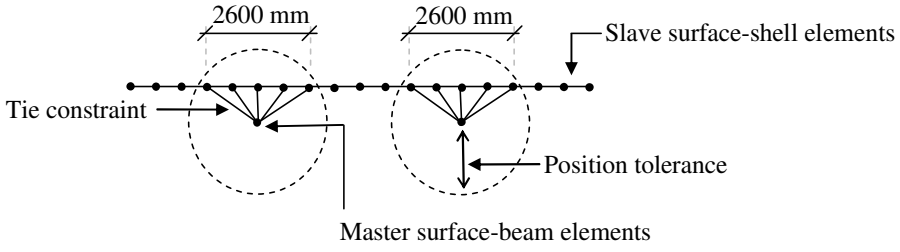

Figure 4.10 *Stiff couplings between the beam elements and shell elements by tie constraints. A width of 2600 mm in the shell was constrained.*

When choosing boundary conditions it is important to consider which structural behaviour the model should represent. The boundary conditions were applied to single nodes of the beam elements. This was a good way of representing the boundary

conditions since the area supported by the bearings was relatively small compared to the length of the span. The rotation about the longitudinal axis and translation in vertical direction were constrained at all nodes that represented the supports. In addition to this, translations in the longitudinal and transversal direction were prevented at the mid supports, see Figure 4.11.

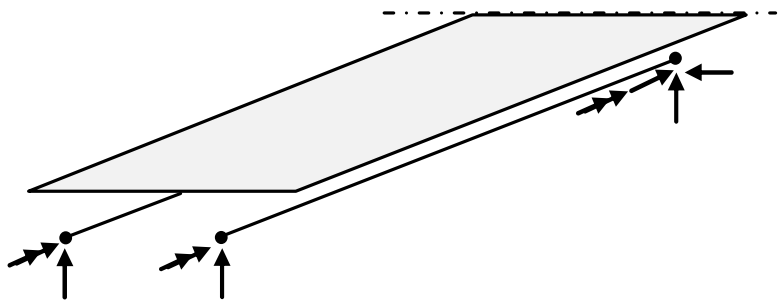

Figure 4.11 Boundary conditions in model 1.

The element type that was used to represent the girders was a three dimensional first order beam element. In each element there was one integration point and the size of the mesh was chosen 0.5 meter. For the bridge deck slab, a first order shell element with reduced integration was used. In each shell element there was one integration point in the centre of the element. The shape of the shell was quadratic and the element sides were 0.0625 meter.

The model was verified and a convergence study was made to confirm that the FE-model showed the expected structural behaviour, see Appendix A.

4.4 Bridge model 2 – Shell model

Bridge model 2 was established by isotropic shell elements, see Figure 4.12. The advantages and disadvantages with the model were explained in Section 3.3 with corresponding Figure 3.2 (g). This model was chosen to represent one of the three FE-models to be compared in this Mater's project since the model is established by structural elements where both the longitudinal and transversal load distribution in the bridge deck slab is taken into account.

As explained in Section 4.3 the bridge deck slab can advantageously be modelled by shell elements since shell elements represent the structural behaviour of the slab in a good way. The shell elements, in model 2, were chosen to have a rectangular shape and the mesh was regular.

A certain width of the shell in the region of the girders was given a thickness by offset of the shell elements. The height of the girders in the model was the same as in the case study bridge; hence the width was adjusted to simulate an equivalent stiffness of the girders for bending longitudinally. As mentioned in Section 3.3 it is important to be aware of that the plate theory implemented in the FE-software holds true for both the shell elements that represent the bridge deck slab and the girders. In Brigade/Plus the thickness is taken into account so that the analysis is carried out by the correct plate theory (Simulia, 2009).

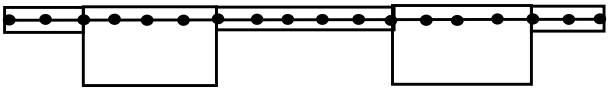

Figure 4.12 Three-dimensional model with isotropic shell elements for both the bridge deck slab and the girders

The boundary conditions were applied in the position of the bearings along one edge of the elements in transversal direction of the girders. Similar to the boundary conditions in model 1 the supported length of the bearings was relatively small compared to the length of the longitudinal span. For that reason it could be seen as a good approximation to only constrain one edge intead of a bigger area. The boundary conditions were chosen to prevent translation in vertical and transversal direction of the bridge at all supports. At the mid support the translation in the longitudinal direction of the bridge was prevented as well, see Figure 4.13.

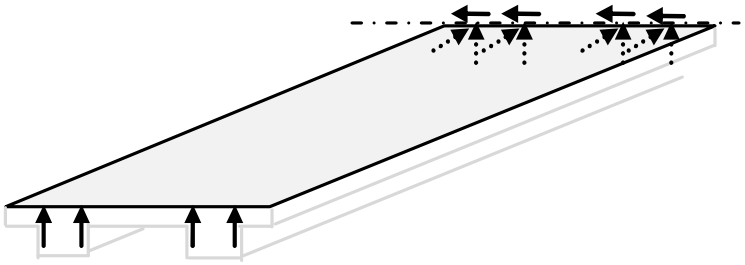

Figure 4.13 Boundary conditions in model 2.

The element type that was used to represent the girders as well as the bridge deck slab was a first order shell element with reduced integration. In each element there was one integration point in the centre of the element. The shape of the shell was quadratic and the size of the mesh was 0.125 meter.

To verify the model for the bridge deck slab, the same verification and convergence study as for model 1 was used, see Appendix A. For the girders, to verify that the plate theory implemented in the model gives good results, a complemented study was made, see Appendix B.

4.5 Bridge model 3 – Continuum model

Bridge model 3 was established by continuum elements, see Figure 4.14. The model was shortly explained in Section 3.3 with corresponding Figure 3.2 (h). The shape of the structure could be modelled in its entirety since simplifications regarding geometry, which was needed when structural elements were used, were not necessary when continuum elements were used. The model was chosen as one of the three FE-models to be compared in this Master's project because continuum elements are based on continuum mechanics and represents a fully three-dimensional structural behaviour.

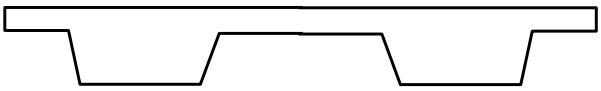

Figure 4.14 Three-dimensional model with continuum elements for the entire bridge structure.

Continuum elements represent a volume and hence the mesh was needed to be adjusted in three directions. Avoiding distortion was especially important when continuum elements were used since *Free Body Cut* was needed in order to get sectional forces, see Section 2.5. In the Free Body Cut surfaces, created to get the variation of the sectional forces transversally in the plate, it was important to include a sufficient number of elements in the surfaces. Otherwise, depending on the loading situation, the results could become mesh dependent.

In the element library in Brigade/Plus there are many available types of continuum element and it can be difficult to choose the most suitable one for the particular application. The Abaqus Analysis User's Manual (Simulia, 2009) gives recommendations of when different element shapes and mathematical models should be used or avoided. Following the recommendations from the Abaqus Analysis User's manual, the shape of the elements was chosen to be hexahedral. Hexahedral elements give the best result for the minimum computational cost when the geometry of the structure is simple and complex details are excluded.

For bending induced linear problems, second order elements with reduced integration should be used instead of first order elements (Simulia, 2009). However, when this Master's project was conducted it was not possible to use second order elements in a *Free Body Cut* calculation and instead incompatible mode elements were used. Incompatible mode elements are a type of first order elements using first order integration. In addition to the ordinary displacement degrees of freedom internal incompatible degrees of freedom are added, hence the elements are good to use in problems dominated by bending. Incompatible mode elements are more expensive to use in terms of computational cost compared to first order elements but less expensive than second order elements. For a convergence study of different types of continuum elements see Appendix C.

As in model 2 the boundary conditions in model 3 was assigned at the position of the bearings along one edge of the elements in transversal direction of the girders. The same translations was prevented as in model 2, see Figure 4.15.

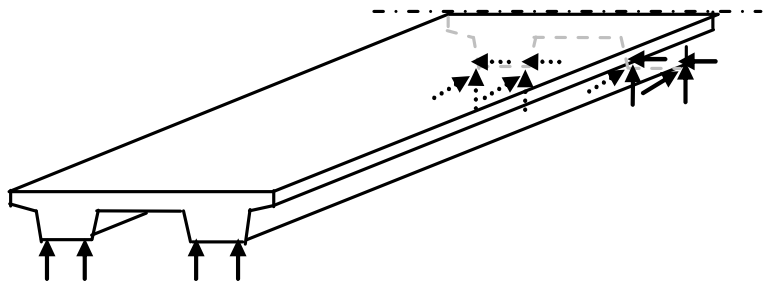

Figure 4.15 Boundary conditions in model 3.

The element type that was used to represent the girders as well as the bridge deck slab was a three-dimensional continuum element type with incompatible modes, which

uses linear integration. In this type of continuum elements there is eight integration points in each element. The shape of the element was hexahedral with equal element sides of 0.125 meter.

For model 3 a convergence study and verification of the results was made to confirm the reliability of the FE-model, see Appendix C.

5 Results and interpretation of results

The bridge deck slab was subjected to two specific load cases, one consisting of a concentrated load and one of a distributed load on a small area, see Section 4.2. In the first load case, the concentrated load was applied on a node between the girders, slightly offset from the symmetry line in both longitudinal and transversal direction. In the second case, the same magnitude of load was applied at the edge of the cantilever at the same distance from the mid support as in the first load case. In addition to these specific load cases, moving vehicle loads were subjected to the bridge deck slab.

In the examination of the structural response for the two specific load cases, shear forces and bending moments in the transversal direction of the bridge deck slab and along the girders were of interest. The main purpose was to compare the load distribution longitudinally in the slab and to investigate the structural response and interaction between the girders. To do a comprehensive examination, both transversal and longitudinal sections were studied in the bridge deck slab. The transversal sections were intended to show the transversal variation of sectional forces and the longitudinal sections were intended to show the longitudinal distribution of the transversal shear forces and bending moments. In addition to these sections, the variation of shear forces and bending moments in the longitudinal direction of the bridge were studied along each girder. The load effect from moving vehicle loads was also studied along the girders.

The same notation of the coordinate system was used throughout the analysis, where the right hand orientation was used and the x-axis was defined along the bridge. The bending moment in the slab and along the girders was about the x-axis and y-axis respectively. All graphs that show shear forces and bending moments along the transversal sections in the slab were defined in positive y-direction. The graphs that show the sectional forces along the longitudinal sections in the slab were created in positive x-direction. Also the graphs that present the total load effect along the girders were created in positive x-direction.

When output data was created to examine sectional forces in the slab, the feature *path* was used for both transversal and longitudinal sections in model 1. In model 2, *path* was used for longitudinal sections and *Free Body Cut* for transversal sections. Model 3 required that *Free Body Cut* was used to create output data, both for transversal and longitudinal sections.

When the transversal sections were created by *Free Body Cut* in model 2 and 3, a Free Body Cut surface was created over a width of 0.5 meter. The surface was then swept in transversal direction to examine the averaged variation of sectional forces in the slab over 0.5 meter. In this Master's project, the distribution width was chosen without adopting the requirements of distribution of loads in TRVR Bro 11 (2011). It should be noted that sectional forces obtained in the results only are valid over the width where the Free Body Cut surfaces are created.

The output data in intersections of the longitudinal and transversal sections can in model 1 be compared because the same feature in Brigade/Plus was used to create output data along all sections. However, in model 2 and 3 the output data in the intersections of the longitudinal and transversal sections cannot directly be compared. This depends on that different features were used to create output data in the different sections in model 2, and that Free Body Cut surfaces were created over different widths in the longitudinal and transversal sections in model 3.

When examine sectional forces along the girders, the feature *path* was used along the beam elements in model 1. In model 2 and 3, Free Body Cut surfaces were created over half of the cross-section of the bridge along the girders. The total load effect along the girders was thereby presented for all three FE-models and the results could directly be compared.

In the diagrams showing the transversal variation of shear force and bending moment in the bridge deck slab, a schematic figure of the position of the load application and the supports are shown above the graphs. Because the FE-models were established differently, the length of the span between the girders became unequally long. For that reason, the vertical lines representing the position of the girders are not in the same position transversally in the slab for the different FE-models.

5.1 Load case 1 - Concentrated Load between the girders

To examine the load effect for the load case of a concentrated load applied between the girders, several sections were studied, see Figure 5.1. The transversal section in the bridge deck slab, going through the loading point, was studied to show the variation of shear force and bending moment between the two girders. To study the longitudinal distribution of the transversal sectional forces, three sections in the bridge deck slab were studied. One longitudinal section was going through the loading point and the other two were on each side of the loading point, closer to the girders. Also, sectional forces along the girders were studied to examine the load effect and interaction between the girders.

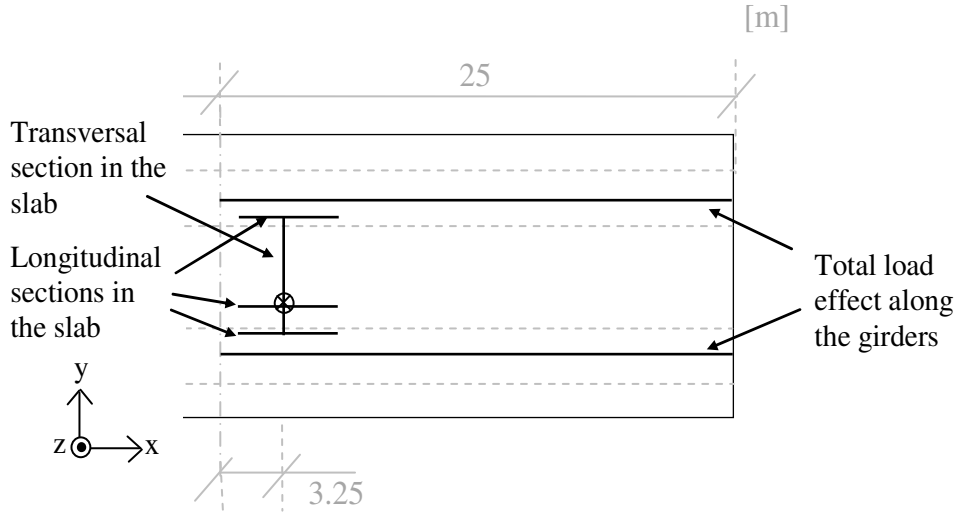

Figure 5.1 Sections in the bridge deck slab where the variation and distribution of shear forces and bending moments were studied. Also the total load effect on the girders was studied. A concentrated load of 360 kN was applied on the slab between the girders.

5.1.1 Variation and distribution of shear force in the slab

In Figure 5.3 and Figure 5.4, the transversal shear force in the slab is shown for model 1, 2 and 3, respectively. The results in model 1 differed from the results in model 2

and 3 to that extent that they were not comparable to be presented in the same graphs and for that reason the results in model 1 are presented separately.

In model 1, see Figure 5.3 (a), the variation of shear force transversally in the bridge deck slab was almost constant between the applied load and the girders. This was due to that the bridge deck slab in model 1 was assigned stiffness in transversal direction of the bridge only. At the point where the load was applied, the shear force changed sign from a magnitude of approximately 1100 kN/m to -2800 kN/m.

The total shear force at the point where the load was applied was much greater than the applied load of 360 kN. This depends on that the magnitude of the shear force in the elements adjacent to the point where the load was applied will go to infinity when the mesh density increases. In model 1, a path was created along the transversal section and the impact of the element size was significant. Because the load was transferred transversally in the bridge deck slab only, the size of the mesh was influencing the sectional forces along the entire section where *path* was used. The total load was transferred over the width of approximately two elements.

The longitudinal distribution of the shear force showed that the applied load affected the bridge deck slab on a width of ten elements. At the section where the load was applied a peak value of the shear force was seen, see Figure 5.3 (b) and (c). It should be noted that the shear force changed sign more than once in the longitudinal direction. This may depend on that there were difficulties to describe the structural behaviour of the slab when the shell elements were assigned stiffness in transversal direction of the bridge only. The reason that a longitudinal shear force distribution occur in the bridge deck slab may depend on torsion and deflection of the girders, which affect the slab. Also the deformed shape of model 1 was such that it was clear that the structural behaviour of the slab could not be described correctly. Figure 5.2 shows the deflection of the bridge deck slab along the longitudinal section that was going through the loading point. It was seen that the deflection of the bridge deck slab was not continuous in the studied section. However, the integration and summation of the shear force along the two longitudinal sections in Figure 5.3 (b) and (c), that were presenting the shear force distribution in the slab, gave a resulting force of 360 kN which was equal to the applied load.

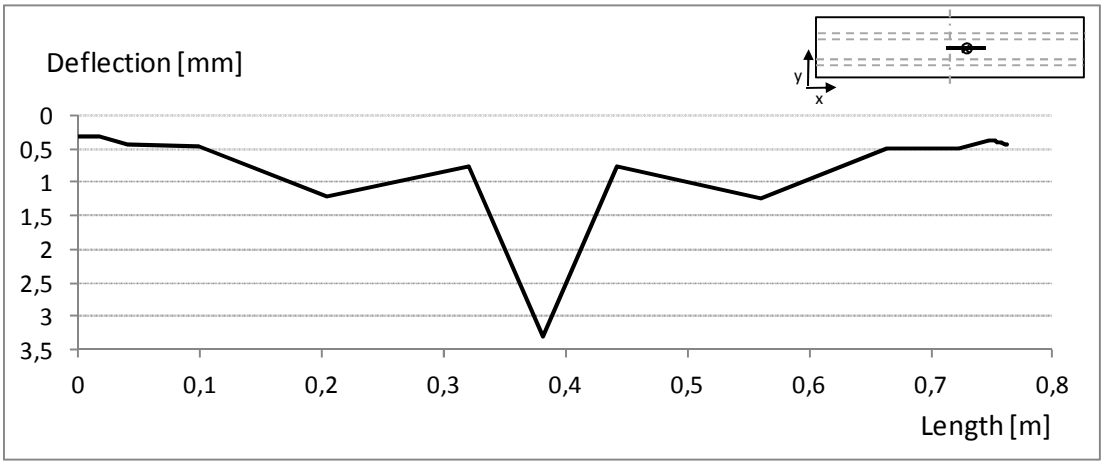

Figure 5.2 Deflection along a longitudinal section in model 1, when the bridge deck slab was subjected to a concentrated load of 360 kN.

The variation of shear force in the transversal sections, in model 2 and 3, was not constant between the girders and the section where the load was applied, see Figure 5.4 (a). Instead, the shear force decreased towards the girders. This was due to that the bridge deck slab was assigned isotropic material properties in model 2 and that model 3 was established by continuum elements. The sectional forces were therefore distributed in longitudinal direction of the bridge deck slab. However, the most pronounced change of the shear force, transversally in the slab, was found at the section where the load was applied. The impact of the size of the mesh, which was seen in model 1, decreased substantially when Free Body Cut surfaces were created over 0.5 meter. The output data from *Free Body Cut* was then calculated as average values of the shear forces in each element in the Free Body Cut surface. The output data from *Free Body Cut* is valid at the width were the Free Body Cut surfaces were created only. The maximum positive and negative shear force was approximately 280 kN/m and -340 kN/m, respectively, for both model 2 and 3. The positive and negative shear force closer to the girders in model 2 and 3 was about 50 kN/m and -150 kN/m, respectively.

Furthermore, the reaction force at the girders and under the load were not as distinguished in model 2 and 3 as in model 1. This was a consequence of how *path* and *Free Body Cut* presented the output data, see Section 2.6. With infinitesimally elements in model 2 and 3, the reaction force would become more distinguished.

Looking at Figure 5.4 (b) and (c) it was seen that the transversal shear force was distributed longitudinally in the bridge deck slab, for both model 2 and 3. The highest magnitude of the shear force was at the section where the load was applied but there were not a distinguished peak value, as in the graph from model 1. The integration and summation of the shear force in the longitudinal sections gave a resulting shear force of 360 kN.

In model 2 and 3, no singularities of the shear forces were seen in the graphs that were presenting the distribution of load. This was because the bridge deck slab could distribute load both transversally and longitudinally in the bridge deck slab. Therefore, in a longitudinal section further away from the loading point the transversal sectional forces, given by *path* and by *Free Body Cut*, were equal in model 2 and 3.

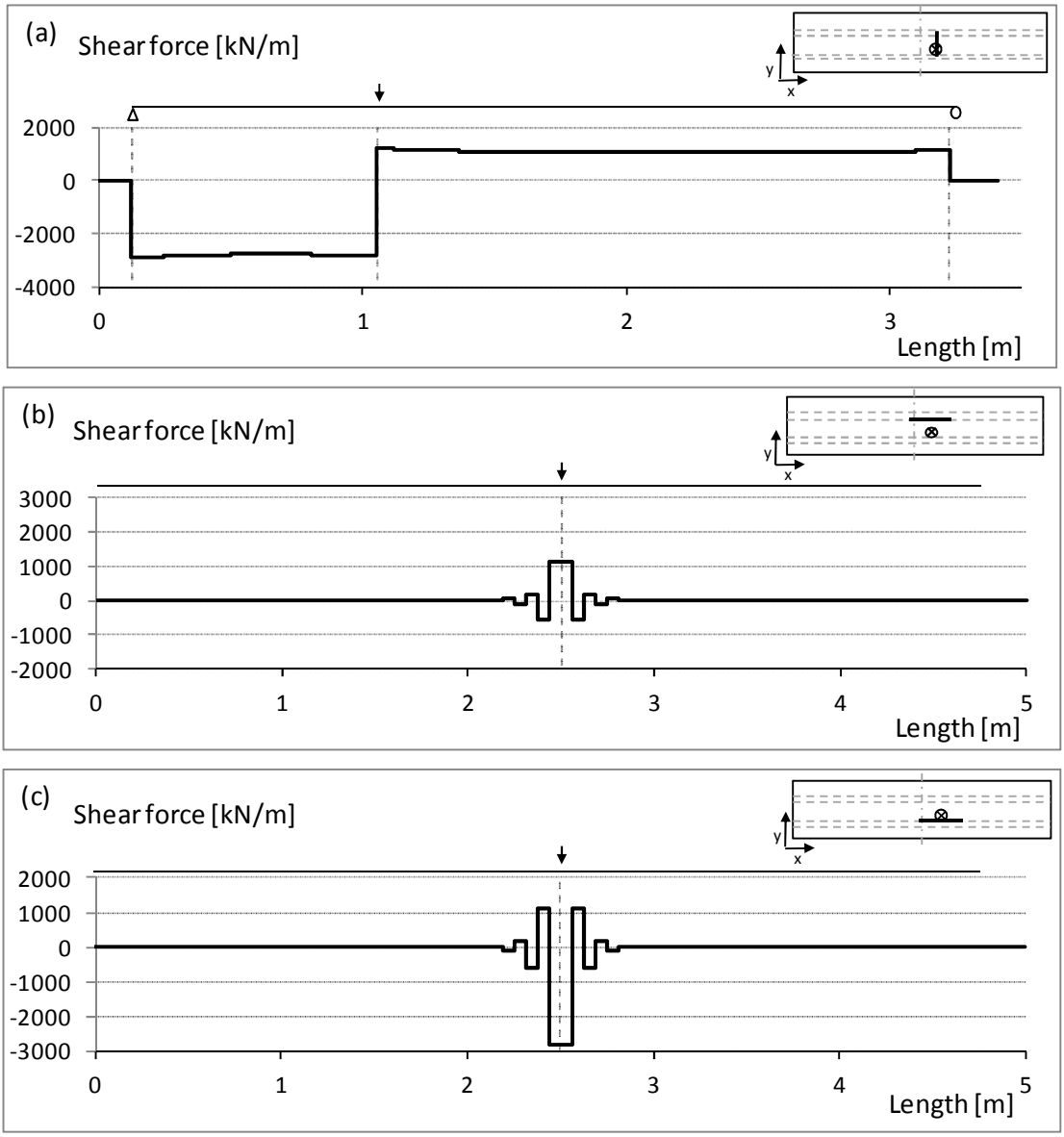

Figure 5.3 Variation and distribution of transversal shear force in model 1, when a concentrated load of 360 kN was applied to the bridge; (a) transversal section between the girders going through the point where the load was applied, (b) longitudinal section close to the girder where the transversal shear force was positive and (c) longitudinal section close to the girder where the transversal shear force was negative.

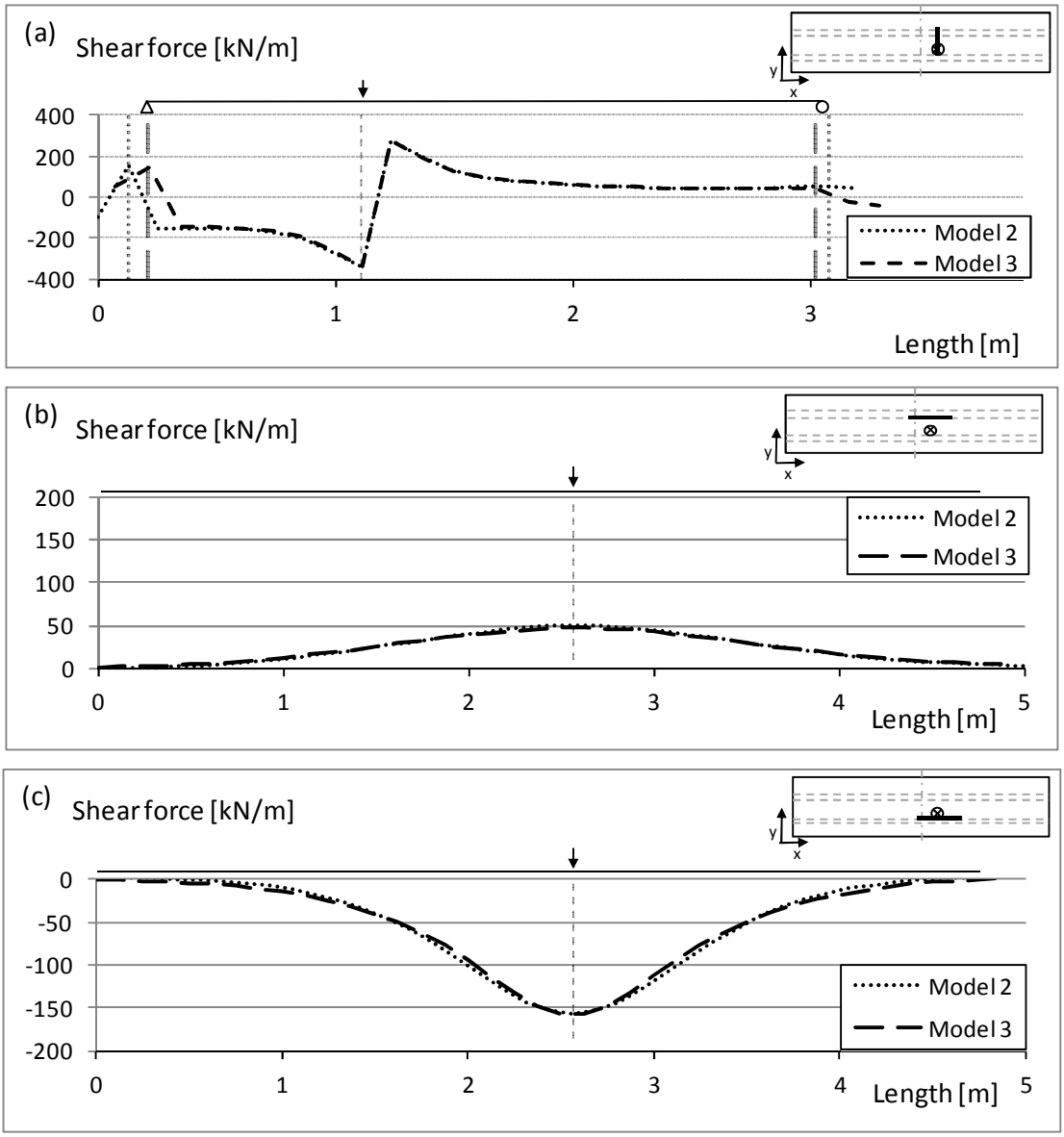

Figure 5.4 *Variation and distribution of transversal shear force in model 2 and 3, when a concentrated load of 360 kN was applied to the bridge; (a) transversal section between the girders going through the point where the load was applied, (b) longitudinal section close to the girder where the transversal shear force was positive and (c) longitudinal section close to the girder where the transversal shear force was negative.*

As mentioned earlier, results in the intersections of the transversal and longitudinal sections cannot directly be compared in model 2 and 3. To be able to compare the output data from the longitudinal sections with the transversal section in model 2 and 3, see Figure 5.4, the longitudinal sections need to be integrated over the same width as the width of the Free Body Cut surfaces in the transversal sections, and calculating an average value of the force. Figure 5.5 show a principal sketch of how this was done for the graph in Figure 5.4 (c). The mean value of the shear force between point a and b in Figure 5.5 then become equal to the shear force in the same point in the transversal section, close to the girder that was closest to the applied load, see Figure 5.4 (a).

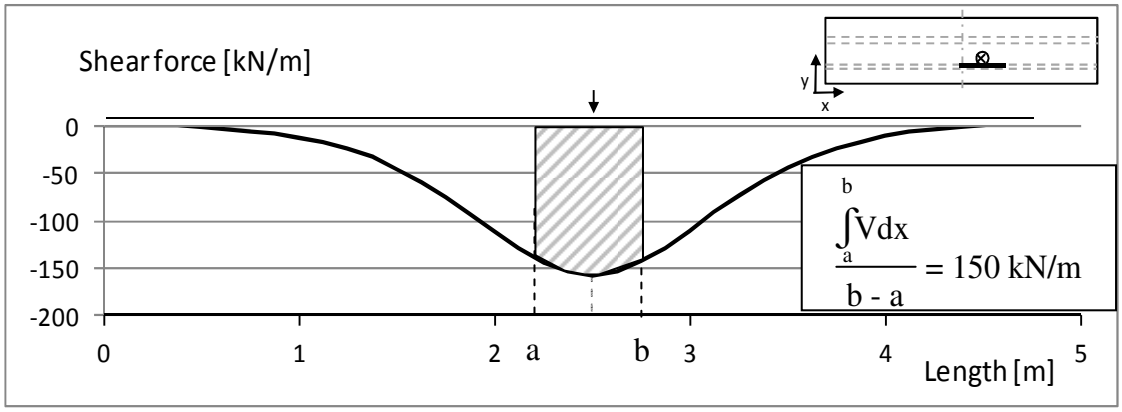

Figure 5.5 Schematic sketch of how the shear forces in the transversal sections were obtained by integrating the graphs of the longitudinal sections.

5.1.2 Variation and distribution of bending moment in the slab

When examined the bending moment from the transversal sections in model 1, it was seen that the concentrated load gave rise to an almost linear moment variation between the girders, see Figure 5.6 (a). The maximum field moment was about 500 kNm/m and the support moments were around 700 kNm/m and 320 kNm/m.

The longitudinal distribution of the bending moment in the sections where the load was applied and where the maximum support moments were found is presented in Figure 5.6 (b), (c), and (d). It could be noted that the bending moment was distributed over a small width and showed distinguished peak values at the section where the load was applied, in the same way as the graphs that show the shear force in model 1.

In model 2 and 3, the variation of the bending moment along the transversal section was close to linear, except close to the load, with a maximum field moment of 100 kN/m for both FE-models, see Figure 5.7 (a). The increased stiffness due to the change of cross-sectional height at the girders gave rise to support moments of about 65 kNm/m and 45 kNm/m in model 2 and support moments of about 50 kNm/m and 35 kNm/m in model 3, at the girder closest to the loading point and the girder farthest from the loading point, respectively. The reason that the support moments in model 2 and 3 were not equal depended on that the theoretical length of the span between the girders was not the same in the FE-models due to different ways of representing the girders.

The distribution of the bending moment in the bridge deck slab was studied close to the girders and in the section where the load was applied. It could be noted that the bending moment was distributed over a certain width for both model 2 and 3, see Figure 5.7 (b) and (d). The maximum bending moment appeared at the section where the load was applied and decreased symmetrically in the longitudinal direction. In the section that was going through the loading point, also a smooth curve of the bending moment could be seen in model 2 but in model 3 a peak appeared over a small width at the loading point, see Figure 5.7 (c).

To verify the support conditions for the slab when the girders act as supports the moment distribution in the slab for the different FE-models was compared to analytical two-dimensional models, see Appendix D.

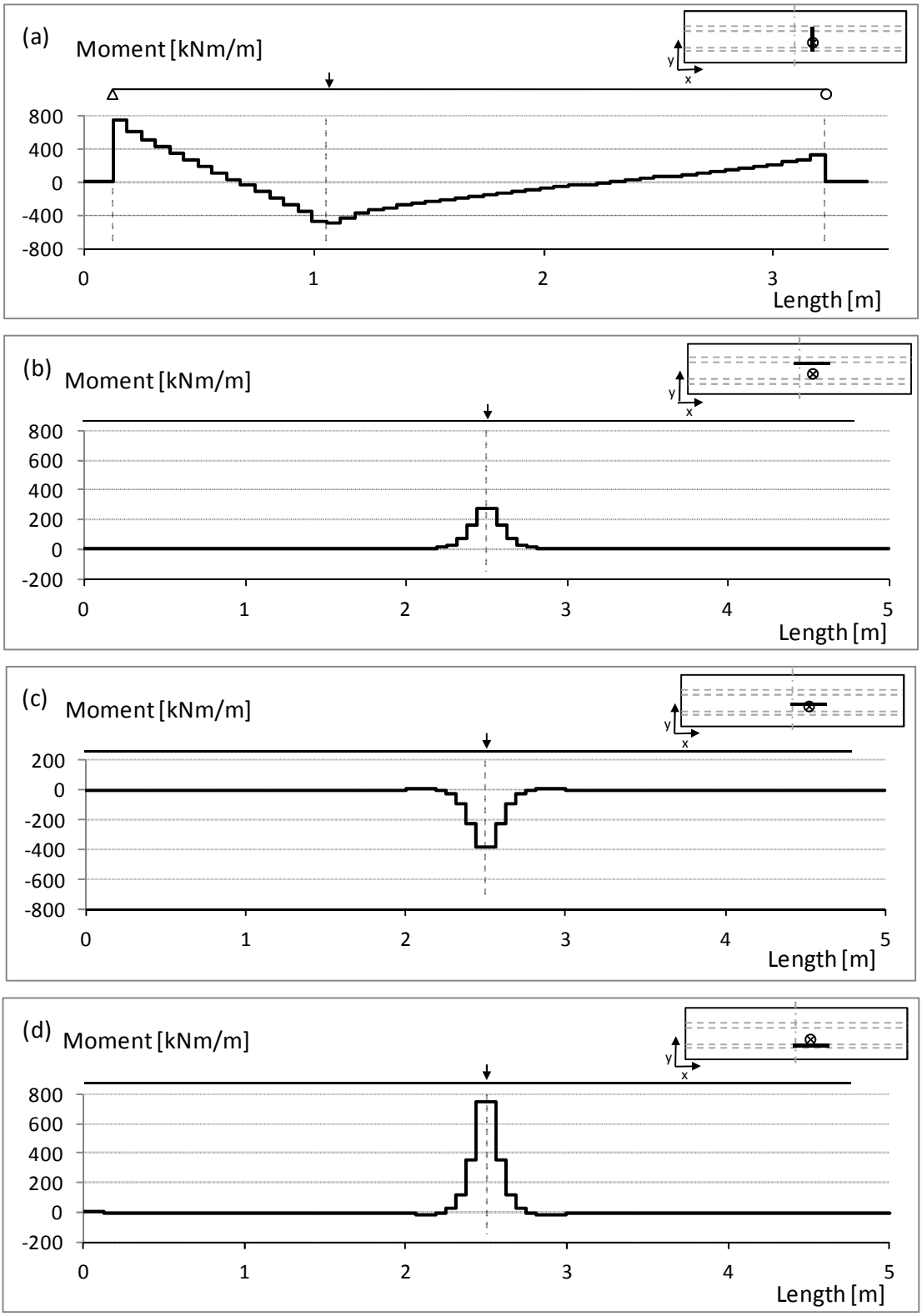

Figure 5.6 *Variation and distribution of bending moment about x-axis in model 1, when a concentrated load of 360 kN was applied to the bridge; (a) transversal section between the girders going through the point where the load was applied, (b) longitudinal section close to one girder (c) longitudinal section through the point where the load was applied and (d) longitudinal section close to the other girder.*

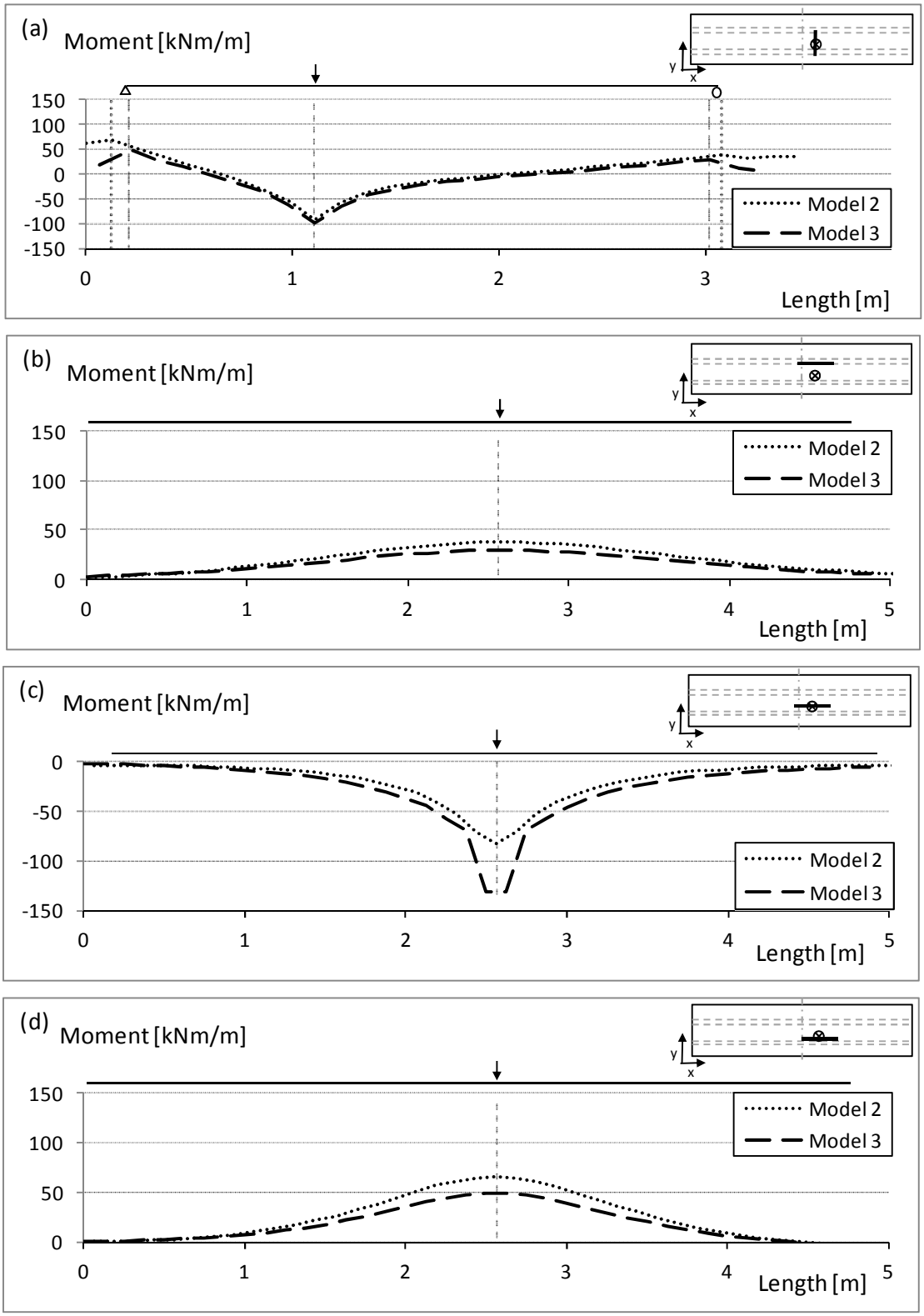

Figure 5.7 *Variation and distribution of bending moment about x-axis in model 2 and 3, when a concentrated load of 360 kN was applied to the bridge; (a) transversal section between the girders going through the point where the load was applied, (b) longitudinal section close to one girder (c) longitudinal section through the point where the load was applied and (d) longitudinal section close to the other girder.*

Similar to the shear force in the bridge deck slab in model 2 and 3, bending moment presented in longitudinal and transversal sections cannot directly be compared. Figure 5.8 presents a principal sketch of the integration of the longitudinal section in model 3, see Figure 5.7 (c). The same bending moment as the maximum field moment in Figure 5.7 (a) was then obtained.

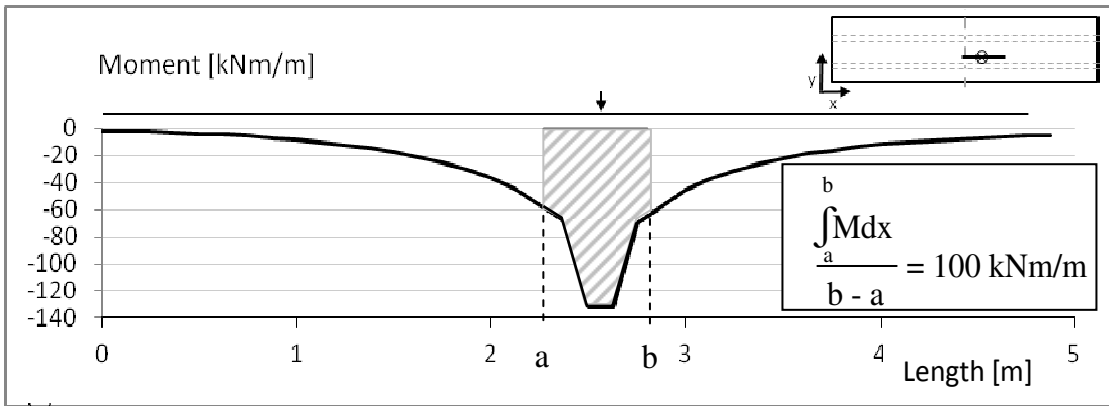

Figure 5.8 Schematic sketch of how the shear forces in the transversal sections were obtained by integrating the graphs of the longitudinal sections.

In Figure 5.7 (c) it was seen that the bending moment distribution in model 2 and 3 differed significantly. To investigate the reason for this, the features *path* and *Free Body Cut* were studied. Both *path* and *Free Body Cut* were then used in model 2 to examine the variation of bending moment in the longitudinal section that was going through the loading point. From this it was clear that *path* and *Free Body Cut* presented the bending moment differently, see Figure 5.9.

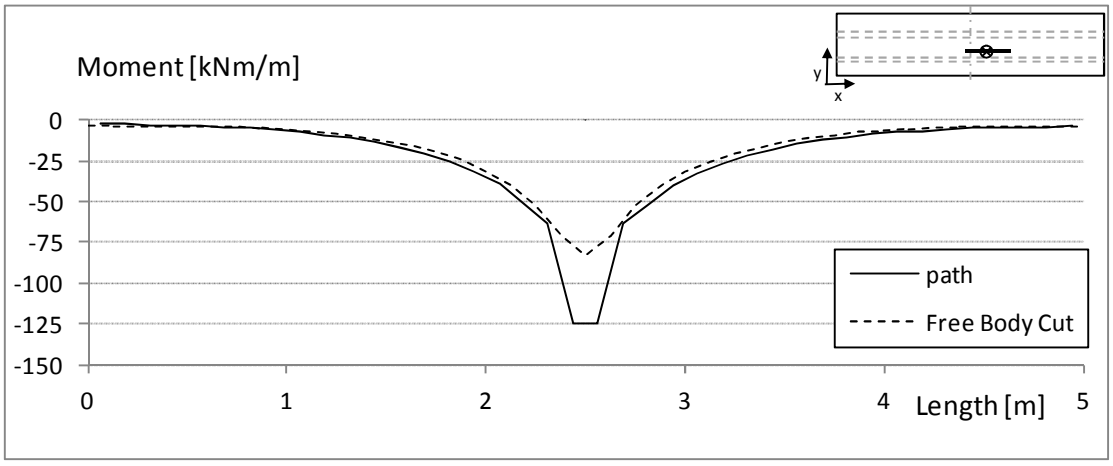

Figure 5.9 Transversal bending moment in a longitudinal section in the bridge deck slab in model 2, when a concentrated load was applied between the girders. The sections were created by the feature path and by the feature Free Body Cut.

To further investigate the reason why *path* and *Free Body Cut* gave different magnitudes of the bending moment close to the loading point, the values of the integration points of the elements transversally in the bridge deck slab were plotted in a graph, see Figure 5.10. By extrapolating the curves from each side of the loading point, an approximation of the bending moment at the section where the load was applied could be obtained. The values obtained from *path* and *Free Body Cut* in the longitudinal section where the load was applied is also presented in Figure 5.10.

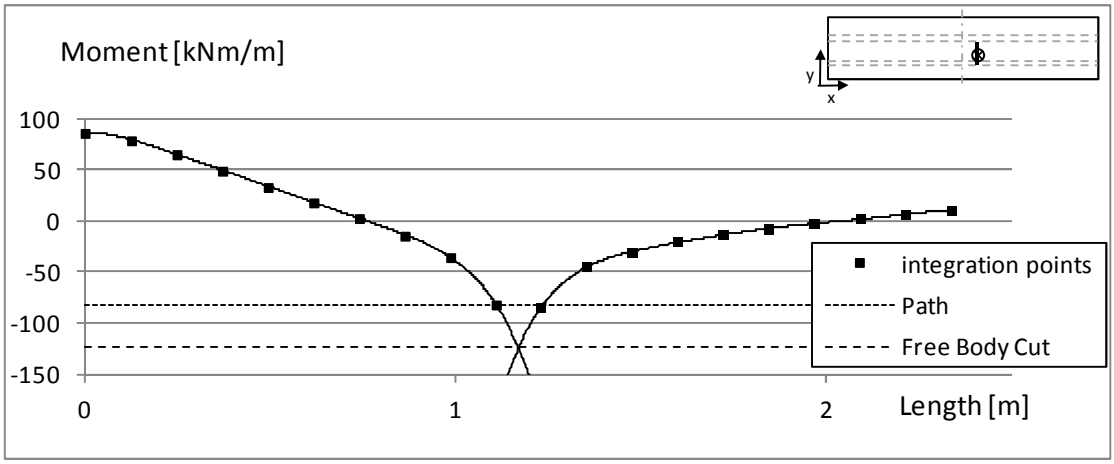

Figure 5.10 A graph showing the bending moment in the integration points of the elements transversally of the bridge deck slab.

From this it was seen that the bending moment under the loading point in the longitudinal section that was created by *Free Body Cut*, see Figure 5.9, was equal to the extrapolated value from the integration points, see Figure 5.10. *Path* on other hand, gave the bending moment in the loading point as a mean value of the closest integration points. This explained why the distribution of bending moment was different in model 2 and 3 along this section. In a design situation of a bridge deck slab there are no concentrated loads, only distributed loads. The differences that were seen between *path* and *Free Body Cut* when one node was loaded only, are for that reason not relevant in design.

5.1.3 Variation of sectional forces along the girders

In Figure 5.11 and Figure 5.12 the shear forces and bending moments along the girders are presented. For all FE-models, it was seen that the girder closest to the applied load attracted more load than the girder farthest away. It was seen that the reaction force over the mid support, of the girder closest to the loading point, was greater for the model 1 compared to model 2 and 3, 250 kN, and 225 kN, respectively, see Figure 5.11 (b). The opposite was seen at the mid support of the girder farthest away from the load, where model 1 showed a support reaction of 100 kN and the other two models showed a support reaction of 120 kN, Figure 5.11 (a).

The reaction force at the right end support of the girder farthest away from the loading point was positive with a magnitude of about 15 kN for all FE-models. The shear force decreased towards the section of the loading point and even changed sign before this section. At the right end support of the girder, closest the loading point, the support reaction was approximately 15 kN for all FE-models. The shear force increased closer to the section where the load was applied and a distinguished reaction force could then be seen there. Model 2 and 3 showed a peak of the shear force at the section where the concentrated load was applied.

The reason that a peak of the shear force appeared in model 2 and 3 can be explained by that Free Body Cut surfaces were created on half of the cross-section of the bridge along the girders. The load was thereby directly included in the Free Body Cut surface in the section where the load was applied. For that reason, it looks like the total load was carried by the girder closest to the load in that section.

The bending moment for the girder closest to the applied load showed that model 2 and 3 got slightly lower bending moment than model 1, see Figure 5.12 (b). The opposite was seen in the graph showing the bending moment along the other girder. The reason to this will be discussed in Chapter 6.

Summation of the load effect from both girders showed that all FE-models gave almost the same total load effects, see Figure 5.13. These load effects were compared to an analytical two-dimensional model and the results agreed well.

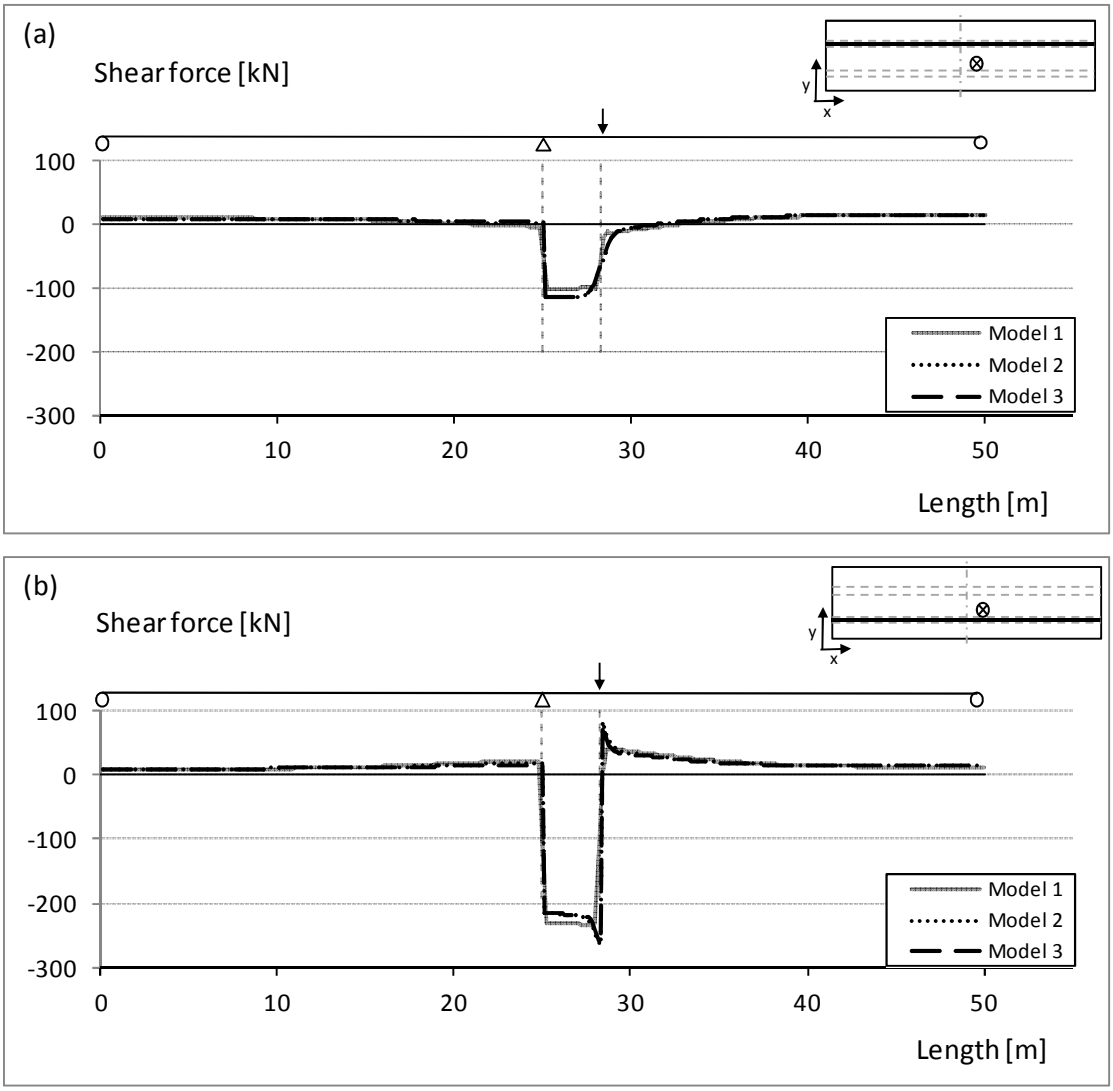

Figure 5.11 Variation of shear force along the girders in model 1, 2 and 3, when a concentrated load of 360 kN was applied on the slab between the girders; (a) total load effect on the girder that was farthest from the applied load and (b) total load effect on the girder that was closest to the applied load.

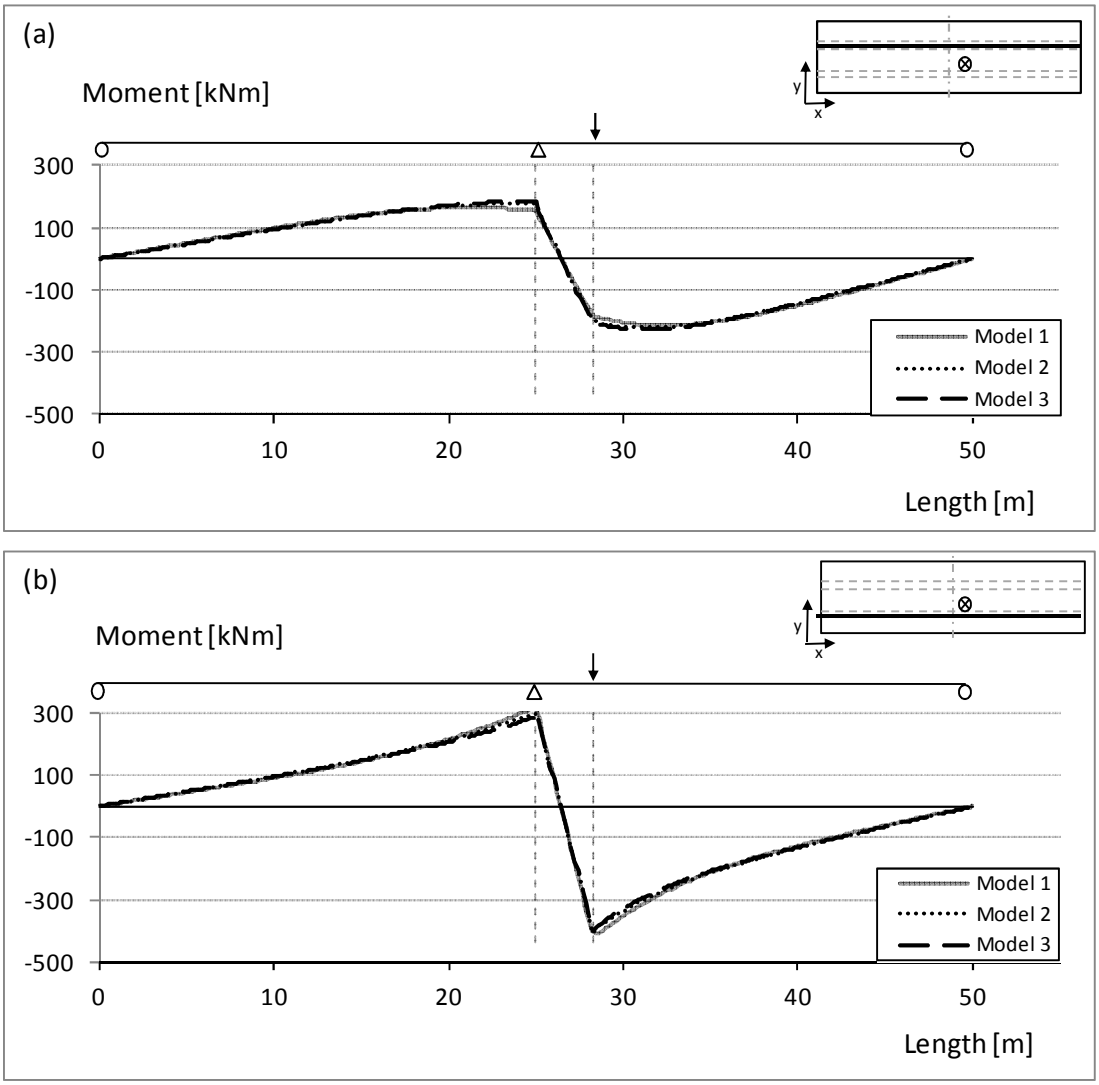

Figure 5.12 Variation of bending moment along the girders in model 1, 2 and 3, when a concentrated load of 360 kN was applied on the slab between the girders; (a) total load effect on the girder that was farthest from the applied load and (b) total load effect on the girder that was closest to the applied load.

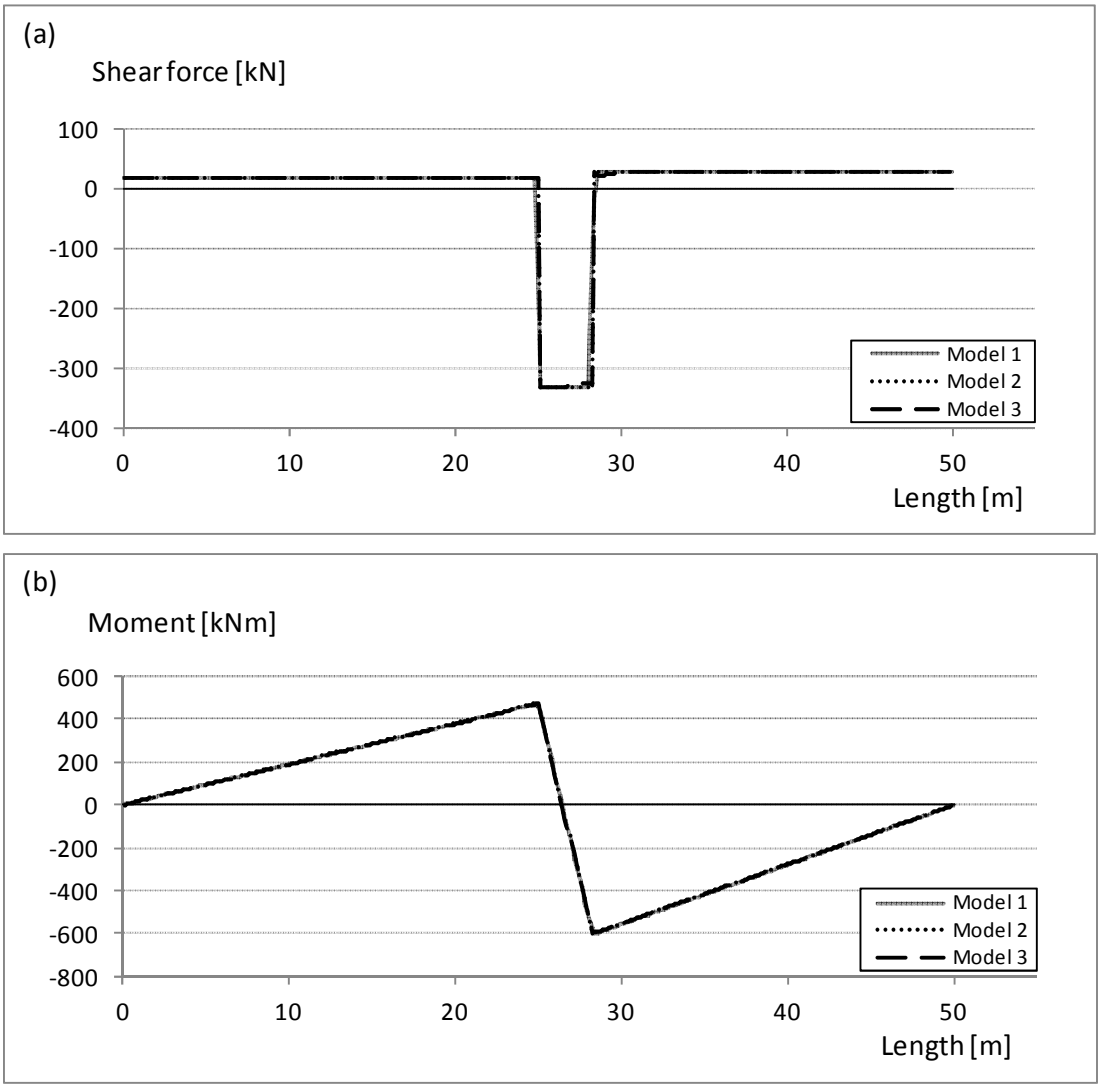

Figure 5.13 Summation of the load effect on both girders in model 1, 2 and 3 when a concentrated load of 360 kN was applied on the slab between the girders; (a) total shear force and (b) total bending moment.

5.2 Load case 2 – Distributed load on a small area of the cantilever

For load case 2, where a distributed load was applied to a small area at the edge of the cantilever, output data along four sections was created, see Figure 5.14. To show the variation of the shear force and bending moment a transversal section in the bridge deck slab, going through the loading point, was studied. To show the longitudinal distribution of the transversal shear force and bending moment, a longitudinal section was studied in the slab close to the girder. Also for this load case, it was of interest to examine the load effect on both girders and the interaction between them.

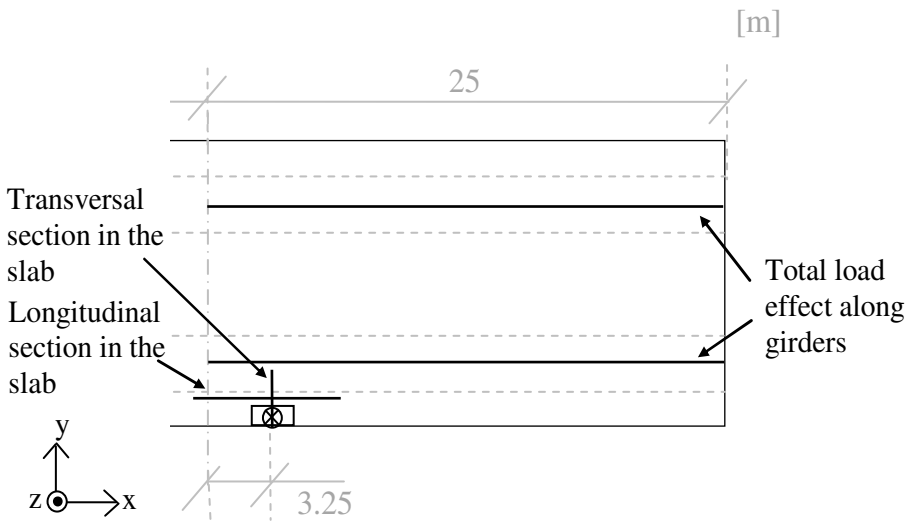

Figure 5.14 Sections in the bridge deck slab where the variation and distribution of shear force and bending moment were studied. Also the total load effect on the girders was studied. A distributed load with a magnitude of 360 kN was applied on the edge of the cantilever.

5.2.1 Variation and distribution of shear force in the slab

In Figure 5.15 and Figure 5.16, the shear force in the slab is presented in model 1, 2 and 3, respectively, when a small area of the cantilever was subjected to a load of 360 kN.

Figure 5.15 (a) presents the shear force variation in model 1 along the transversal section, from the applied load to the closest girder. The shear force was build up successively over the elements where the load was applied to a magnitude of about 640 kN/m. Thereafter, the shear force was slightly increased towards the girder where a support reaction of about 750 kN/m appeared. However, due to the assigned stiffness to model 1, a constant magnitude of the shear force was expected. When transversal sections on each side of the examined section were studied it was seen that the magnitude of the shear force decreased closer to the girder. It can therefore be assumed that the shear force variation over a certain width would be constant.

The reason that the shear force in model 1 was greater than the applied load depended on that the bridge deck slab could transfer load in transversal direction of the bridge only, see the explanation in Section 5.1.1 for load case 1. This was also the reason why a peak value of the shear force appeared at the section where the load was applied, see Figure 5.15 (b). As for the shear force diagram for load case 1, the shear force changed sign more than once in the longitudinal direction. Integrating the shear force over the longitudinal section gave a resulting force of 360 kN.

The graph that present the shear force variation in model 2 and 3, showed that the shear force builds up over the area where the cantilever was loaded, see Figure 5.16 (a). It could also be noticed that the shear force continued to increase even after the area with applied load. The maximum shear force in model 2 and 3 was about 260 kN/m and 270 kN/m, respectively. The shear force was thereafter slightly decreasing towards the girder, to a magnitude around 150 kN/m in both FE-models. The reason that the shear force continued to increase even after the area with applied

load was a consequence of how *Free Body Cut* presents the output data. In Brigade/Plus a distributed load is represented by nodal forces and the integration point in the element outside the loaded area is thereby affected by the total load. Due to how output data was presented from *Free Body Cut*, see Section 2.6, the magnitude of the shear force was calculated from the applied load in a correct way, but the result was presented in the wrong point in the slab.

In Figure 5.16 (b), the distribution of the shear force in model 2 and 3 along the longitudinal sections is shown. It was seen that the maximum value appeared at the section where the load was applied and decreased in longitudinal direction. The shear force was distributed over a certain width and did not show a distinguished peak. Integrating the graphs that were presenting the shear force distribution, gave a resulting shear force of 360 kN for both FE-models.

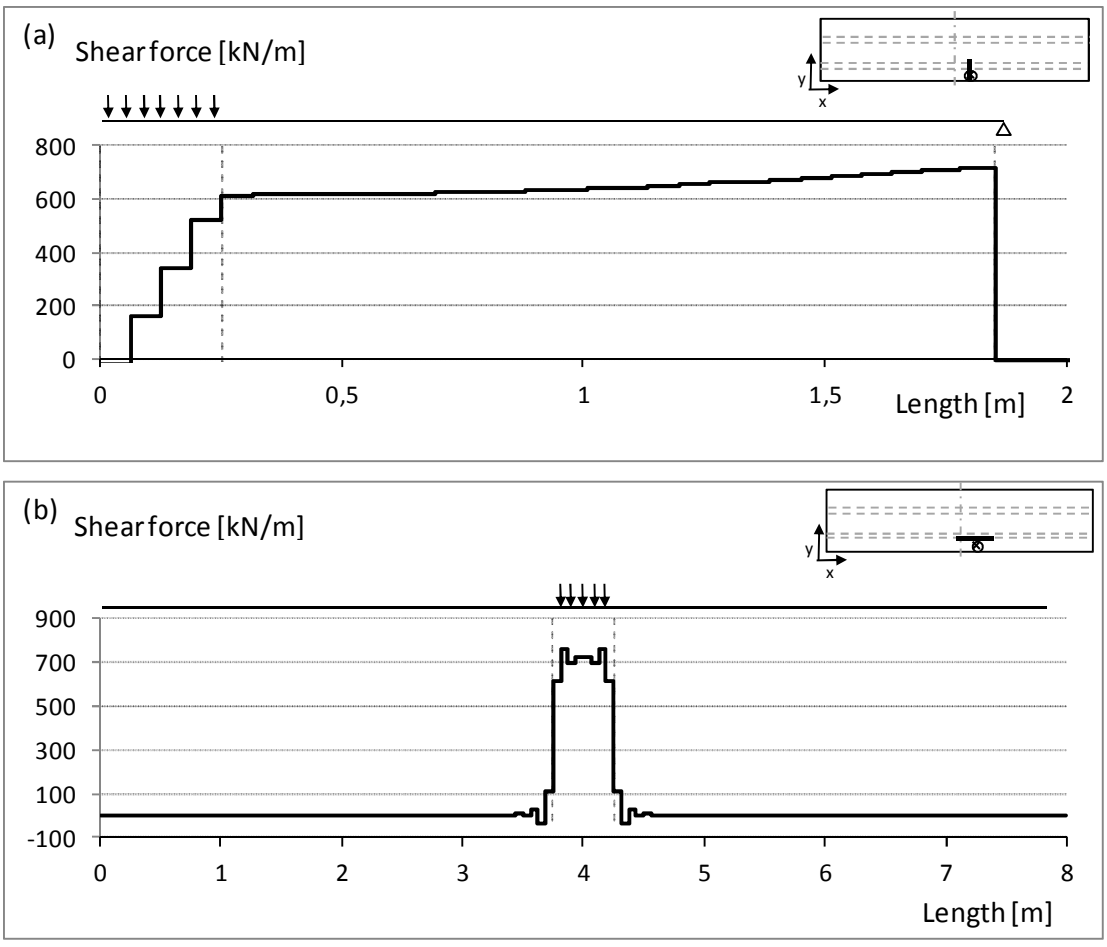

Figure 5.15 Variation and distribution of transversal shear force in model 1, when a distributed load of 360 kN was applied to a small area on the edge of the cantilever; (a) transversal section between the loading point and the closest girder, (b) longitudinal section close to the girder.

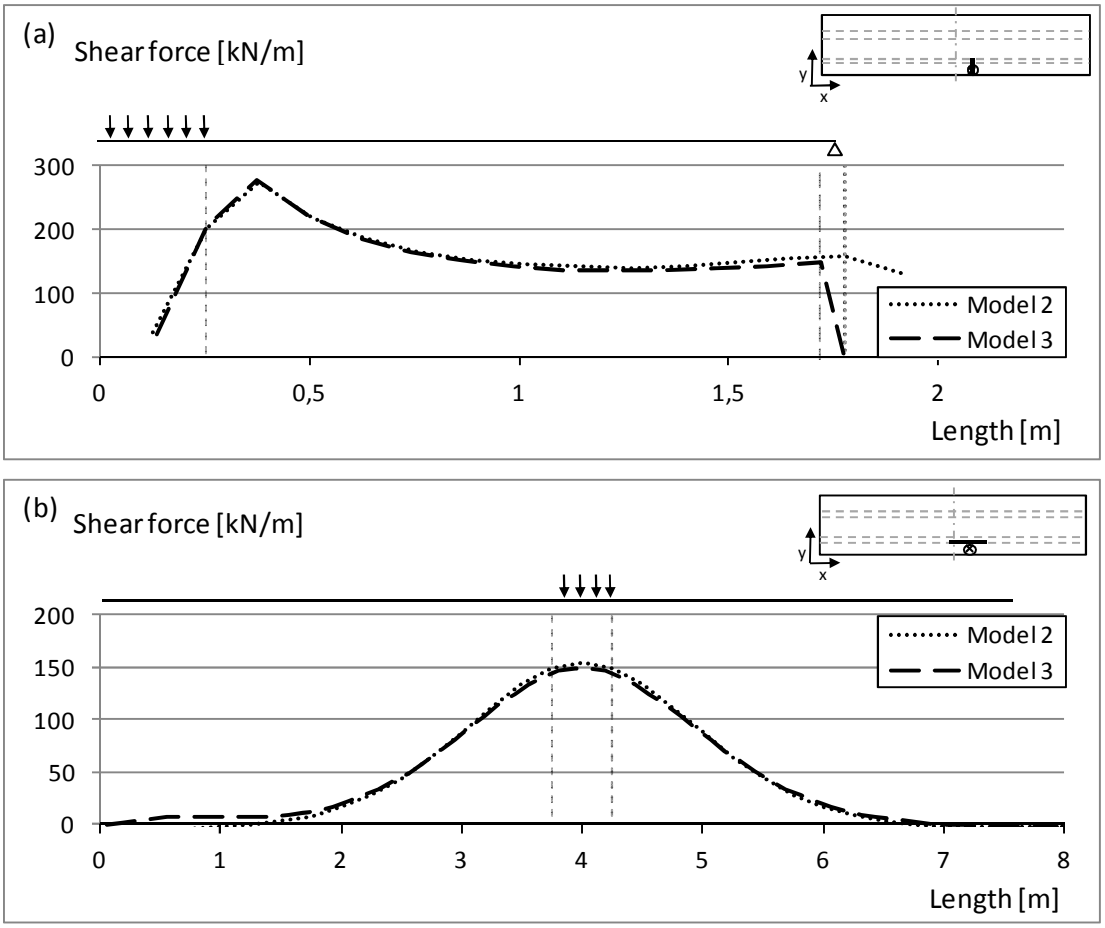

Figure 5.16 Variation and distribution of transversal shear force in model 2 and 3, when a distributed load of 360 kN was applied to a small area on the edge of the cantilever; (a) transversal section between the loading point and the closest girder, (b) longitudinal section close to the girder.

5.2.2 Variation and distribution of bending moment in the slab

Figure 5.17 and Figure 5.18 show the variation and distribution of the bending moment in model 1, 2 and 3, respectively. All graphs presented a more or less linear increase of the bending moment towards the girder, from a bending moment of zero at the end of the cantilever.

The support moment for the different FE-models differed extensively. Model 1 showed a support moment of 1100 kNm/m, see Figure 5.17 (a). The graph presenting the variation of bending moment in model 2 and 3 showed a support moment of about 170 kNm/m and 160 kNm/m, respectively, see Figure 5.18 (a). The reason that model 1 showed much greater bending moment compared to model 2 and 3 depends on the impact of mesh density due to the orthotropic material properties assigned to the slab.

As for the distribution of shear force, the bending moment in model 1 was distributed over a small width close to the girder and showed a peak value in the section where the load was applied, see Figure 5.17 (b). The graphs that were showing the distribution of bending moment in model 2 and 3 were smoother and distributed the moment over a larger width, see Figure 5.18 (b).

To verify the support conditions for the slab, when the girders act as supports, the moment distribution in the slab for the different FE-models was compared to an analytical two-dimensional model, see Appendix D.

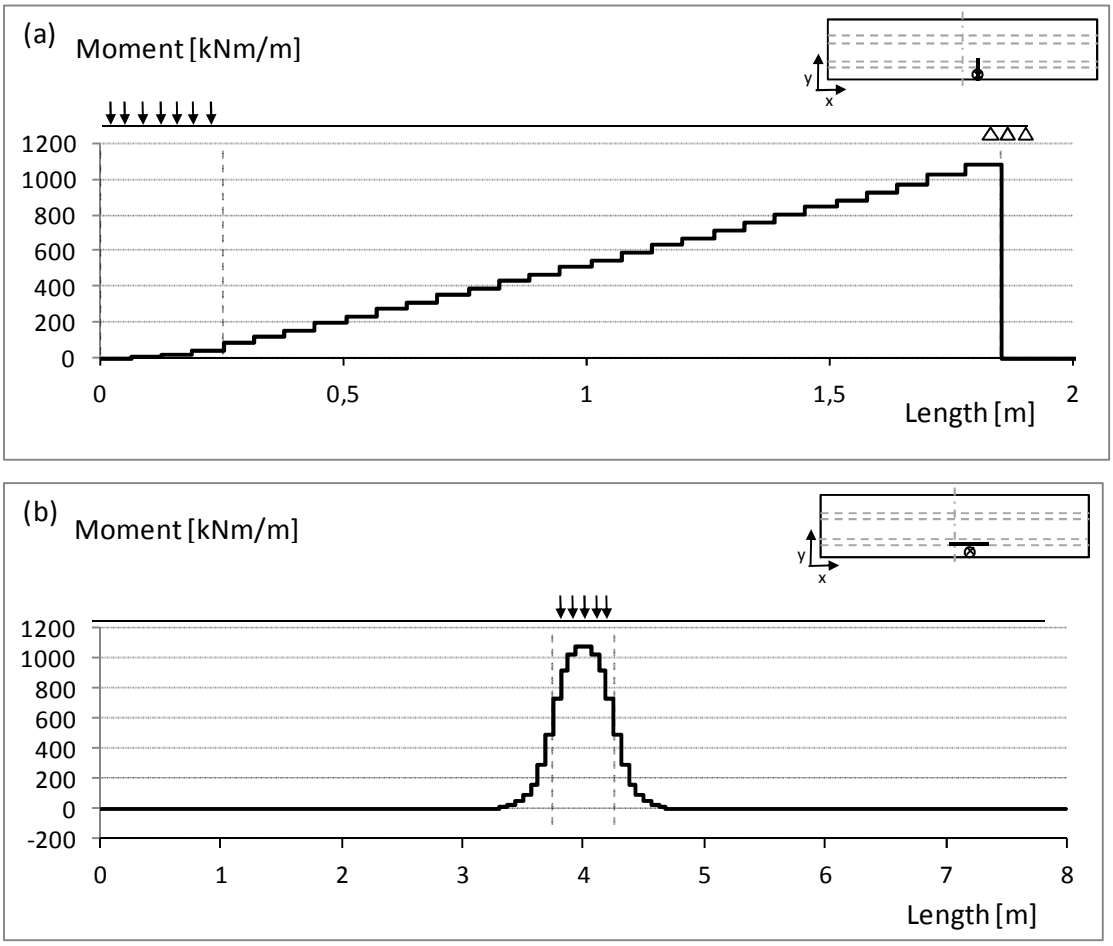

Figure 5.17 *Variation and distribution of bending moment about x-axis in model 1, when a distributed load of 360 kN was applied to a small area on the edge of the cantilever; (a) transversal section between the loading point and the closest girder and (b) longitudinal section close to the girder.*

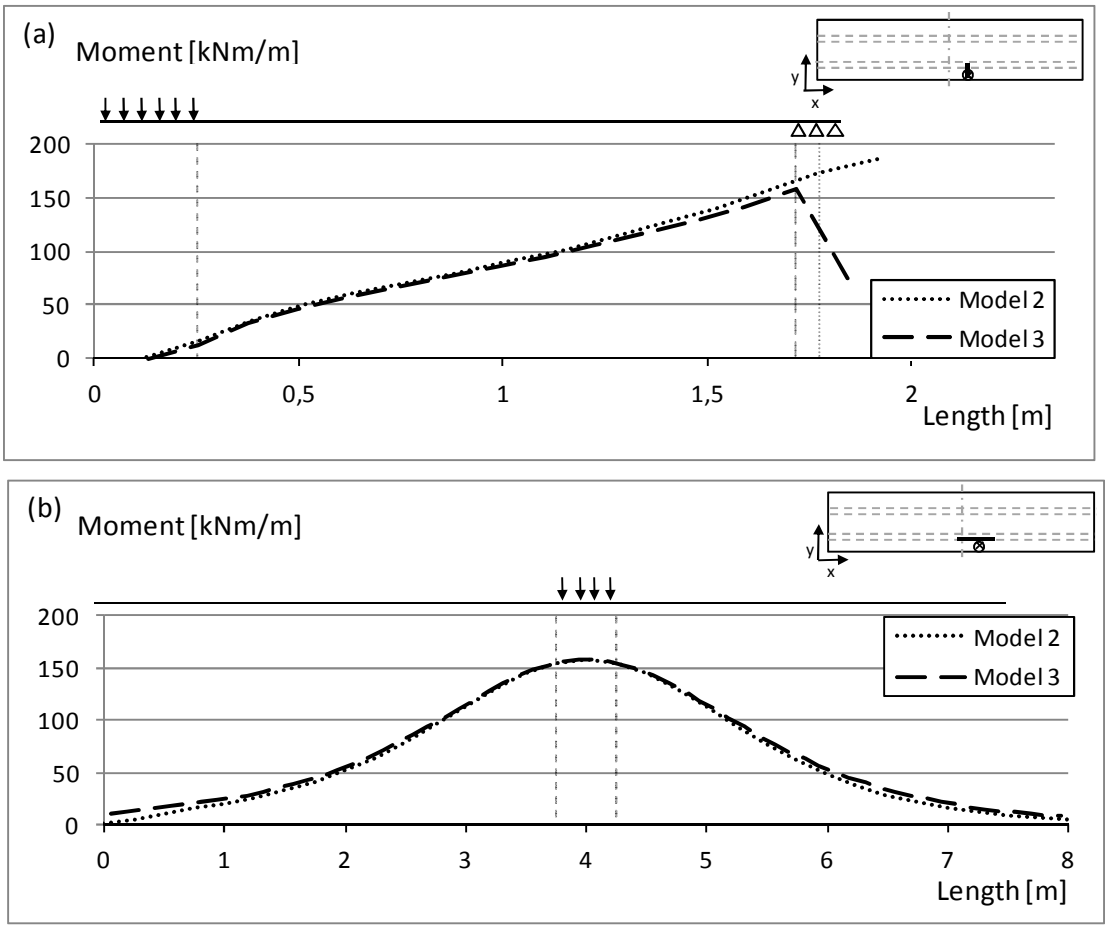

Figure 5.18 Variation and distribution of bending moment about x-axis in model 2 and 3, when a distributed load of 360 kN was applied to a small area on the edge of the cantilever; (a) transversal section between the loading point and the closest girder and (b) longitudinal section close to the girder.

5.2.3 Variation of sectional forces along the girders

In the graphs below, the shear forces and bending moments along both girders are presented, see Figure 5.19 and Figure 5.20, respectively.

When examined the shear force variation along the girder that was closest to the applied load, it was seen that model 1 and 2 showed the same variation but model 2 showed a slightly higher reaction force at the mid support compared to model 1, see Figure 5.19 (b). Model 3, showed a support reaction that was lower than the reaction force in the other FE-models, and in the section where the load was applied the graph showed a peak of the shear force. Similar to load case 1, the peak of the shear force depended on that the total load was included in the Free Body Cut surface in that section.

The shear force along the girder farthest away from the load was small in model 1 and 2. In model 3 a support reaction appeared at the mid support.

When examined the variation of bending moment along the girders it was seen that all models showed similarities in the moment variation. At the girder close to the load,

model 2 showed the highest magnitude of the bending moment, see Figure 5.20 (b). The bending moment in model 1 was slightly less than the bending moment in model 2, and model 3 showed the lowest bending moment.

For the girder farthest away from the applied load the magnitude of the bending moment along the girder was much smaller compared to the girder close to the load, see Figure 5.20 (a). Comparing the magnitude of the bending moment it was noted that model 3 showed the highest bending moment and model 2 showed the lowest bending moment, for the girder farthest away from the applied load. The bending moment in model 1 was somewhere in between.

In load case 2, compared to load case 1, the differences of the interaction between the girders were seen more clearly in model 1, 2 and 3. Again, the summation of the load effect from both girders showed that all FE-models gave almost the same total load effects, see Figure 5.21.

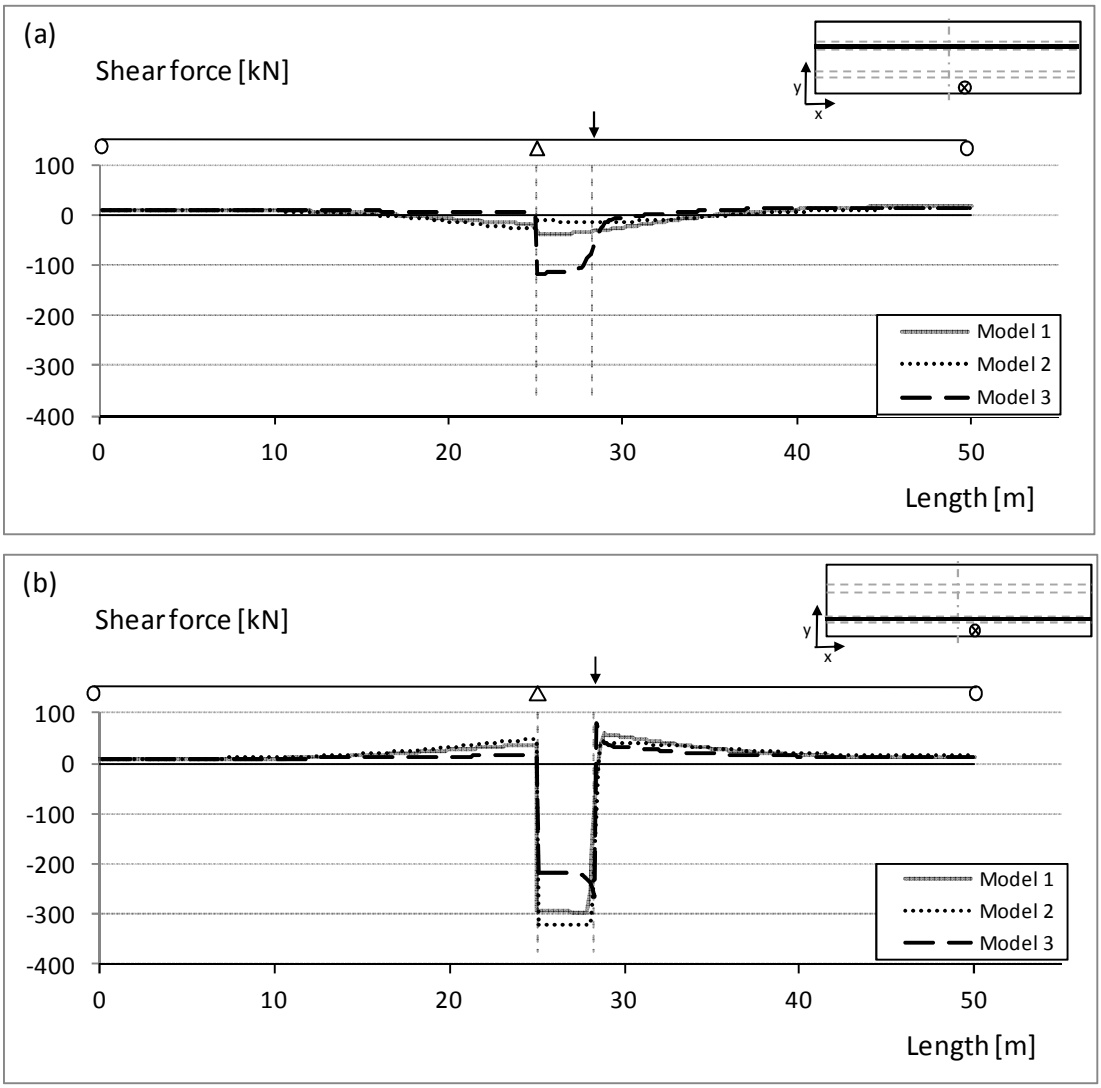

Figure 5.19 Variation of shear force along the girders in model 1, 2 and 3, when a load of 360 kN was applied to a small area of the cantilever; (a) total load effect on the girder farthest from the applied load and (b) total load effect on the girder closest to the applied load.

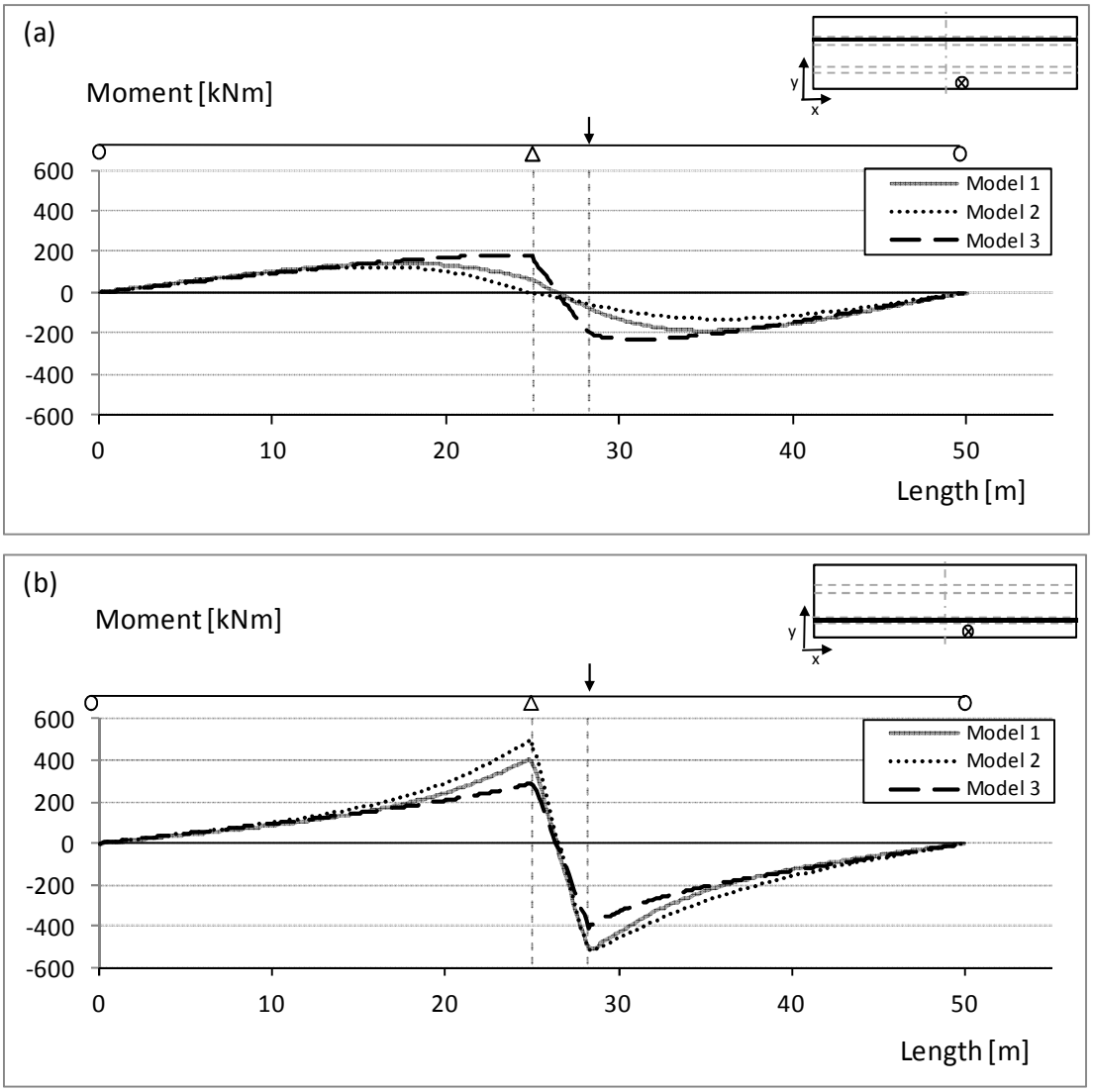

Figure 5.20 Variation of bending moment along the girders in model 1, 2 and 3, when a load of 360 kN was applied to a small area of the cantilever; (a) total load effect on the girder farthest from the applied load and (b) total load effect on the girder closest to the applied load.

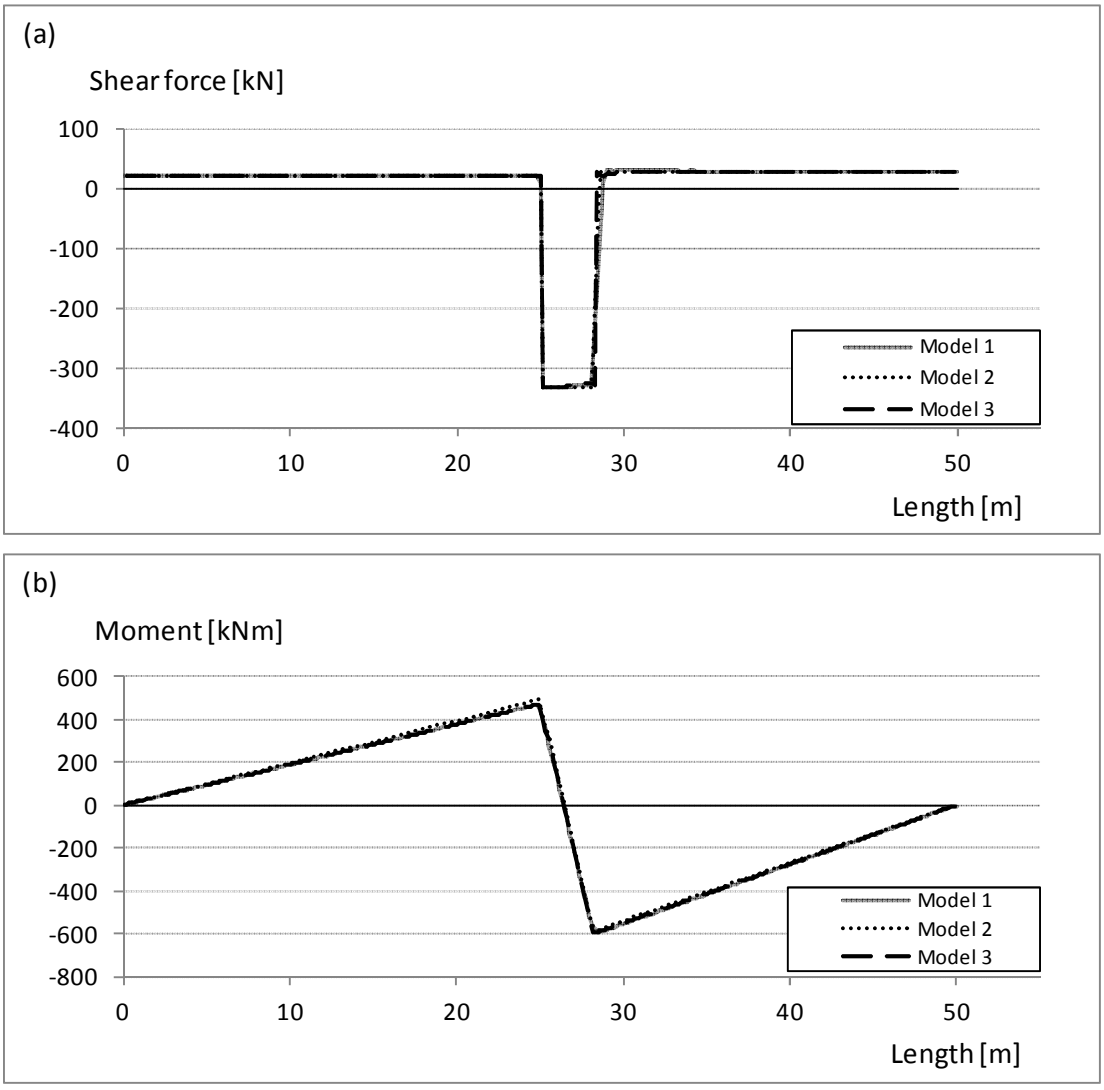

Figure 5.21 Summation of the load effect on both girders in model 1, 2 and 3 when a load of 360kN was applied to a small area of the cantilever; (a) total shear force and (b) total bending moment.

5.3 Load case with moving vehicle loads

As described in Section 4.2, four different load models can be imported in Brigade/Plus and in this Master's project the vehicle loads from load model 1 were studied. The vehicle loads consist of two vehicles with a bogie pressure of 270 kN and 180 kN, respectively.

In Figure 5.22 and Figure 5.23, the variation of maximum and minimum shear force and bending moment along the girders for all examined load positions are presented. The vehicle lines were created symmetrically on the bridge deck slab and for that reason both girders showed the same variation of the sectional forces.

In Figure 5.22 it was seen that the variation of shear force was almost the same in all FE-models. In some regions, the shear force in model 1 was slightly lower than the shear force in model 2 and 3. In Figure 5.23 on other hand, there was a significant lower bending moment in model 1, compared to the other two FE-models. The biggest difference was seen in the field where the maximum bending moment was about

2500 kNm, 2800 kNm and 2800 kNm in model 1, 2 and 3, respectively. The bending moment in model 1 was about 10 percent lower than in model 2 and 3.

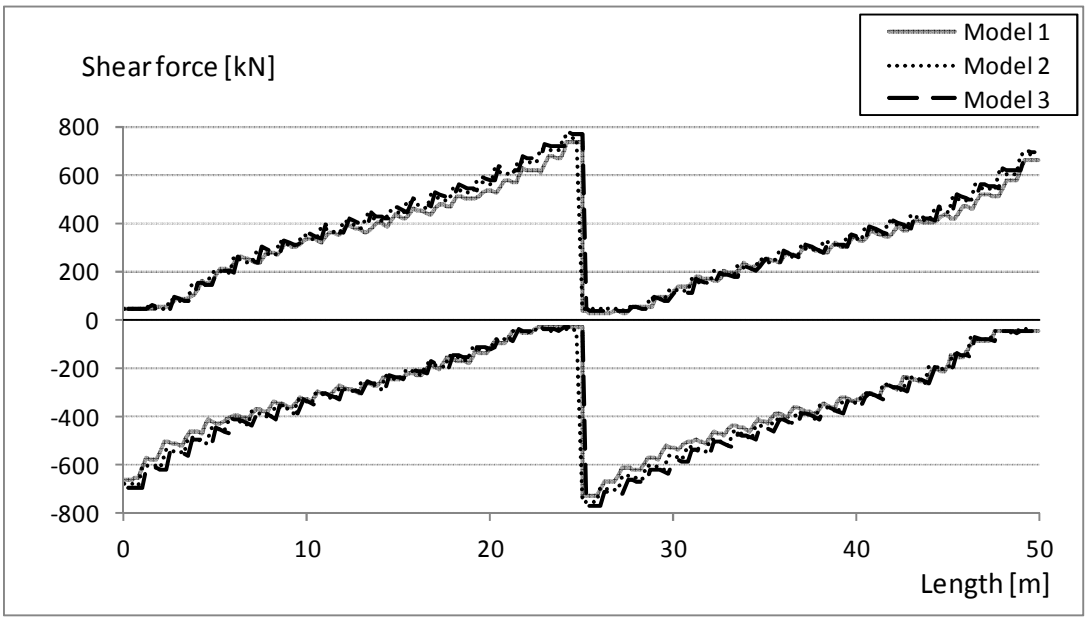

Figure 5.22 Variation of shear force along the girders for the three FE-models. The bridge deck slab was subjected to moving vehicle loads from load model 1.

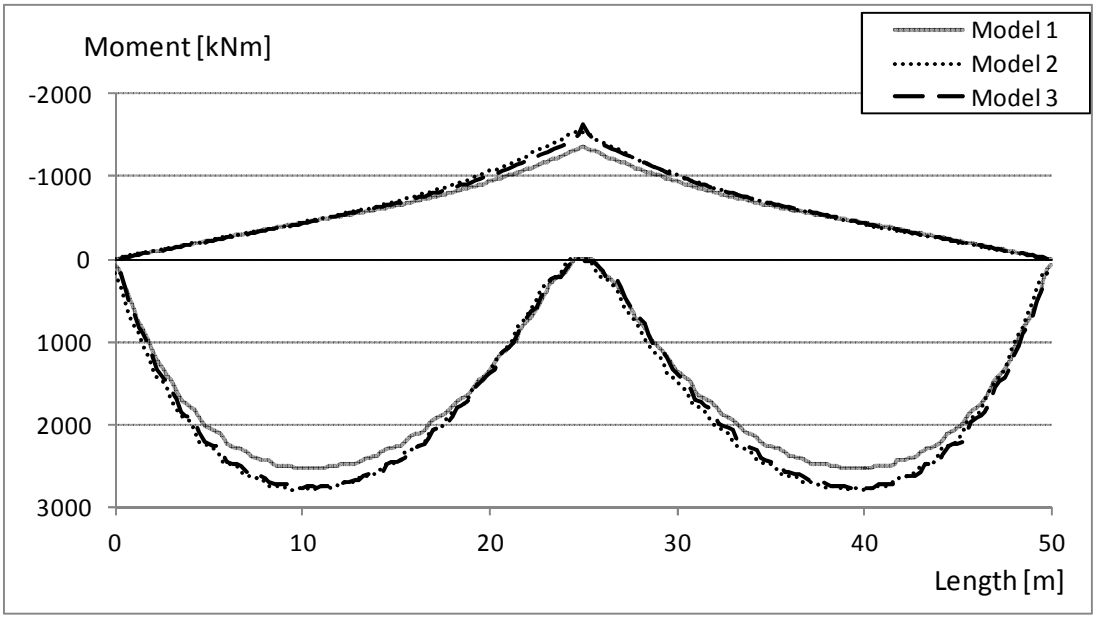

Figure 5.23 Variation of bending moment along the girders for the three FE-models. The bridge deck slab was subjected to moving vehicle loads from load model 1.

To examine the reason why model 1 showed lower sectional forces compared to model 2 and 3, the model was recreated and the tied width of the slab was decreased. Instead of constraining a width of 2.6 meters of the slab above the girders, the nodes straight above the gravity centre of the girders were constrained only. If the area where the slab was constrained to the girders in model 1 was decreased, the shear

force and bending moment along the girders increased, see Figure 5.24 and Figure 5.25. The bending moment in field then became about 4.3 percent higher in model 1 compared to model 2 and 3.

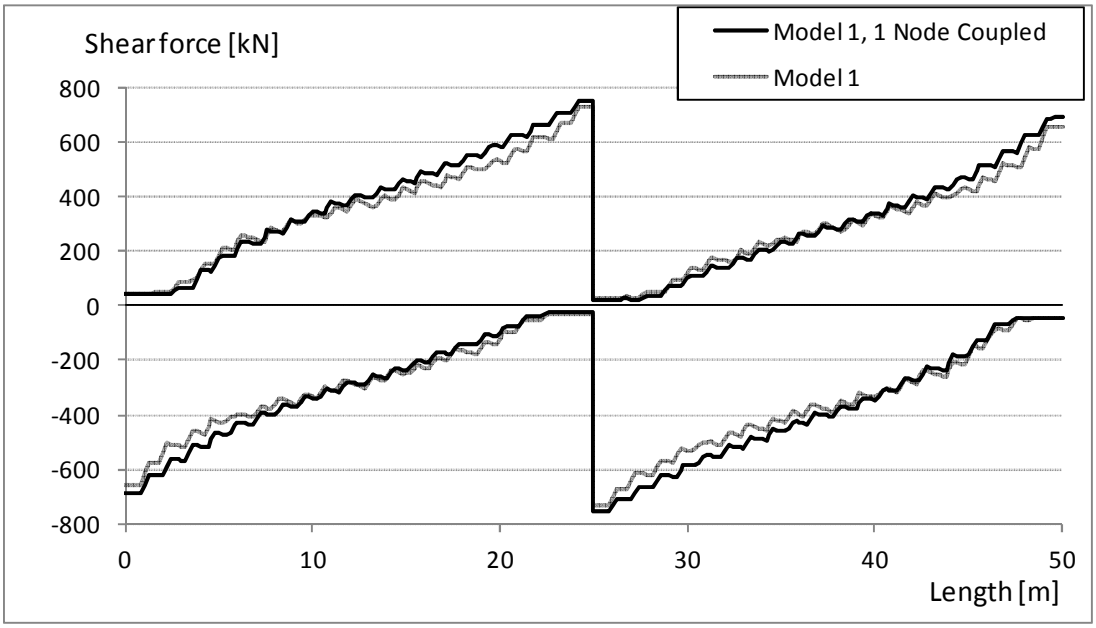

Figure 5.24 Variation of shear force along the girders in model 1, if all nodes in the slab above the girders were constrained and if only one node in the slab was constrained. The bridge deck slab was subjected to the moving vehicle loads from load model 1.

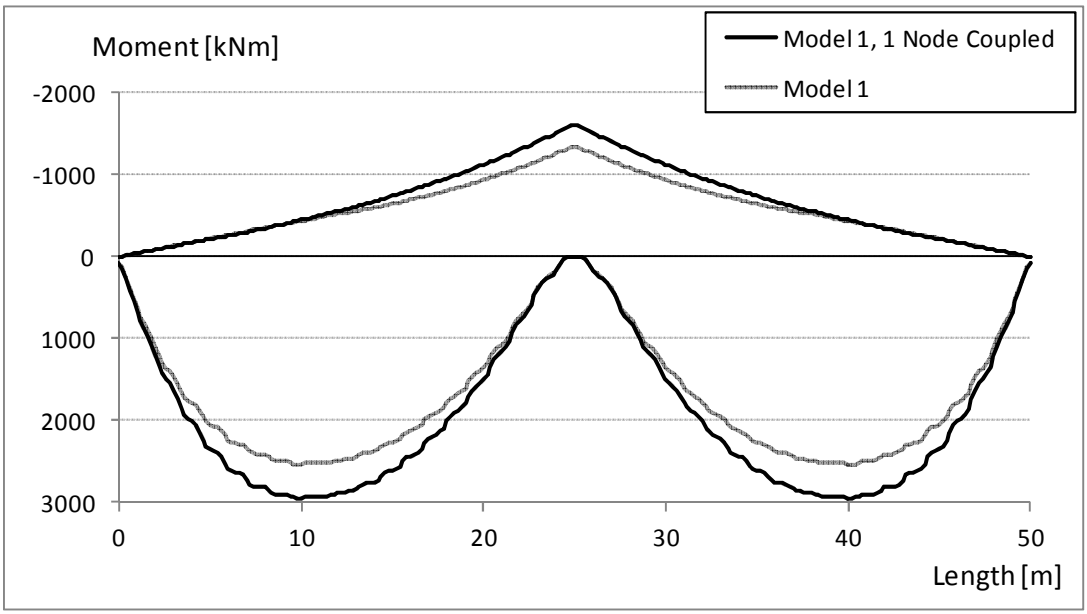

Figure 5.25 Variation of bending moment along the girders in model 1, if all nodes in the slab above the girders were constrained and if only one node in the slab was constrained. The bridge deck slab was subjected to the moving vehicle loads from load model 1.

6 Discussion

The FE-models that represented the case study bridge were created in different ways, which was expected to influence the results from the FE-simulation. Model 1 was intended to transfer the load transversally in the bridge deck slab only, without any longitudinal load distribution. Model 2 and 3 were given structural properties where the longitudinal distribution of load in the bridge deck slab was taken into account. Therefore, sectional forces in model 1 are not comparable to sectional forces in model 2 and 3.

Many differences of the sectional forces in the bridge deck slab between model 2 and 3 can be explained by how the feature *path* and the feature *Free Body Cut* in Brigade/Plus calculate and present the output data, see Chapter 5. However, to explain the differences in the three FE-models which were seen in the analysis of the load effect on the girders, further studies were needed, which are discussed in this chapter. The chapter also contains a discussion of the advantages and disadvantages with the different FE-modelling techniques.

6.1 Interpretation of the results concerning the girders

When the three FE-models were established in Brigade/Plus the geometry of the case study bridge was modelled in different ways so that all FE-models simulated an equivalent longitudinal bending stiffness. This resulted in that the bridge deck slab, for the different FE-models, became unequally stiff in transversal direction of the bridge.

Model 1 and 2 are established by structural elements where beam theory and plate theory simplifies the structural response of the structural members included in the FE-models. Model 3 is established by continuum elements, based on continuum mechanics. Therefore, model 3 can be expected to describe the elastic response of the structural parts included in the FE-model similar to the structural response of the case study bridge.

The bridge can in transversal direction conceptually be replaced by a theoretical model where the slab is supported on vertical and rotational springs, see Figure 6.1. These springs represent the vertical and rotational restraint that the girders provide to the slab, through their flexural and torsional stiffness. In case the rotational springs are infinitely weak, the slab can be seen as simply supported in transversal direction of the bridge and the system would be statically determinate. The different ways of defining boundary conditions for the three FE-models do however affect the torsional restraint of the girders differently and, consequently, the rotational restraint of the slab. The boundary conditions will therefore have an impact on the results, and the slab cannot be seen as simply supported on the girders.

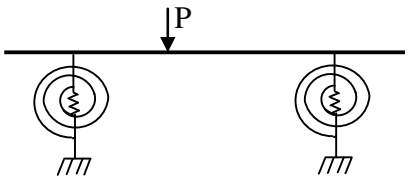

Figure 6.1 Theoretical model of a slab supported on vertical and rotational springs.

Rotations around the longitudinal axis of the girders were prevented by the boundary conditions at the supports, see Chapter 4. In model 1, one node of the beam elements at each support were constrained and in model 2, one edge of the shell elements at each support were constrained. This means that the boundary conditions were constraining the entire cross-section of the girders over the supports from deforming. This corresponds to that both the vertical and rotational springs in the theoretical model are infinitely stiff in the support sections. In model 3, the boundary conditions were applied to constrain the edge of the continuum elements at the bottom of the girders only. The cross-section of the girders was thereby allowed for some deformation and the section where the slab connected to the girders was allowed for some rotation. This corresponds to that both the vertical and, in particular, the rotational springs in the theoretical model provide some flexibility in the support sections.

The differences that was seen in the graphs that presented the variation of shear force and bending moment along the girders for the different FE-models, see Figure 5.11-5.12 and Figure 5.19-5.20, depend on four parameters: the stiffness of the slab in transversal direction, how the connection between the slab and the girders was modelled, the vertical stiffness provided by the girders and the rotational stiffness provided by the girders. The relation between these parameters for the case study bridge demands for further investigations, and it is not possible to state a correct relation between these depending parameters that holds for all bridge structures.

6.1.1 Load case 1

The results for load case 1, when the bridge deck slab was loaded between the girders, depend on the four parameters stated above. The relation between the parameters implied that the shear force in the region between the loading point and the mid-support was higher at the girder closest to the applied load in model 1 compared to model 2 and 3, besides the section where the load was applied, see Figure 5.11 (b). Also the bending moment in model 1 was the highest in this girder, see Figure 5.12 (b). The opposite was seen at the girder farthest away from the load.

The only conclusion that can be given from load case 1 is that the current rigidities and dimensions means that model 1 gives higher shear force and bending moment compared to model 2 and 3 at the girder closest to the load. For other rigidities and dimensions of the case study bridge, the FE-models would not necessary show the same results.

6.1.2 Load case 2

Examining the diagrams of shear forces and bending moments for load case 2, when the cantilever was loaded, there were big differences between the FE-models. The magnitude of the shear force between the load and the mid support was much lower at the girder close to the loading point in model 3 compared to model 1 and 2, see Figure 5.19 (b). The opposite was seen at the girder farthest away from the load. This means that there was a greater interaction between the girders in model 3 compared to model 1 and 2.

To investigate the differences which were seen in Figure 5.19 (a) and (b), the boundary conditions in model 3 were studied. Instead of applying the boundary conditions to the bottom edge of the girders the entire cross-section of the girders was

constrained to prevent vertical translation and rotation over the supports. The analysis showed that the variation of shear force and bending moment then became the same as in model 1 and 2. It can therefore be argued that the differences of the variation of shear force and bending moment along the girders that were seen in the FE-models for load case 2 depend on the possibility for the cross-section to deform.

When the entire cross-section over the supports was constrained, as it was in model 1 and 2, it led to that no interaction between the girders, at the sections where the boundary conditions were applied, could take place. In the section where the load was applied the girders were allowed for some deflection and rotation and therefore there was some interaction between the girders. This was reflected in the shear force and moment diagrams for model 1 and 2, where some shear force and bending moment was taken by the girder farthest away from the load.

6.1.3 Case of moving vehicle loads

For the case of moving vehicle loads, it was seen that the variation of maximum sectional forces for all load positions along the girders was almost the same in all FE-models but model 1 showed slightly lower shear force and bending moment compared to model 2 and 3, see Figure 5.22 and Figure 5.23.

From the investigation of the load position that gave the design values along the girders, it was seen that both vehicles were positioned in the same transversal section of the bridge. The heaviest vehicle was placed at the vehicle line on the cantilever and the lighter vehicle was placed at the vehicle line created 4.5 meters from the cantilever.

At a first examination it appeared that the FE-models were explaining the load effect on the girders in a correct way for moving vehicle loads. However, when analysing what was seen in load case 1 and 2 for the different FE-models more in detail, the conclusion could be drawn that the similarity of the shear force in the FE-models rather was a consequence of the geometric symmetry, choice of the positions of the vehicle lines and how output data was presented.

In Chapter 5, it was explained how *Free Body Cut* presents output data if loads are included in the Free Body Cut surfaces. If a Free Body Cut surface is created in the same section where a load is applied to the bridge deck slab, the total shear force from that load is given in the weighted gravity centre of that Free Body Cut surface. In the case of moving vehicle loads, Free Body Cuts were created in all sections along the girders and the vehicle loads were therefore always included in a Free Body Cut surface, when consider axle loads. This means that the transversal distribution of vehicle loads to the girders was not taken into account in a correct way. The case study bridge was chosen to represent a modern Swedish bridge and the dimensions of the bridge cross-section can be seen as general. In Swedish bridge design, two axle loads from vehicles are defined. For one and two girder bridges, the load positions that govern the design values of shear forces along the girders is such that each girder will be designed to have enough capacity to carry the total load from both vehicles; the distribution to the second girder for a typical two-girder bridge will be negligible. For this reason, *Free Body Cut* can in practice be used even if the total shear force from the axle loads is included in the Free Body Cut surfaces. For that reason, all three FE-models can be used to describe sectional forces along the girders when designing with moving vehicle loads. However, because the output data was

calculated and presented by *Free Body Cut*, the interaction between the girders in model 3 became ignored in the results of shear forces.

The reason why model 1 showed slightly lower design values of shear forces, compared to model 2 and 3, depends partly on the position of the lightest vehicle. Two of the wheels were placed on the slab slightly outside the constrained part of the slab and the wheel pressure from these wheels was therefore distributed to both girders. If vehicle lines would have been created on the bridge deck slab between the girders only, for the case study bridge, the load effect on the girders would not have been similar in the three FE-models. In model 1, the load would be distributed transversally between the girders in a correct way. In model 2 and 3, the creation of Free Body Cut surfaces would result in that the girder where loads are included in a Free Body Cut surface would appear to carry the total load, regarding shear force.

Another reason why model 1 showed slightly lower design values of shear forces and also bending moments, compared to model 2 and 3, depends on the width of the part of the slab that was tied to the beam elements. To analyse this, model 1 was recreated and only the nodes in the slab centrically above the beam elements were constrained. Both the shear force and the bending moment along the girders did increase with this FE-model. This can be explained by that the rigidity of the slab in transversal direction of the bridge decreased when the constrained width of the slab decreased.

6.2 Advantages and disadvantages with the different FE-modelling techniques

6.2.1 Model 1

Model 1 was established with equivalent cross-sections of the girders, where the moment of inertia for the entire bridge cross-section was included. The calculations of equivalent cross-sectional properties required some work and if the geometry of the structure would have been complex the workload would have increased.

It can be argued how well the supports need to be modelled for the case study bridge. In model 1, the boundary conditions were applied to one node of the beam elements. It would have been more correct to offset the boundary conditions vertically, to the position of the bearings and add rotational springs to allow for some rotation of the girders. Another way to account for the rotation of the girders would have been to include the substructure in the FE-model.

Concerning the mesh, it was easy to generate a mesh in model 1 without distortions. A relatively coarse mesh of the beam elements converged for bending. To get an interaction between the girders and the bridge deck slab, the different element types were coupled by tie constraints. For sectional forces to be used in design for the girders it may be on the safe side to only constrain the nodes of the slab straight above the gravity centre of the girders.

Model 1 can be used to design the girders longitudinally but a supplemented analysis for the design of the bridge deck slab is needed. In model 1 the shell elements were given orthotropic properties without any stiffness in longitudinal direction of the bridge. Loads applied on the bridge deck slab were for that reason transferred directly to the girders, without any longitudinal distribution. The magnitude of the sectional forces in the bridge deck slab became mesh dependent but the integration of the

transversal sectional forces along the bridge proved that the slab gave a correct load effect on the girders.

Model 1 was established in three dimensions but the use of beam elements and orthotropic shell elements, without stiffness in longitudinal direction of the bridge, implied that a two-dimensional behaviour for the bridge deck slab and for the girders were considered separately. Because the shell elements were constrained to the beam elements, there was an interaction between the slab and the girders.

To perform the analysis of model 1, not much computational time was needed. The output data was easy to get with *path*. However, it was only the output data for the girders that was of interest for this bridge model. Furthermore, contour plots of sectional forces and displacements could be visualised, which was a good help for understanding the structural behaviour of the FE-model.

6.2.2 Model 2

In model 2 the girders were represented by shell elements that were given an offset at the position of the girders. The girders were modelled with equivalent cross-sections, but equivalent sectional properties were easy to find for the case study bridge and the geometry was easy to create.

The boundary conditions were applied along an edge of the shell. The boundary conditions were constraining the entire cross-section with the centre of gravity of that cross-section as rotational centre. In the same way as for model 1 it can be argued that rotational springs or the substructure should be included in the model, to allow for some rotation of the girders.

The mesh was easy to generate and there were only two directions to adjust the mesh for. An advantage with model 2 was that both *Free Body Cut* and *path* could be used to analyse the variation and distribution of sectional forces in the bridge deck slab and along the girders. Additionally, contour plots of the sectional forces and deformations could be used to visualise the results.

Model 2 described the structural behaviour in a correct way where the variation and distribution of loads could be analysed in its entirety in the bridge deck slab. To obtain sectional forces to be used in design of the bridge deck slab, the structural engineer can directly distribute the sectional forces in the slab by creating Free Body Cut surfaces over a chosen width. The post-processing of obtaining design values for the bridge deck slab then decreases substantially. However, Free Body Cuts need to be created in the mesh of the model before the FE-analysis is performed and therefore it needs to be known in advance in which sections sectional forces are of interest.

To get the total load effect along the girders, Free Body Cut surfaces were needed to be created over half the bridge cross-section along the girders. However, if loads were applied to the bridge deck slab, at sections where Free Body Cut surfaces were defined, the total loads were included in the calculation of sectional forces for those surfaces. Therefore, it was not possible to get sectional forces to be used in design in those sections of the girders. In sections without applied load, the load distribution was reflected in the results in a correct way. The interaction between the girders was not taken into account in a correct way since the girders in model 2 could not deform over the cross-section due to the use of shell elements.

6.2.3 Model 3

In model 3 the geometry of the case study bridge could be modelled without simplifications. All structural parts of the FE-model were assigned correct sectional properties.

The boundary conditions in model 3 were advantageously applied along an edge of the continuum elements in the bottom of the girders. The rotational stiffness of the girders became for that reason more similar to the stiffness of the case study bridge. Because model 3 was established by continuum elements, the boundary conditions constrained the bottom of the cross-section only and the cross-section was therefore able to deform in three directions.

It was time consuming to generate the mesh in model 3. This was because there were three directions to adjust the mesh for. If a dense mesh along one edge was preferred, but a coarse mesh was acceptable along another edge, it was very difficult to generate a structured mesh with regular shapes. Because model 3 was needed to be analysed with *Free Body Cut* to get sectional forces, it was important to get a structured mesh without distortions.

Continuum elements, used in model 3, are based on a strain-displacement relation. Contour plots of sectional forces could therefore not be visualised. In addition to this, the Free Body Cut surfaces was needed to be created before the FE-simulation, hence the most critical sections can mistakenly be ignored.

When continuum elements were used, simplifications of the structural behaviour were not needed. Model 3 was therefore describing the interaction between the girders in a correct way since the cross-section could deform in three dimensions. The slab could be designed in its entirety where the load distribution in longitudinal direction of the bridge was taken into account. The sectional forces in the bridge deck slab can be calculated over a distribution width directly by creating the Free Body Cut surfaces with widths equal to the distribution width. However, in the same way as in model 2, it is to be aware of that the shear forces in sections where loads are applied and included in a Free Body Cut surface is not calculated and presented in a correct way.

7 Conclusion

From the investigation of the specific load cases with concentrated loads, the conclusion can be stated that model 1 can be used to design the girders of the case study bridge for both shear forces and bending moments. The bridge deck slab distributes the load transversally between the girders in a correct way and the total load effect on the girders was proven to be correct. Despite this, the structural behaviour of the slab of the case study bridge cannot be described by model 1 due to the assigned orthotropic material properties. However, the slab is contributing to the interaction of the girders.

Model 2 and 3 can be used to design the girders as well as the bridge deck slab of the case study bridge for both shear forces and bending moments when specific load cases are of interest. Both FE-models have similar distribution of the load longitudinally in the bridge deck slab. However, it is to be aware of that the output data do not describe shear forces in the sections where loads are included in Free Body Cut surfaces in a correct way. In sections where no loads are included in Free Body Cut surfaces, the shear forces are correctly described. In design of the bridge deck slab, regarding shear forces, a section where load is applied is not governing the design values of the shear forces. For that reason *Free Body Cut* can be used to design the bridge deck slab regarding shear forces.

An advantage with model 3 compared to model 2 is that the interaction between the girders is much greater, due to the possibility for the cross-section in model 3 to deform.

For design with moving vehicle loads all FE-models can be used to describe sectional forces along the girders for the case study bridge. However, the advantage of the interaction of the girders regarding shear forces, which was seen in model 3 for the specific load cases, cannot be seen in the results from analysis of moving vehicle loads.

8 Further investigations

In this Master's project, the structural behaviour of three different FE-models was examined for a case study bridge. The purpose was to compare shear forces and bending moments and to study how longitudinal load distribution in the bridge deck slab and the interaction between the girders influenced these results, when the bridge deck slab was subjected to specific load cases. In addition to this, sectional forces for moving vehicle loads were compared to study the effect of the different modelling techniques on the design of the girders.

In TRVR Bro 11 (2011), there are two methods to determine distribution widths of shear forces in the bridge deck slab. The most common method is based on the relation between span length and slab thickness and the second method is based on the longitudinal load distribution obtained from FE-simulation. To do a comprehensive comparison of the structural behaviour for the different FE-models, design values of sectional forces in the bridge deck slab is still to be investigated. The most favourable way of determine distribution widths in the bridge deck slab according to TRVR Bro 11 (2011) could then be evaluated.

To be able to state general conclusions of the different modelling techniques in a design situation, supplementary analyses are needed. A further investigation to this Master's project could be to study other dimensions of the bridge structure, with cases of asymmetric geometries and horizontal curvature of the bridge. Also, the influence of boundary conditions compared to including the substructure in the FE-model could be examined. In addition to shear forces and bending moments also torsion could be studied.

When the case study bridge was represented by a FE-model established by continuum elements, it was seen that there was an interaction between the girders when the bridge deck slab was subjected to specific load cases of concentrated loads. However, when moving vehicle loads were studied, the interaction between the girders was not accounted for in the result due to how output data was calculated and presented. It could be further investigated if the interaction that was seen for specific load cases in model 3 could be utilized in a design situation by a reduction of the sectional forces along the girders. If a relation between the interaction of the girders and e.g. cross-sectional geometry, support conditions and material properties could be found, the advantages from continuum mechanics could be included in design of the girders.

9 References

Bathe, K.-J., 1996. *Finite Element Procedures.* New Jersey: Prentice-Hall, Inc. .

Blaauwendraad, J., 2010. *Plates and FEM Suprises and Pitfalls.* s.l.:Springer Science +Business Media B.V..

CEN, 2003. *Eurocode 1: Actions on structures, Part 2: Traffic loads on bridges, EN 1991-2.* Brussel: European Committee for Standardization.

Davidson, M., 2003. *Strukturanalys av brokonstruktioner med finita elementmetoden-Fördelning av krafter och moment.* Göteborg: Brosamverkan Väst.

Liu, G. R. & Quek, S. S., 2003. *The finite element method; A practical course.* Oxford: Butterworth-Heinemann.

Ottosen, N. & Petersson, H., 1992. *Introduction to the finite element method.* Edinburgh: Pearson Education Limited.

Rombach, G., 2011. *Finite-element Design of Concrete Structures Practical problems and their solutions.* Second edition ed. London: ICE Publishing.

Rugarli, P., 2010. *Structural Analysis with finite elements.* London: Thomas Telford.

Scanscot Technology AB, 2013. *Brigade/Plus User's Manual.* version 5.1 ed. s.l.:Scanscot Technology AB.

Simulia, 2009. *Abaqus 6.9 Analysis User's Manual, vol4.* USA: Simulia.

Trafikverket1, 2011. *TRVK Bro 11.* s.l.:Trafikverket.

Trafikverket2, 2011. *TRVR Bro 11.* s.l.:Trafikverket.

Appendix A. Model 1

In appendix A, additional investigations for model 1 are presented. The appendix addresses the convergence study and verification of model 1, that ensures the reliability of the established FE-model. How the coupling between the beam and shell elements was made and how this influenced the structural behaviour is also presented.

A.1 Convergence study of model 1

In the convergence study, the bridge deck slab was subjected to two different load cases, one consisting of a uniformly distributed load of 25 kN/m^2 applied to the entire bride deck slab and one of a line load of 15 kN/m applied at the edge of the cantilever. The self-weight was excluded in the convergence study. In the convergence study, only the nodes in the shell above the gravity centre of the girders were constrained to the beam elements.

To verify the mesh density two sections were studied. The first section was along one of the girders and the second section was transversally in the slab, at one end of the bridge.

The convergence study for the girders was studied when the bridge deck slab was subjected to the distributed load. The study showed a rapid convergence for bending moment and deflection with mesh refinement, see Figure 1 and Figure 2. For the girders it could be concluded that an element size of 2 meters was good enough to describe deflection, and 0.5 meter when bending moment was of interest.

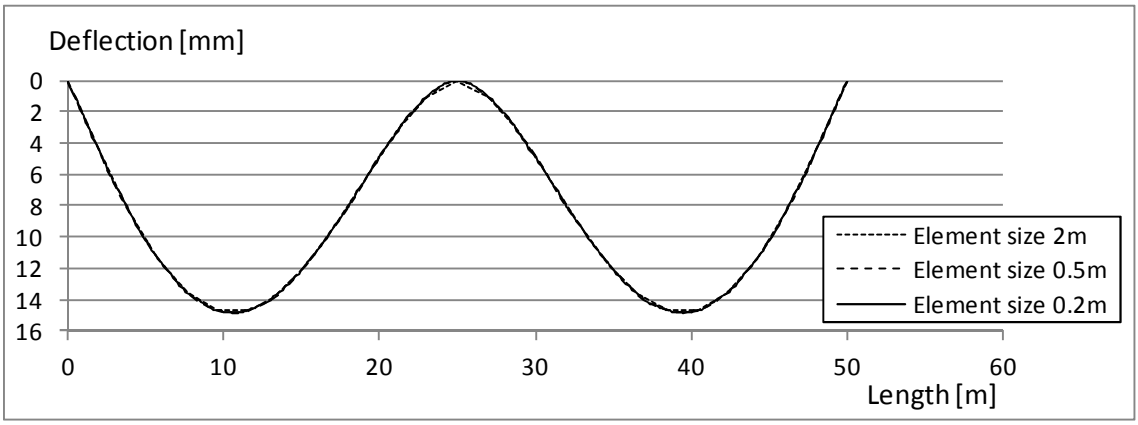

Figure 1 *Deflection for the girder with mesh refinement. The bridge deck slab was subjected to a uniformly distributed load of 25 kN/m^2.*

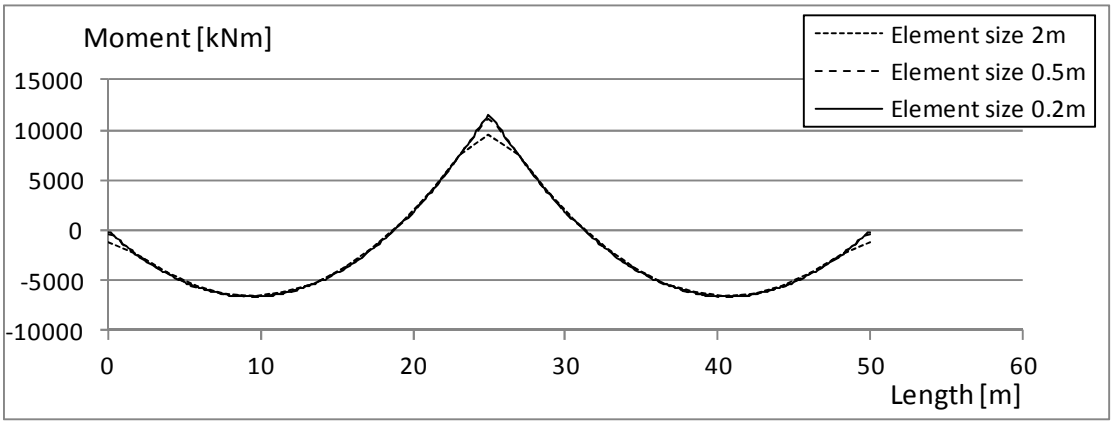

Figure 2 *Moment variation along the girder with mesh refinement. The bridge deck slab was subjected to a uniformly distributed load of 25 kN/m^2.*

The convergence of the bridge deck slab was done with respect to the uniformly distributed load and the line load. The shell element described deflection very well, even for a coarse mesh, which can be seen in Figure 3. To capture the bending moment, a denser mesh was needed and convergence was reached for an element size of 0.5 meters, see Figure 4 and Figure 5.

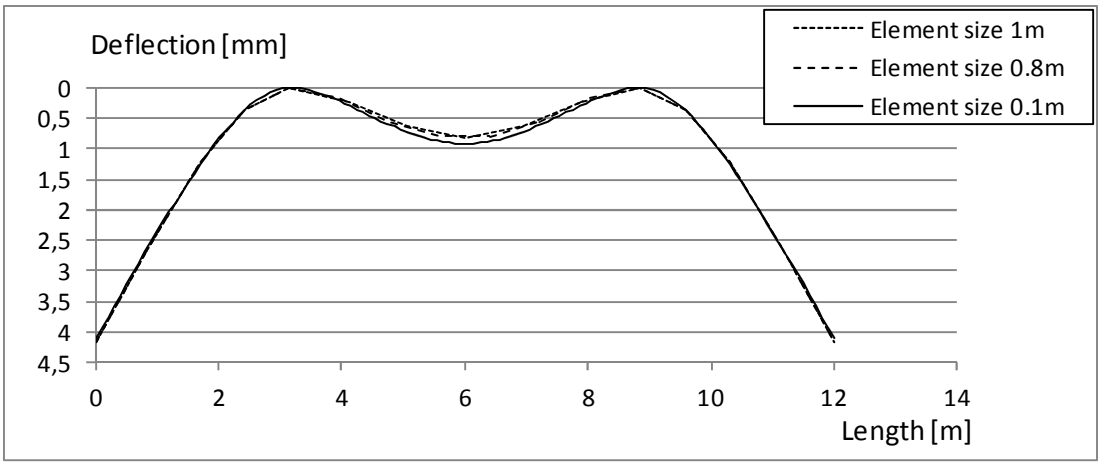

Figure 3 *Deflection for the bridge deck slab transversally with mesh refinement. The bridge deck slab is subjected to a uniformly distributed load of 25 kN/m^2.*

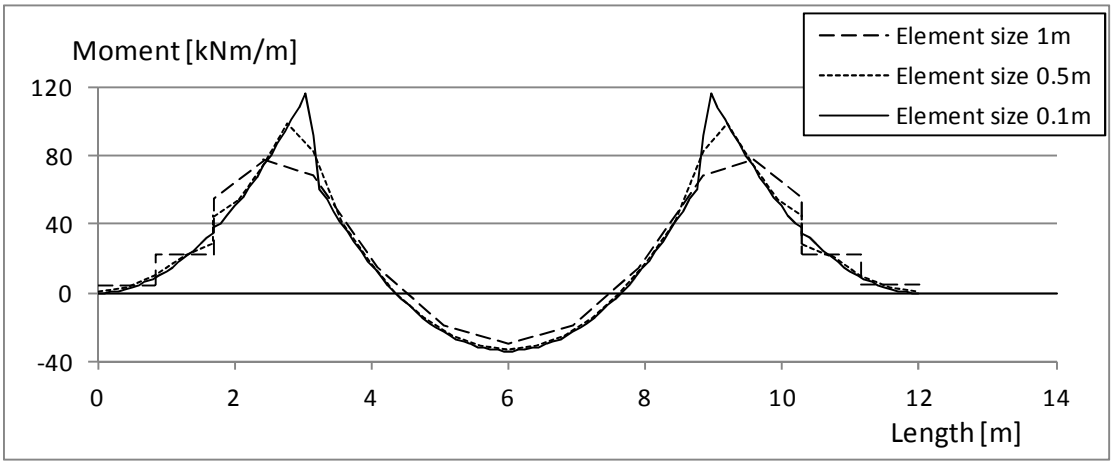

Figure 4 *Transversal moment for the bridge deck slab with mesh refinement. The bridge deck slab was subjected to a uniformly distributed load of 25 kN/m2.*

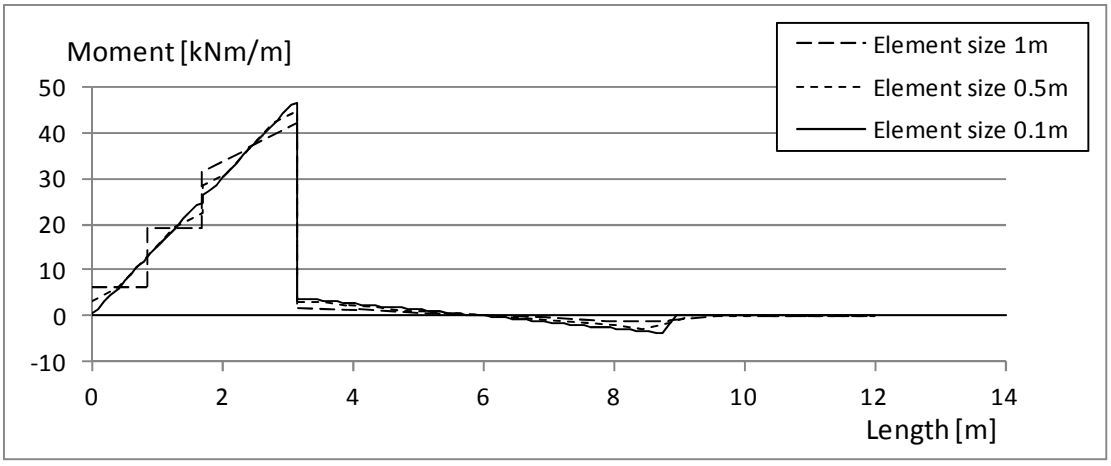

Figure 5 *Transversal moment for the bridge deck slab with mesh refinement. The cantilever of the bridge deck slab was subjected to a line load of 15 kN/m.*

The convergence study showed that an element size of 0.5 meter for the beam elements was good enough to describe moment. For the shell elements a mesh of 0.5 meter converged and in order to have regular shapes of the shell elements the elements were chosen to be quadratic with equal element sides.

A.2 Verification of model 1

To verify model 1, two different load cases were studied and the results from the FE-model were compared to hand calculations. In the first load case the bridge deck slab was subjected to an evenly distributed load of 25 kN/m^2 and in the second load case a line load of 15 kN/m was applied along the edge of the cantilever of the bridge. The data used in the analytical analysis can be seen in Table 1.

Table 1 Data used in the analytical analysis.

Length of the bridge span	l_{span}	25 m
Width of the bridge	d_{slab}	12 m
Moment of inertia	I_x	0,685 m^4
Young's modulus	E	34 GPa
Uniformly distributed load	q	25 kN/m^2
Uniformly distributed line load	$q_{lineload}$	15 kN/m

For the distributed load the analytical result and the result from the FE-model, for the maximum field moment and support moment for the girders longitudinally of the bridge, were compared. To ensure that the cross-section was given the correct cross-sectional properties, the maximum deflection was compared as well. The calculations and the analytical results for the bending moment over the mid support, the maximum field moment and maximum deflection, can be seen in Equation (1), (2) and (3), respectively.

$$M_{support} = \frac{q*l_{span^2}}{8} * \frac{d_{slab}}{2} = 11\,720\ kNm \quad (1)$$

$$M_{field} = \frac{9q*l_{span^2}}{128} * \frac{d_{slab}}{2} = 6\,592\ kNm \quad (2)$$

$$w_{max} = \frac{0.521*q*l_{span^4}*\frac{d_{slab}}{2}}{100EI_x} = 13.1\ mm \quad (3)$$

To ensure that the structural behaviour of the bridge deck slab in transversal direction of the bridge was correct, the transversal bending moment close to the girder was verified when the cantilever of the bridge was loaded with the line load. When subjected the cantilever to a line load, it gave rise to a statically determinate moment at the girder, close to the load. Equation (4) shows the calculated bending moment.

$l_{cantilever} = 3.15\ m$

$$M_{cantilever} = q_{lineload} * l_{cantilever} = 47.25\ \frac{kNm}{m} \quad (4)$$

In the table below, see Table 2, the bending moment and deflection that was determined analytically are compared to the values given in the FE-model. It can be seen that the bending moments from the FE-model agreed well with the hand calculations but that the deflection became 13 percent greater in the FE-model compared to the analytical value. It can be concluded that the established model explained the bending moment in a good way and the results in further investigations can be trusted.

Table 2 *Comparison between hand calculations and the results from the FE-model.*

	Hand calculations	**FE-model**	**Ratio**
$M_{support}$	11 720 kNm	11 440 kNm	0.98
M_{field}	6 592 kNm	6 606 kNm	1.00
w_{max}	13.1 mm	14.8 mm	1.13
$M_{cantilever}$	47.25 kNm/m	46.47 kNm/m	0.98

A.3 Coupling of beam and shell element with tie constraints

When the bridge was modelled it was important to evaluate which structural behaviour that was to be achieved. In the transversal direction the width of the supporting girders was relatively big compared to the length of the span, hence the width of the girders had a significant influence on the load effect.

Rombach (2011) describes how to model the couplings between a one-way slab and supporting walls in the best way. Figure 6 show four different ways of modelling the supports where three of the approaches (a), (b) and (c), are recommended to use and shows a good correlation between the result in a FE-model and the exact solution. The first line support, (a), is a pinned support of one node only. In (b), the pinned support is coupled to a number of nodes in the slab to simulate an infinite stiff element that can rotate around the centre node and (c) shows a three-dimensional model. The line support (d) is a pinned support of all nodes above the support and should not be used.

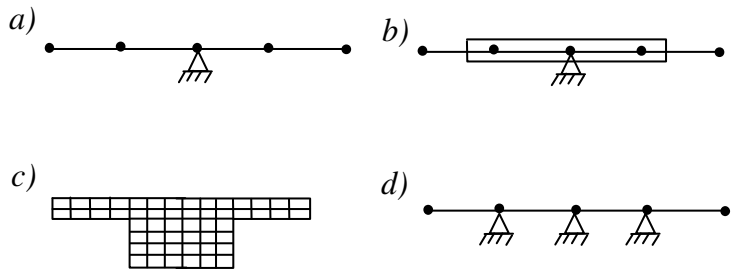

Figure 6 *Different ways of modelling line supports of slabs; a) pinned support of one node, b) pinned support of one node and coupling, c) three-dimensional model and d) pinned support of all nodes above the support.*

The bridge deck slab that was modelled with orthotropic shell elements, without any stiffness in longitudinal direction of the bridge, was supported on two girders. When the tie constraints were used to couple the beam elements and the shell elements, the structure could be compared to the theory described by Rombach (2011). It should however be noted that the girders could not be seen as rigid supports since they could deflect when the slab was loaded. Therefore, there were interdependency between the girders and the bridge deck slab in another way than between a slab on supporting walls. The theory could for that reason not be compared directly and adopted fully for the actual case study bridge in this Master's project.

When modelling the bridge with beam and shell elements the coupling between the different element types could be made in different ways. In this Master's project the tie constraints were used. It was important to connect different element types in a correct way so that the effect from one element was reflected in the neighbouring elements (Rugarli, 2010). Because the shell elements and the beam elements had a different number of degrees of freedom, the tie constraints transferred the effects from the slave elements to the master elements. In this Master's project the shell elements were chosen to be slave elements and the beam elements were chosen to be master elements. The coupling with tie constraints was made by a node to surface connection. By specifying a position tolerance, all nodes in the slave region that laid within the tolerance were constrained to the nodes in the master region. The coupling was stiff and did not allow for any deformations.

When the nodes between the beam elements and shell elements were constrained, an assumption that the slab was undeformed above the girders was made, i.e. there was no curvature. Due to the high difference in stiffness between the beam and slab sections, this assumption could be seen as correct.

When the deflection and moment diagrams were studied in the transversal direction in the bridge deck slab, see Figure 7 and Figure 8, it was obvious that the number of constrained nodes in transversal direction affected the structural behaviour. Both the bending moment and the deflection were zero over the region that was constrained because no deformations of the cross-section of the girders were allowed.

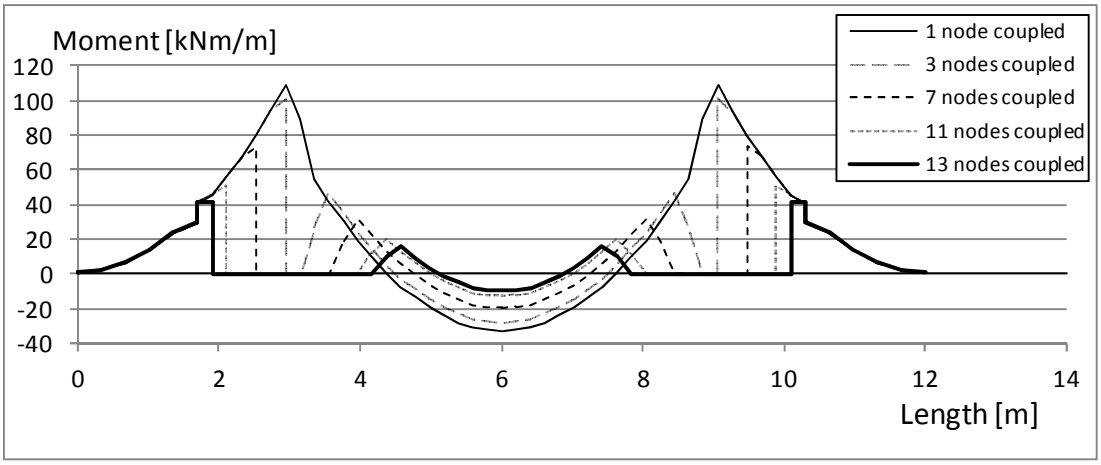

Figure 7 *Moment diagram in transversal direction where different numbers of shell nodes were constrained to the beam nodes. Between 4.4 and 7.6 meter, there was a critical region in design. A uniformly distributed load of 25 kN/m^{2}was applied on the bridge deck slab.*

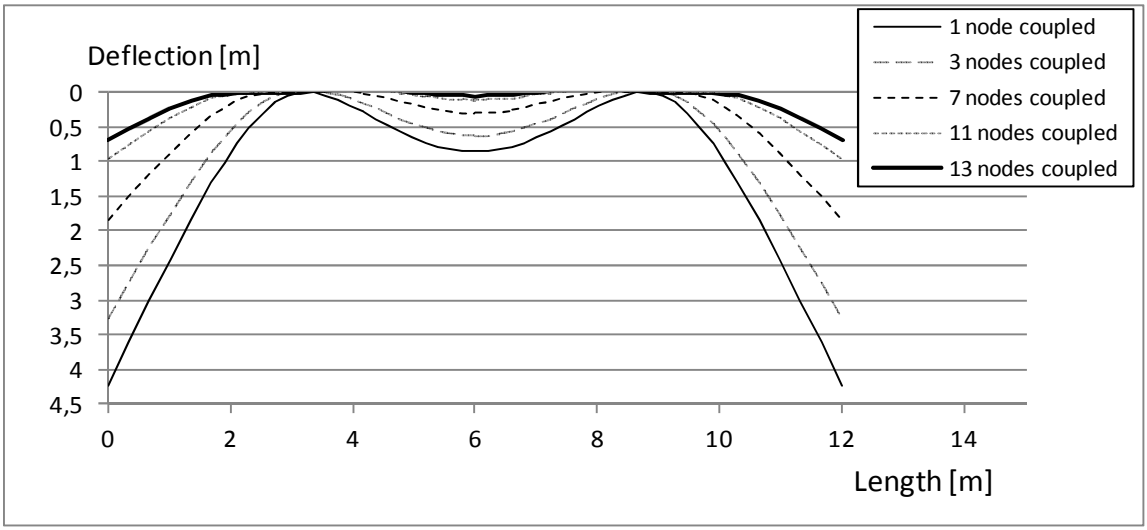

Figure 8 *Deflection diagram in transversal direction in the field, where different number of shell nodes were constrained to the beam nodes. A uniformly distributed load of 25 kN/m^{2}was applied on the bridge deck slab.*

In the moment diagram, see Figure 7, different magnitudes of the bending moment in the slab over the girders were seen depending on the number of constrained nodes. If only one node in the transversal direction in the slab was coupled, namely the node above the centre of the girder, the slab was free to rotate in relation to the girder. If several nodes were coupled, the transversal stiffness increased.

Without further thought, it was easy to believe that the case of one coupled node gave the design moment, but after further reasoning this must not necessary be true. In Figure 9, only the most extreme diagram are shown for the bending moment, i.e. the case of one constrained node only and the case when all nodes above the girders were constrained.

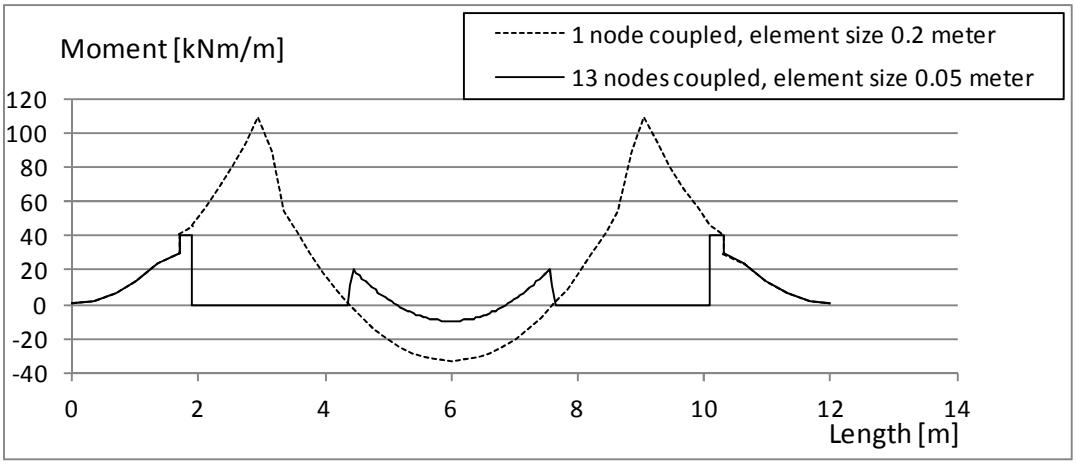

Figure 9 *Moment diagram of a section in transversal direction. The curves represent the bending moment if one node in the shell was constrained to the beam nodes and if all nodes in the shell over the girders were constrained to the beam nodes.*

In the region 4.4 - 7.6 meters it was seen that there was small or no need for top reinforcement in the slab between the girders, if the graph showing one coupled node was believed. Instead, the need for bottom reinforcement was essential. When the entire area in the slab above the girders was constrained, the support moment occurred in the connection of the slab and the girders. If this way of modelling was believed, the support moments between the girders gave a need of top reinforcement in the slab that was not taken into account if only one node in the bridge deck slab was constrained. In field, the need for bottom reinforcement decreased substantially. In a design situation it should be remembered that the inner level arm for the girder section is much greater than for the slab. Depending on the difference of level arm and difference of maximum bending moment in the top of the section, it is not obvious which way of coupling that governing the design values of the sectional forces.

In model 1, it was decided to constrain a width of 2.6 meters of the shell to the beam nodes. This was due to reflect the same structural behaviour of the bridge deck slab as in model 2 and 3.

Appendix B. Model 2

In appendix B, additional investigations for model 2 are presented. The appendix addresses the convergence study and verification of the model that ensures the reliability of the established FE-model.

B.1 Convergence study of model 2

The mesh in the bridge deck slab in model 2 was chosen considering the convergence study made for model 1. An element size of 0.5 meter described the structural behaviour satisfactorily.

To study if the girders described the structural behaviour in a correct way, the bending moment and deflection in the girders longitudinally was verified, see the section Verification of model 2.

In model 2, the feature *Free Body Cut* was used. A Free Body Cut must contain a certain amount of elements for the sectional forces to converge. This was studied for Free Body Cut surfaces, created over a width of 0.5 meter, in a transversal section in the bridge deck slab. Figure 10 and Figure 11 show the variation of shear force and bending moment, respectively, along the transversal section. It was seen that an element size of 0.25 meter described the structural behaviour satisfactorily.

To have the same size of the mesh as in model 3, the mesh was chosen to 0.125 meter in the bridge deck slab, see Appendix C. This was due to be able to compare the results from the FE-models independently of the mesh.

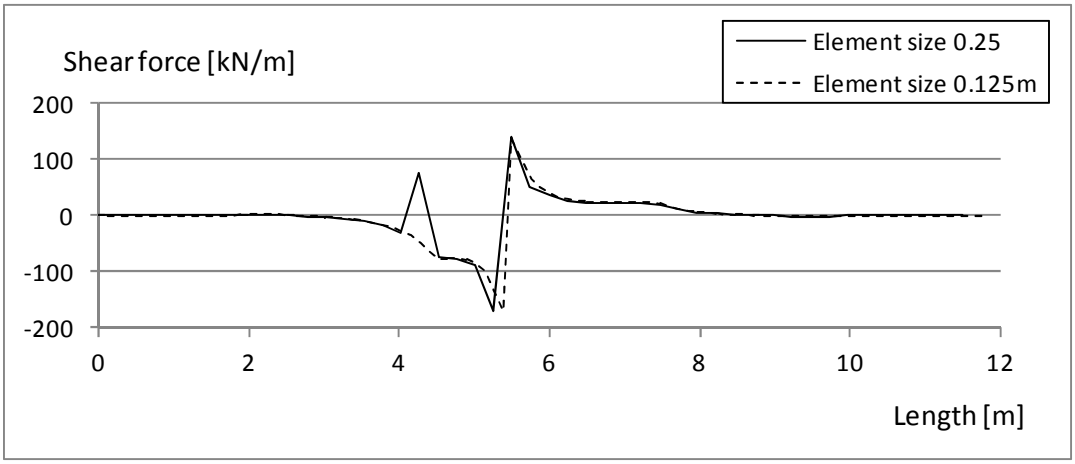

Figure 10 *Transversal shear force along a transversal section in the bridge deck slab, created by the feature Free Body Cut.*

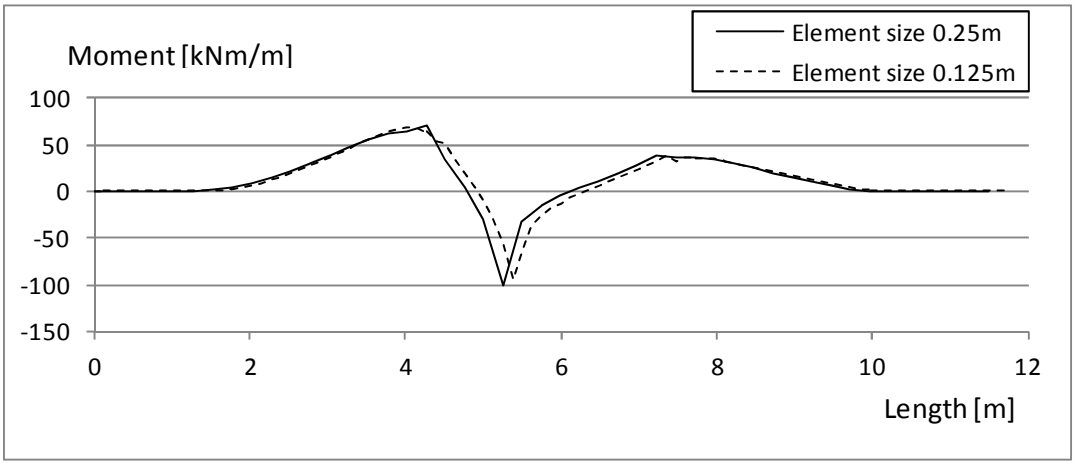

Figure 11 *Transversal bending moment along a transversal section in the bridge deck slab, created by the feature Free Body Cut.*

B.2 Verification of model 2

The verification of model 2 was made in the same way as for model 1. For the explanation of the verification and input data, see Appendix A.

The analytical values of the bending moment over the mid support, the maximum field moment and maximum deflection, is shown in Equation (5), (6) and (7) respectively. The statically determined transversal bending moment close to the girder is shown in Equation (8).

$$M_{support} = \frac{q*l_{span^2}}{8} * \frac{d_{slab}}{2} = 1.172 * 10^4\ kNm \tag{5}$$

$$M_{field} = \frac{9q*l_{span^2}}{128} * \frac{d_{slab}}{2} = 6.592 * 10^3\ kNm \tag{6}$$

$$w_{max} = \frac{0.521*q*l_{span^4}*\frac{d_{slab}}{2}}{100EI_x} = 13.1\ mm \tag{7}$$

$$l_{cantilever} = 1.775\ m$$

$$M_{cantilever} = q_{lineload} * l_{cantilever} = 26.6\ \frac{kNm}{m} \tag{8}$$

In the table below, see Table 3, the bending moment and deflection determined analytically are compared to the results from the FE-model. It was seen that the bending moments from the FE-model agreed well with the hand calculations. The deflection became 8 percent greater in the FE-model compared to the analytical value. It was concluded that the established model described bending moment in a good way and the results in further investigations can be trusted.

Table 3 *Comparison between hand calculations and the results from the FE-model.*

	Hand calculations	**FE-model**	**Ratio**
$M_{support}$	11 720 kNm	11 750 kNm	1.00
M_{field}	6 592 kNm	6 580 kNm	1.00
w_{max}	13.1 mm	14.1 mm	1.08
$M_{cantilever}$	26.26 kNm/m	26.70 kNm/m	1.02

Appendix C. Model 3

Appendix C, presents additional investigations made for model 3. In order to understand which continuum element type that was best suited for the investigation, convergence studies were made for different element types.

To ensure the reliability of the model, convergence and verification studies are presented. To increase the understanding of how to use the feature *Free Body Cut* and interpret the results correctly an additional investigation of this is also presented.

C.1 Convergence study of model 3

The convergence study of model 3 was made for the same load cases as for model 1 and 2. A distributed load of 25 kN/m^2 was applied uniformly on the bridge deck slab and a line load of 15 kN/m was applied at the edge of the cantilever.

When examined the bending moment, the feature *Free Body Cut* was used. For the bending moment in the girders, half of the bridge cross-section was included in the Free Body Cut surfaces. To study the bending moment transversally in the bridge deck slab, the Free Body Cut surfaces were created in the middle of the span, where two element edges longitudinally was included. The section where the deflection of the girder was studied was created along the lower edge of one of the girders.

Since the mesh of a continuum can be adjusted in three directions the element size longitudinally was kept constant to 0.5 meter while examined the dependency of the number of elements over the height of the girders and bridge deck slab. When convergence was reached, the element sides were adjusted to not exceed a ratio of 2:1.

It was found in the convergence study that *Free Body Cut* did not calculate the bending moment correctly when second order elements were used. Therefore it was decided to use linear element types. In a bending induced problem it is favourable to use the element type C3D8I with incompatible modes instead of C3D8R with reduced integration (Simulia, 2009). However, the convergence study was made to compare these two element types.

In order to differentiate the notations of the curves in the graphs in the diagram legends the first number tells how many elements that were used over the height of the girders and the second number tells the number of elements that were used over the cantilever and bridge deck slab between the girders.

Looking at the convergence of the bending moment at the girders it was seen that both element types converged for a very coarse mesh with three elements over the height of the girders and one element in the slab, see Figure 12. However, when examined the deflection it was recognised that the element type C3D8I converged more rapidly compared to the element type C3D8R, see Figure 13. It should be noted that the bending moment and deflection converged in the opposite way than structural elements. A converged bending moment was lower than a moment that had not converged.

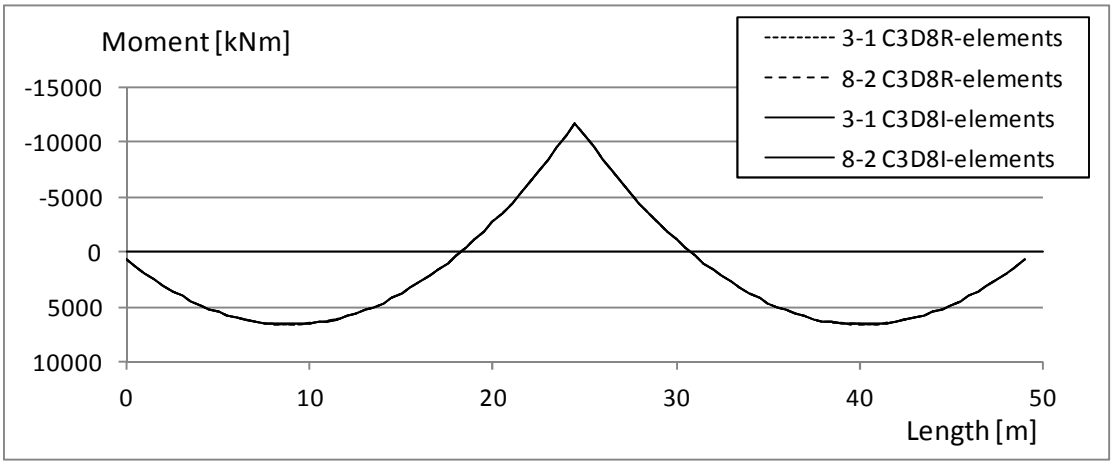

Figure 12 *Bending moment along the girders with mesh refinement. The element types C3D8R and C3D8I were used. A uniformly distributed load of 25 kN/m^2 was applied on the bridge deck slab.*

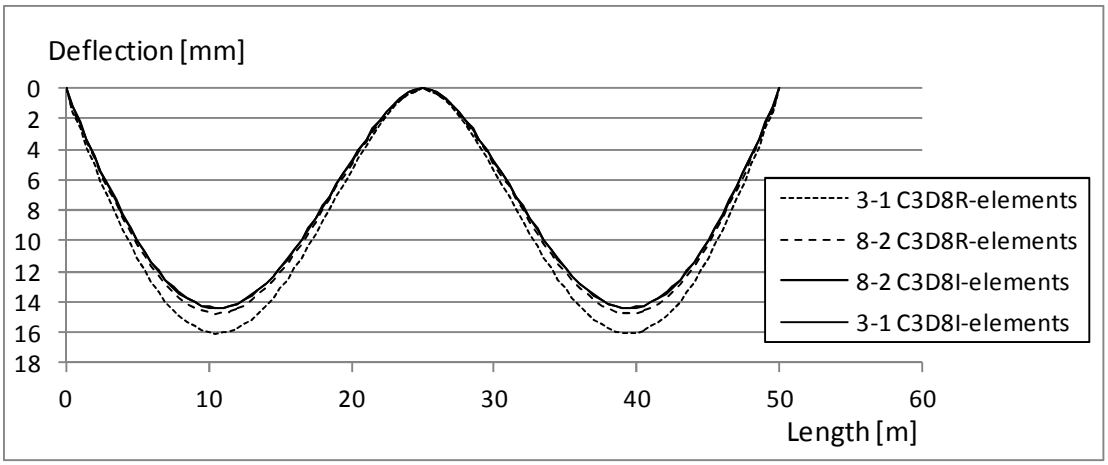

Figure 13 *Deflection along the girders with mesh refinement. The element types C3D8R and C3D8I were used. A uniformly distributed load of 25 kN/m^2 was applied on the bridge deck slab.*

Investigating the bending moment transversally demands for a higher number of elements over the height of the girders and bridge deck slab compared to the convergence of the bending moment at the girders. This was because the structure was not as slender in the transverse span compared to the longitudinal span. The convergence for moment transversally for the different element types is presented in Figure 14 and Figure 15. When compared the capability for the different element types to describe moment transversally, it was clear that the element types distinguished more from each other than if the bending moment along the girders was studied. The reason why the diagrams in Figure 14 and Figure 15 were assymetric was due to the creation of Free Body Cuts. When generating a Free Body Cut, a normal vector to the Free Body Cut surfaces was needed to be formulated. The exposed side of the cut is dependent on the direction of the normal vector and if the vector was given in the direction from the less stiff part to the more stiff part of the structure, the bending moment over the support was captured, otherwise it was not.

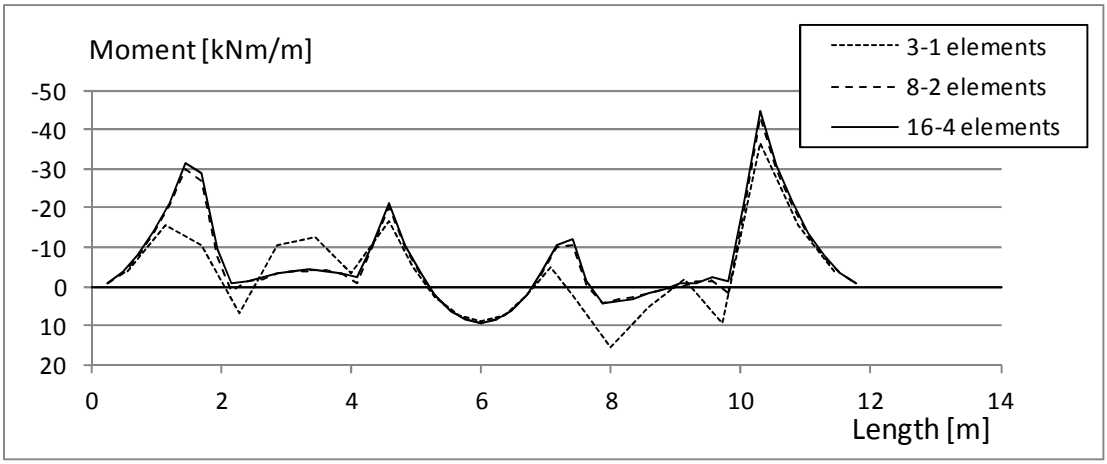

Figure 14 *Transverse moment with mesh refinement when the element type C3D8R was used. A uniformly distributed load of 25 kN/m^2 was applied to the bridge deck slab.*

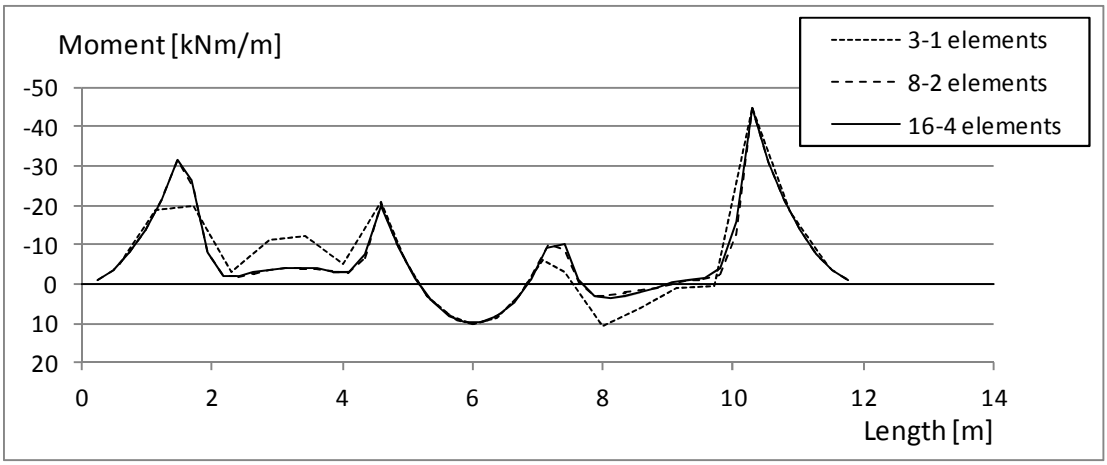

Figure 15 *Transverse moment with mesh refinement when the element type C3D8I was used. A uniformly distributed load of 25 kN/m^2 was applied to the bridge deck slab.*

The convergence of the deflection transversally, see Figure 16, distinguished the incompatible mode elements. It should be noticed that the section where deflection was examined was chosen to be in the mid span where the largest deflection was to be expected. Since the mesh also influences the deflection of the girders longitudinally, it is to be remembered that the chosen mesh does influence the convergence of load effects in both longitudinal and transverse direction.

It was seen that the elements with reduced integration was not good to describe bending for the coarse mesh with three elements over the height of the girders and one element over the bridge deck slab. To be able to examine the convergence of the deflection, the C3D8R elements with the coarsest mesh was excluded, see Figure 16.

As for the convergence of the girders it was seen that C3D8I did describe bending better than C3D8R even in transversal direction of the slab. All the three curves where C3D8I was used, described deflection very well while C3D8R did not converge for the mesh refinement that was performed.

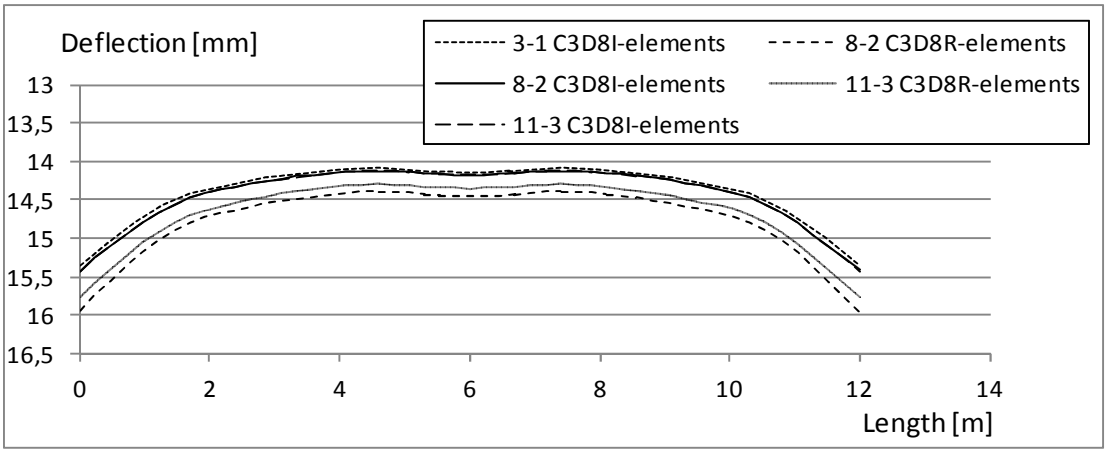

Figure 16 *Deflection transversally with mesh refinement and different element types. A uniformly distributed load of 25 kN/m^2 was applied on the bridge deck slab.*

When the line load was applied at the edge of the cantilever, only the transverse moment variation was examined, see Figure 17 and Figure 18. The results showed that both element types were able to capture the statically determinate moment even for coarse mesh. However, the incompatible mode elements converged more rapidly.

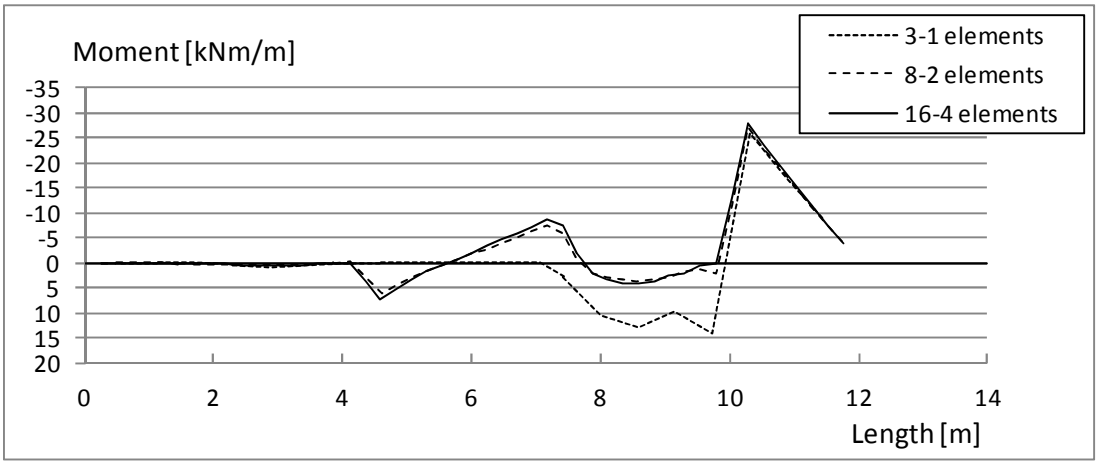

Figure 17 *Transversal moment for the bridge deck slab with mesh refinement. The cantilever of the bridge deck slab was subjected to a line load of 15 kN/m. The element type C3D8R was used.*

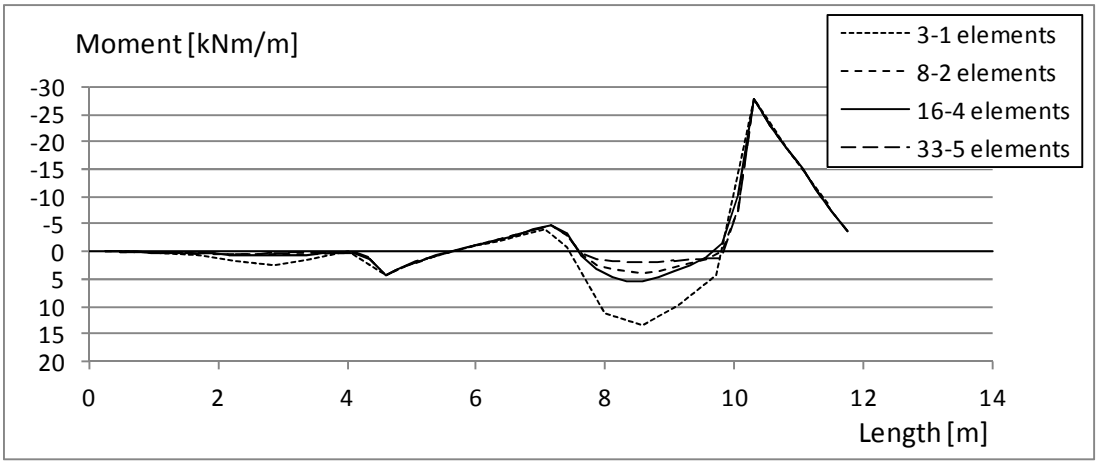

Figure 18 *Transversal moment for the bridge deck slab with mesh refinement. The cantilever of the bridge deck slab was subjected to a line load of 15 kN/m. The element type C3D8I was used.*

The convergence study for the continuum elements showed that more elements over the height of the cross-section gave a more accurate way of describing bending. The comparison between the element types C3D8R and C3D8I showed that incompatible mode elements were preferably used if bending was to be described. The conclusion from the convergence study was that the element type C3D8I should be used in the analyses and that 8 and 2 elements should be used over the girders and bridge deck slab, respectively.

The convergence was performed with a constant element length of 0.5 meters longitudinally and transversally in the bridge deck slab, and in order to stay within the recommendations of a ratio of 2:1 between the element sides, the elements were adjusted to 0.25 meters. A control was made with the adjusted mesh to be sure that it had converged.

As mentioned earlier, the feature *Free Body Cut* was used in model 3, to get sectional forces. To know how many elements a Free Body Cut must contain to show the correct magnitude of the bending moment and shear force, Free Body Cut surfaces were created in a transversal section in the bridge deck slab. The Free Body Cut surfaces were created with a width of 0.5 meter.

Figure 19 and Figure 20 present the shear force and bending moment, respectively, along the transversal section in the bridge deck slab. It was seen that an element size of 0.25 meter has not converged. An element size of 0.125 meter, show the same variation of shear force and bending moment as the same graphs in the convergence of model 2. An element size of 0.125 meter could for that reason be concluded as converged.

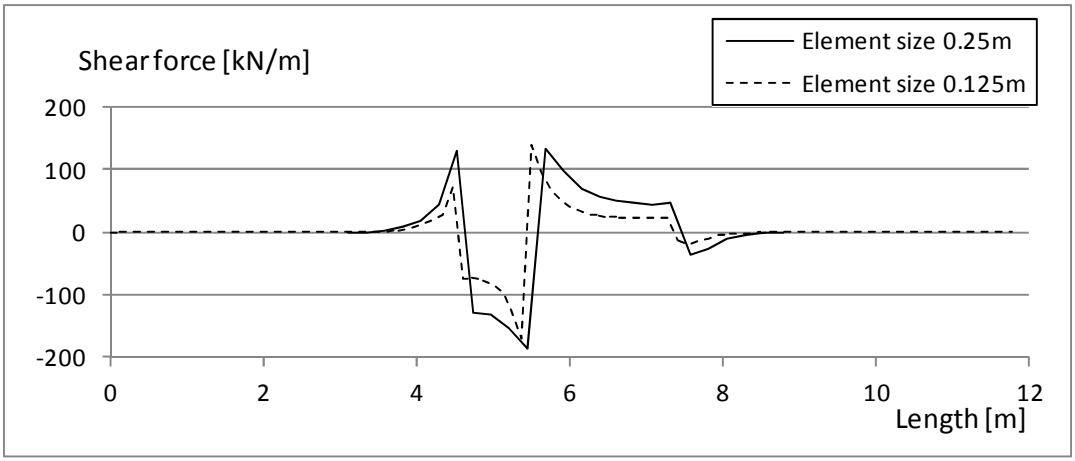

Figure 19 *Transversal shear force along a transversal section in the bridge deck slab, created by the feature Free Body Cut.*

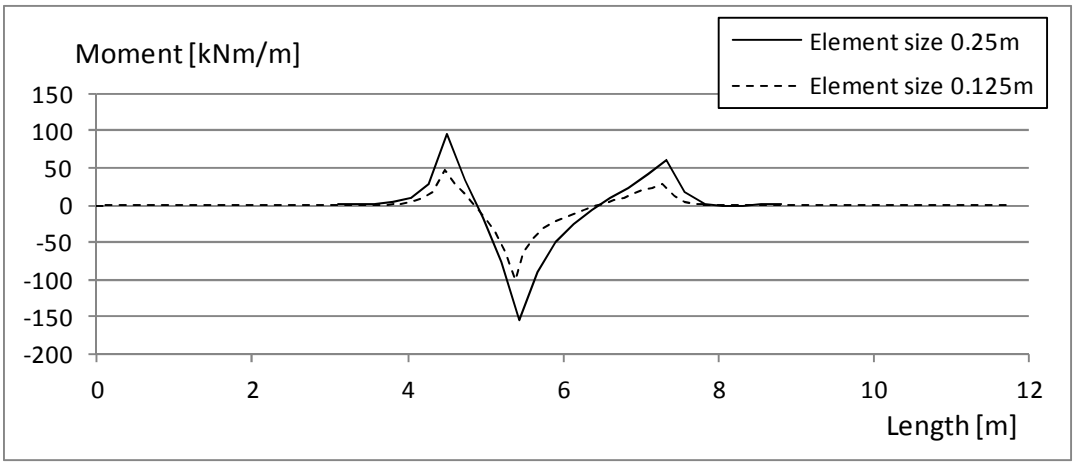

Figure 20 *Transversal bending moment along a transversal section in the bridge deck slab, created by the feature Free Body Cut.*

C.2 Verification of model 3

The verification of model 3 was made in the same way as model 2 and 3. For the explanation of the verification and input data, see Appendix A.

The analytical values of the bending moment over the mid support, the maximum field moment and maximum deflection, are shown in Equation (9), (10) and (11), respectively. The statically determined transversal bending moment close to the girder is shown in Equation (12).

$$M_{support} = \frac{q * l_{span^2}}{8} * \frac{d_{slab}}{2} = 1.172 * 10^4 \; kNm \tag{9}$$

$$M_{field} = \frac{9q * l_{span^2}}{128} * \frac{d_{slab}}{2} = 6.592 * 10^3 \; kNm \tag{10}$$

$$w_{max} = \frac{0.521 * q * l_{span}{}^4 * \frac{d_{slab}}{2}}{100 E I_x} = 13.1\ mm \quad (11)$$

$$l_{cantilever} = 1.7\ m$$

$$M_{cantilever} = q_{lineload} * l_{cantilever} = 25.5\ \frac{kNm}{m} \quad (12)$$

In the table below, see Table 4, the bending moment and deflection determined analytically is compared to the results from the FE-model. It was seen that the bending moments from the FE-model agreed well with the hand calculations. The deflection became 8 percent greater in the FE-model compared to the analytical result. It was concluded that the established model described bending moment in a good way and the results in further investigations can be trusted.

Table 4 *Comparison between hand calculations and the results from the FE-model.*

	Hand calculations	FE-model	Ratio
$M_{support}$	11 720 kNm	11 750 kNm	1.04
M_{field}	6 592 kNm	6 580 kNm	1.09
w_{max}	13.1 mm	14.2 mm	1.08
$M_{cantilever}$	25.5 kNm/m	27.5 kNm/m	1.00

C.3 Influence of the normal vector for a Free Body Cut

As mentioned earlier in Appendix C, the sectional forces along sections where *Free Body Cut* is used are dependent on the normal vector to the Free Body Cut surfaces. If the normal vector was given in the direction from the less stiff section to the more stiff section the support values were captured but otherwise they were not.

In Figure 21, the variation of bending moment transversally in the bridge deck slab is presented along a section with *Free Body Cut*. The mesh in the bridge deck slab was 0.25 meter. For the two curves, the normal vectors for the Free Body Cut surfaces were defined in different ways and the curves were for that reason not equal. The symmetric curve presents the variation of bending moment if the normal vectors were defined from the less stiff sections to the more stiff sections when the stiffness where the cross-section of the bridge changed. The other curve presents the bending moment if the normal vectors were defined in the same direction in all Free Body Cuts. The bridge deck slab was subjected to a uniformly distributed load of 25 kN/m^2.

Further investigations showed that for a very dense mesh, the definition of the direction of the normal vectors became less important. Along a section, transversally in the bridge deck slab, a mesh of 0.02 meters showed a moment variation that was

symmetric even if the direction of the normal vectors were the same for all Free Body Cut surfaces. Because of this, the user of the FE-software has two options when defining the Free Body Cuts. The direction of the normal vectors to the Free Body Cut surfaces have to be defined from the less stiff sections to the more stiff sections of the bridge or the mesh must be dense enough to omit the dependency of the definition of the direction of the normal vectors.

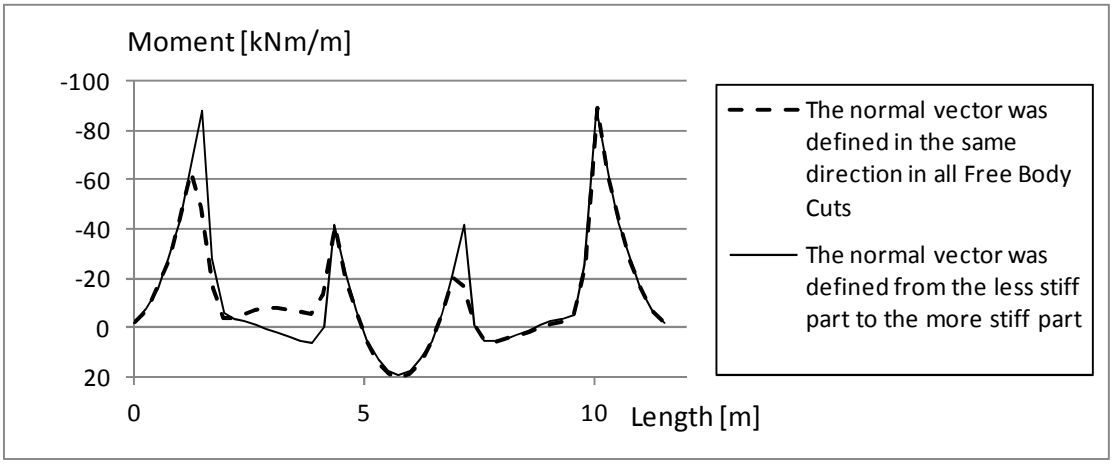

Figure 21 *Variation of bending moment transversally in the bridge deck slab if the normal vectors to the Free Body Cut surfaces were defined in different ways. A uniformly distributed load of 25 kN/m^2 was applied on the bridge deck slab.*

Appendix D. A study of the support conditions of the slab

To examine the structural behaviour of the slab close to the girders for the three FE-models, the transversal bending moment was compared to analytical models, where the moment was calculated from beam tables. For load case 1, analytical two-dimensional models of both simply supported and fully rigid supports were studied and for load case 2 the statically determinate bending moment was studied.

The applied load was known and from the established models the distance between the support moments and the section where the load was applied was measured. The theoretical span for load case 1 and the length of the cantilever for load case 2 for the different FE-models differed slightly, since the girders were represented differently.

D.1 Load case 1

The different support conditions for the analytical two-dimensional models and the FE-models are presented in Figure 22. The transversal moment distribution was integrated along three sections in the bridge deck slab along the bridge. Two sections were close to the girders and one was through the loading point. The variation of the total bending moment in transversal direction of the bridge is presented and compared to the results from the analytical models in Figure 23.

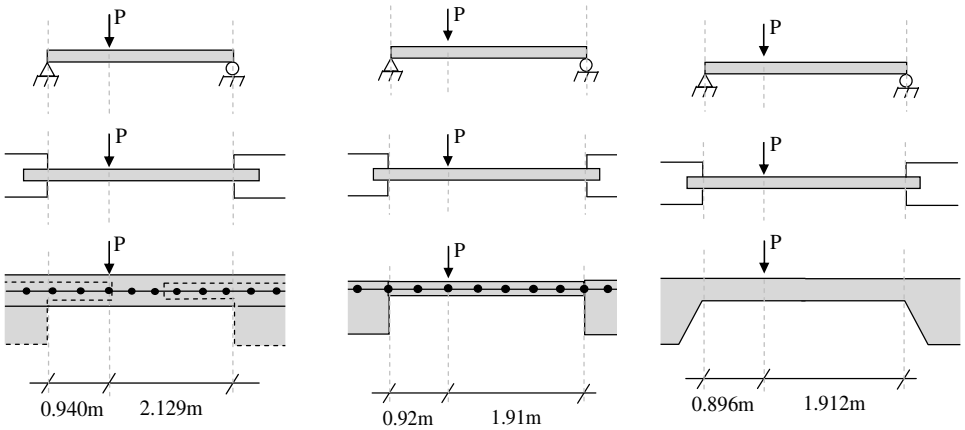

Figure 22 Support conditions for; (a) model 1, (b) model 2 and (c) model 3.

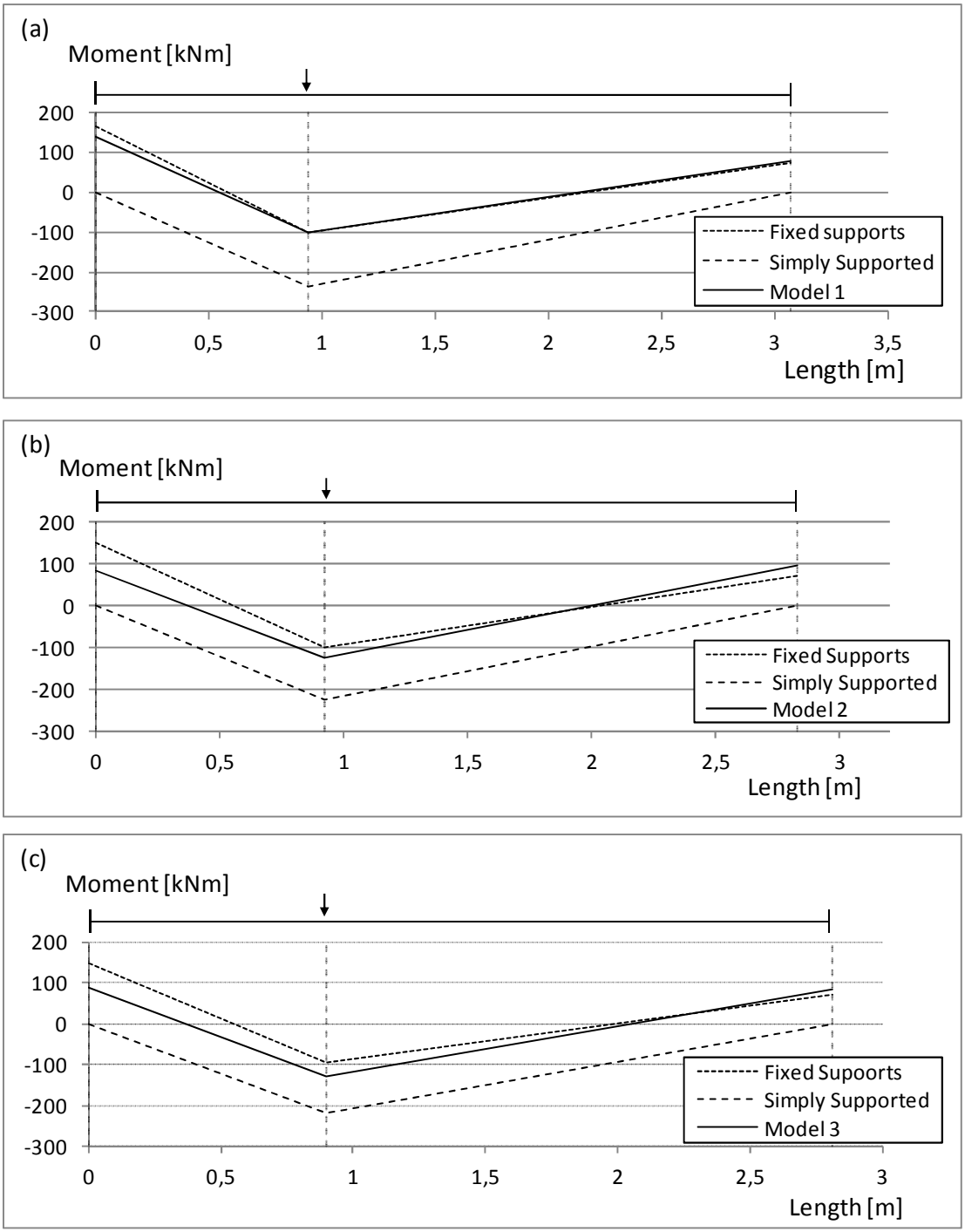

Figure 23 *Variation of the bending moment for the FE-models and a case of simply supported and fixed supports, when concentrated load of 360 kN was applied to the bridge deck slab between the girders. The variation was shown for; (a) model 1, (b) model 2 and (c) model 3.*

From Figure 23 it was seen that all FE-models gave an interaction that represented more closely the condition of fixed supports than simply supports. It was also seen that the support moment at the girder closest to the load was smaller than for fixed supports, but that the support moment at the girder farthest away from the load was slightly higher than for a fixed support condition. The same observations holds for all FE-models, but were more significant in model 2 and 3.

Since none of the established FE-models corresponded to fixed supports or a simply supported condition, the correctness of the models was checked: a straight line between the support moments in Figure 23 was created and the total moment between the line and the maximum field moment was calculated. The total moment should then correspond to the theoretical moment under the load for the corresponding simply supported beam, see Figure 24.

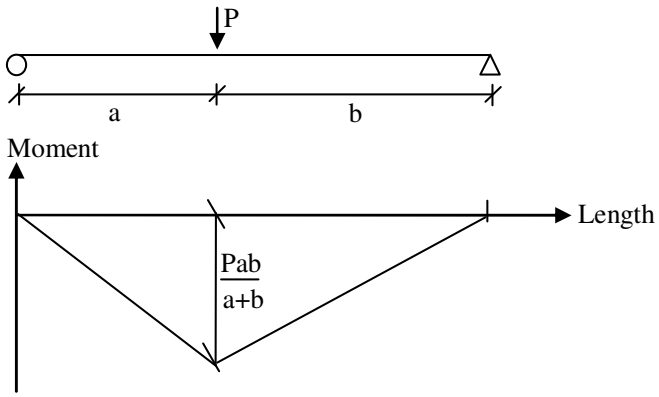

Figure 24 *Schematic moment diagram, showing how the total bending moment between the maximum field moment and the drawn line was calculated for a simply supported beam.*

Table shows a comparison between the total bending moment from FE-analysis and the theoretical bending moment. All models deviated to some extent and gave a total moment lower than expected. It was seen that the chosen averaging of nodal forces, from the output data, influenced the integrated value due to approximation errors. The bending moments shown in Table 5are integrated values from three longitudinal sections and therefore the deviation might be significant.

Table 5 *Comparison of the total bending moment in the FE-models and the analytic model.*

	Model 1	**Model 2**	**Model 3**
Analytically	234.8 kNm	223.5 kNm	219.7 kNm
FE-model	219.5 kNm	216.0 kNm	215.7 kNm
Ratio	0.94	0.97	0.98

D.2 Load case 2

The loading situation for load case 2 gave rise to a statically determinate support moment at the girder which could be calculated by the load times the lever arm, and then be compared to the integrated bending moment from the established FE-models.

Figure 25 shows the transversal support condition for the different FE-models and a case of fixed support. In Table 6, the support moments are compared and it could be seen that the moments from the different models agreed well with the two-dimensional analysis. When the study of the support conditions was made for load case 1, the analytical result and the results from the FE-analysis deviated more than for load case 2. This might depend on that only one longitudinal section was needed to be integrated for load case 2. The approximation errors had then lower impact on the results compared to the approximation errors for load case 1.

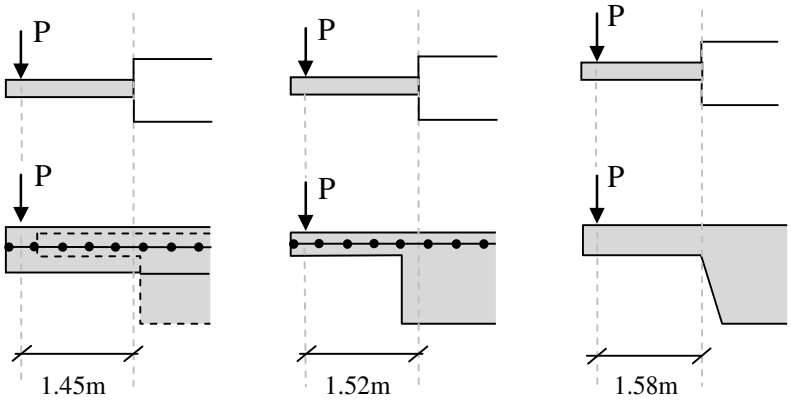

Figure 25 *Support conditions for; (a) model 1, (b) model 2 and (c) model 3.*

Table 6 *Comparison of the total bending moment in the FE-models and the analytic model.*

	Model 1	Model 2	Model 3
Analytically	522.0 kNm	547.5 kNm	568.8 kNm
FE-Model	521.1 kNm	545.0 kNm	567.6 kNm
Ratio	1.00	1.00	1.00